Assessment of Radiological Doses Associated with Natural Radioactivity from soil in the communities close to Uranium mines in Namibia

This thesis is submitted to the:

Department of NUCLEAR SAFETY AND SECURITY

SCHOOL OF NUCLEAR AND ALLIED SCIENCES

UNIVERSITY OF GHANA, LEGON

By

NAMENE TEKULA NEKWAYA

(10644403)

BSc. Physics and Geology (UNAM)

Postgraduate Dip. (Applied Radiation Science and Technology)

(NUST)

In partial fulfilment of the requirement for the award of

MPhil Nuclear Science and Technology degree

JULY, 2019

DECLARATION

I hereby declare that all information in this document has been obtained and presented in accordance with academic rules and ethical conduct. I also declare that, as required by the rules and conduct, I have fully cited and referenced all material and results that are not original to this work.

…… ……

Namene T. Nekwaya **Date**

Student

…… ……

Prof Augustine Faanu **Date**

Principal Supervisor

…… ……

Dr. David Kpeglo **Date**

Supervisor

DEDICATION

I dedicate this body of work to my late Father, Niclaas Nekwaya, my dearest Mother Helena Nekwaya and my siblings.

ACKNOWLEDGMENT

I would like to thank The Almighty God for giving me the wisdom, foresight and tenacity to see through my work till the end. I wish to express my sincere gratitude to my supervisors, Professor Augustine Faanu and Dr David Kpeglo for all your intellectual and academic support during the period of my studies. Secondly I would like to acknowledge Dr D. Adotey for his immense assistance in the retrieval of our samples at the airport customs. I would also like to thank Mr Vilho Shawapala for his assistance during the sample collection, it was a demanding job and it will always be appreciated. I am and will always be grateful for the financial support the International Atomic Energy Agency (IAEA) has given me through International Atomic Energy Fellowship. Most importantly I would like to thank my government (Namibia) for nominating me to be the IAEA Fellow for 2018/2019, will always be grateful. I would officially like to thank the Ghana Atomic Energy Commission for providing a space to prepare my samples and to conduct my NORMs analysis I am grateful for the opportunity to study at the School of Nuclear and Allied Sciences (SNAS), and I would like to thank the Dean, the administrators and all the lecturers for aiding me in attaining knowledge. I would like to thank Bernard Osei, Maruff Abubakar, and Eugenia Yeboah for their laboratory assistance at the Ghana Atomic Energy Commission.

TABLE OF CONTENTS

LIST OF TABLES

LIST OF FIGURES

LIST OF ABBREVIATIONS

UNSCEAR – United Nations Scientific Committee on the Effects of Atomic Radiation

BSS – Basic Safety Standards

Bq/kg – Becquerel per kilogram

GPS – Geographical positioning System

G.A.E.C – Ghana Atomic Energy Commission

ICRP – International Commission on Radiological Protection

BIER – Biologic Effects of Ionizing Radiation

NORM – Naturally Occurring Radioactive Materials

mSv – millisievert

H_{ex} –External hazard indices

HPGe – High Purity Germanium

IAEA – International Atomic Energy Agency

nGy/h – nano Gray per hour

Ra_{eq} – Radium equivalent activity

MeV – Mega electronvolt

NaI(TI) – Sodium iodide (Thallium) Detector

µSv – microsievert

HNBR - High Natural Background Radiation

H_E - Annual Dose Equivalent

LCR – Lifetime Cancer Risk

DNA – Deoxyribonucleic acid

LET – Linear Energy Transfer

U - Uranium

Th - Thorium

K - Potassium

GM – Geiger Muller

MCA – Multi channel analyser

ADC – Analogue to digital converter

AR – Arandis

ABSTRACT

Primordial radionuclides are ubiquitous in the environment and they exist in different ranges of concentration levels in minerals. Some human activities such as uranium mining can result in a rise of concentration of naturally occurring radioactive materials (NORM) and lead to exposure conditions. This necessitates a need to radiologically map and determine the extent of exposure of people who work in the mines and communities that live nearby as they can be the primary exposed population. The aim of this project was to assess the radiological doses of the members of the public who live in towns (Arandis, Walvis Bay, Swakopmund and Henties Bay) that are close to the uranium mines in the Erongo region of Namibia. A total of 28 soil samples were collected from the four towns and analysed for the activity concentration of ^{226}Ra, ^{232}Th and ^{40}K using non-destructive Gamma spectrometry system with a high purity Germanium (HPGe) detector. Genie 2000 software was used to accumulate and analyse spectra. The average activity concentration for Arandis for ^{226}Ra was 58.28± 9.88 Bq/kg, for ^{228}Ra (^{232}Th), the average concentration was 195±83.0Bq/kg, ^{40}K is the radionuclide with the highest activity concentration of 617±85.4Bq/kg, Arandis has the highest activity concentrations than all other towns. In Swakopmund; ^{40}K was the radionuclide with the highest average concentration from the radionuclides that were measured and the value was 379.15 ± 97.5 Bq/kg. Swakopmund had an estimated average activity concentration of ^{232}Th to be 56.29±18.2 Bq/kg, whereas the average activity concentration of ^{226}Ra was estimated to be 28.70 ± 11.2 Bq/kg which makes it the lowest activity concentration from the radionuclides that were measured. For Walvis Bay the radionuclide with the highest average activity concentration was ^{40}K and its value was 285.9±116.9 Bq/, ^{232}Th was found to have an average concentration of 14.44±6.51 Bq/kg, ^{226}Ra activity concentration for Walvis Bay had the lowest

activity concentration average value of 12.3±5.19 Bq/kg than the rest of the radionuclides, making it have the lowest activity concentrations than all the other towns. Henties Bay had a high average activity concentration for ^{40}K of 648.28±31.1 Bq. The average concentration for ^{232}Th was 140.30 ± 76.2 Bq/kg, the activity concentration for ^{226}Ra was found to have an average concentration of 58.80±10.1Bq/kg. The mean annual effective dose values were below the recommended reference value in all the towns. The radium equivalent activity for all the towns except Arandis was below the limit of 370 Bq/kg. The mean external hazard indices, and internal hazard indices values for soil in the towns of; Walvis Bay, Swakopmund, and Henties Bay were below the limit except for Arandis. The results obtained indicate radiation from NORMs at the mining towns show insignificant public exposure.

CHAPTER ONE

INTRODUCTION

1.1 Background

Natural radioactive elements are found in geological environments. The presence of the radionuclides depends on the geological structure. Due to the variation in the natural settings of the environment, there will therefore be different levels of radionuclides in the soils in many areas of the world (UNSCEAR, 2000).

If the levels are high it could lead to harmful exposure of many people living in close proximity. According to the United Nations Scientific Committee on Effects of Atomic Radiation Report, the biggest factor responsible for the environment and human beings for radiation exposure is a result of the background radiation that is always forever present. The world's average annual effective dose is determined to be 2.4 mSv (UNSCEAR, 2000), however, significantly higher ionizing radiation exposures is observed for people who live in environments which are known to have naturally higher background radiation areas (UNSCEAR, 2008).

Natural background radiation is the quantity of exposure of radiation that a human being from the public receives due to radiation sources that comes from the natural environment such as soil, water, air, rocks, and the vegetation and the cosmic radiation that comes from outer space and the Earths closest Star, the Sun. Infinitesimal amounts of naturally occurring radionuclides exist in the human body, which is often taken up through diet, (UNSCEAR, 2008) which result in the person being able to radiate inwardly.

Exposure to ionising radiation emitted by individual radionuclides of naturally occurring radioactive material (NORM) can be hazardous to humans and the environment and can exist to be hazardous for thousands of years if no remedial action

is taken. The world's average radiation dose rate due to exposure to NORM is generally low in most environments. However, certain human activities can increase the concentration of NORM and/or alter exposure conditions. Subsequently, this can give rise to above background radiation dose to receivers. Such exposure needs to be controlled through regulation to ensure that adequate protection to individuals as well as to the environment (Smith, 1992).

Namibia's radiation levels is reported to be 0.3 mSv per year, around the coast where the uranium deposits are located. Majority of the people who reside in the coastal cities and towns (Swakopmund, Arandis, Walvis Bay, Usakos, and Swakopmund) the population-weighted average of the cosmic radiation for the region is similar to the population-weighted world average of 0.38 mSv per year, as reported by UNSCEAR (UNSCEAR, 2000).

Mining practices can result in several factors which can contribute to the exposure of radiations through inhalation, external skin contact (which is the commonest form of exposure), ingesting of water and food that can contain contents which can have radioactive properties (Smith, 1992). Mine workers and people who live in communities are at a higher risk due to mining activities which can ultimately result in significant exposure to ionizing radiation. Various mines such as Rossing Uranium, Langher Heinrich Uranium and Swakop Uranium are the fully operational mines which are in the region of this study.

There are two exposure situations from primordial radionuclides which are external and internal radiation exposures. The contributing factors for external radiation exposures come from gamma radiation being emitted by radionuclides in the soil which are ^{238}U, ^{232}Th and ^{40}K. Whereas internal exposures result in the intake and uptake of

radionuclides through inhaling radioactive gaseous products and ingesting radioactive content which consequentially effect organs when in contact with alpha and beta particles and external gamma dose radiation. Radon has decay products which have short half-lives and they form a major part of exposure due to inhalation and are the most important among the inhalation of natural radiation (UNSCEAR, 2010).

This study will focus on the radiological state of four towns that with some being close to Uranium mines enabling this type of situation to be treated as an existing exposure situation where reference levels will be used.

According to the International Basic Safety Standards (BSS), there exists important fundamental requirements to protect people and the environment from the harmful effects of ionizing radiation and this is made possible by ensuring that there is adequate regulatory control (IAEA, 2014).

These requirements are dependent on the 2007 recommendations of the International Commission on Radiological Protection the 2007 recommendations which focuses on the characteristics of three exposure situations. The current radiological protection principles is utlilised in the context of the three exposure situations which are; emergency, planned, and exsiting exposure situations. Procedures are utilised when making a decision on the nature of the extent of the radiation protections strategies regarding the nature of the exposure situtation (ICRP, 2007).

The International Basic Safety is applied to both natural laws and international legal instruments and may be considered to include human being, biota, abiota, physical surroundings and their interactions (IAEA, 2014).

1.2 Statement of problem

In March 2014, local environmental groups; Earth Life Namibia and LARRI in collaboration with a Brazilian university and an independent radiation specialised laboratory based in France, undertook their own research and made a report which concluded that mining activities in the south western coast are the possible causes of health effects due to mining activities (Kohrs, 2014). In contrast the company came out publicly to indicate there are no significant negative environmental impacts due to mining activities. As result of this disagreement between the two bodies, there is a need for an independent research to ascertain the levels of NORM within the mines and their nearby communities and towns that surround them, by using more than one methodology to be able to characterize the radiological state holistically. This is because, NORM could be one of the hazards of concern since the mining of uranium could result in waste residues with significant levels if not adequately controlled.

Generally there is a knowledge gap amongst the public understanding of the consequences of uranium mining and processing in terms of the possible health risks and health effects it may bring, and understanding the levels of NORMs and radioactivity around the nearby communities.

In view of the above, this study is being carried out in the aforementioned areas to establish the levels of NORM. The distribution of the concentration of radionuclides in the Namibian soils is of main interest, more especially on the south western coast of the country because of insufficient radiological mapping and frequent human activity (mining projects being approved for extraction of NORM). A strong effort to study the coastal area is in line with the Government of Namibia to continuously monitor different levels of radiation in the country.

1.3 Objectives

1.3.1 Main Objective

The overall objective is to assess the radiological impact and doses of the members of the public living in the four areas.The research focus is on determining the levels and the extent of the exposure of the naturally ocurring radionuclides of ^{226}Ra/ ^{228}Ra decay series as well as ^{40}K within the major four towns of the Erongo region.

1.3.2 Specific Objectives

i. Determine the activity concentration of ^{226}Ra, ^{228}Ra and ^{40}K in the soils and compare with and with the world's average values and published work on similar studies done in the same region and the rest of the world.

ii. Calculate the mean absorbed dose rate

iii.. Estimate the mean annual effective dose for the four towns which will furthermore lead to the deduction of the extent of public exposure of people in the nearby communities.

iv. Determine the external hazard index,internal index and the radium equivalent activity

v. Determine the lifetime cancer risk for the members of the public who live in that area.

1.4 Significance of the Research

This work is necessary in order to obtain data to be able to assess the radiological impact on inhabitants around the uranium mines and the nearby communities in particular. This data will be important for regulatory purposes since it will help in the enforcement of the regulations of the mines to implement more efficient safety and protective measures, if there is no compliance with the mining licence requirements or to ensure if the mine is meeting the regulatory requirements of practice.

This research work in itself can also serve as research data for further research and influence mining policy and decision making. This study is also important to minimize, and in some cases eliminate future problems that are associated with the radiological implications of the nearby communities that are in close proximity to the Uranium mines.

1.5 Structure of the Thesis

This study is divided into five chapters. Chapter one gives background information on human exposure and health effects of naturally occurring radioactive materials, source of background radiation, an overview of Namibia's radiological mapping, background information on exposure, exposure pathways and health effects, statement of the problem, the main objectives, and significance of the research. Chapter two presents the literature review of naturally occurring radioactive materials, their source, existence, levels, and regulations on their safe containments as well as protocols for their analyses. It also features literature of the biological effects due to radiation. In addition it includes previous research work. Chapter three describes the procedure and instruments used to achieve the objectives of the study. A presentation of the main results and the assessment is outlined in chapter four. Chapter five gives a summary of the results obtained and presents general conclusions and recommendations.

CHAPTER TWO

LITERATURE REVIEW

This chapter provides the reviews of relevant literature on similar studies carried out on the study of naturally occurring radioactive materials, their existence and levels. It also features literatures of various body of work that serve as an underlying base of knowledge of nuclear science and research.

2.1 Naturally occurring radioactive materials

Naturally occurring radioactive material (NORM) are long-lived radionuclides such as ^{238}U, ^{232}Th and ^{40}K (UNSCEAR, 2000). These NORMs are known to be naturally radioactive which means they are present in our natural environment and they continue to decay spontaneously into other radionuclides that are either unstable or stable nucleus with the emission of alpha and beta particles and gamma radiation. A good estimation of the total radiation dose in terms of the world population has indicated that 96 % is from natural sources (air, soil, water, human body and etc.) whereas the other 4 % is from artificial sources. Natural radioactivity and terrestrial gamma dose originating from NORM depend essentially on geological conditions (UNSCEAR, 2000). Hence, concentrations of natural radioactivity in soil vary from one region to another in the world. Human activities such as mining or mineral processing have the potential to increase the exposure to these radionuclides in comparison to the naturally occurring situation (UNSCEAR, 2008).

In the past, regulatory control of NORM, has largely been focused on the uranium mining and milling industry, as it is part of the nuclear fuel cycle. However, over the past three decades, there has been a growing awareness arising from the recognition of

increased levels of NORM in non-nuclear industries, such as phosphate and petroleum industries. The control of exposure encompasses both indoor and outdoor environments, whether in dwellings or in workplaces, including industries involving NORM (ICRP, 2007).

2.2 Sources of naturally occurring radioactive materials

There are three (3) sources responsible for naturally occurring radiations. The first one is internal radiation. The second type is the oldest source which is cosmic radiation, which is related to the beginning of the universe about 13 to 14 billion years ago. The third (3) source is from primordial radioactive elements that were created when the earth was born about 4.5 billion years ago (UNSCEAR, 2008).

2.2.1 Internal radiation

This type of radiation is due to the internal composition of human bodies such as radioactive isotopes ^{40}K and ^{14}C from birth till death. The human body is known to contain traces of radioactive isotopes that expose its tissues to constant low level radiation. However the absorbed dose and detriment is negligible (Ahmed, 2007).

2.2.2 Cosmic radiation

The outer space consists of radiation that comes from a variety of sources such as the sun which emits mainly alpha particles and protons and exploding stars known as supernovas which consists mainly of electrons and protons. These primary particles enter the earth's atmosphere and interact with the atmospheric molecules (nitrogen,

oxygen, argon) to produce secondary cosmic rays (neutrons, pions, protons, and kaons) that bombard the earth's surface and have sufficient energy to penetrate deeply into the ground and the sea (UNSCEAR, 2000).

These cosmic rays are responsible for burning skin sensation and cancer in human beings who continue to be exposed to sun rays for extended periods of time. In regions of the world where the ozone layer has depleted tend to be worse. In addition to these localized sources of radiation there is a background radiation of lower intensity and it comes from the underlying ground and environment. This radiation is thought to be the remnants of the so called big bang that created this universe. It is known as cosmic microwave background radiation since the photon spectrum peaks in the microwave region of the electromagnetic spectrum. Although these photons reach the earth's surface but due to their low energies, they are not deemed harmful (UNSCEAR, 2008).

Apart from gamma energy photons, there exists other particles as well that are constantly being produced in the outer space. Many of them, never reach the earth either due to magnetic deflection which is the atmosphere. Particles, like muons, electrons, and neutrinos, are produced in the cosmos when other particles interact with atoms in the earth's atmosphere. Some of these particles reach earth's surface time but due to their very low energies and low cross section, they do not pose any significant health hazard (Ahmed, 2007).

The dose rate in air from the directly ionizing part of cosmic radiation is set to be 32 nGy/hr at sea level whereas the neutron part results in an effective dose rate of 3.6 nGy/hr with both components intensity increasing with altitude (UNSCEAR, 2008).

^{3}H and ^{14}C is one the most significant pair of cosmogenic radionuclides that are used to derive doses from man-made environmental releases. A high concentration of

cosmogenic radionuclides exists in the upper stratosphere due to its altitude and latitude dependency. The annual effective dose from cosmogenic radionuclides are estimated to be 12 µSv from ^{14}C, 0.15 µSv from ^{22}Na, 0.01 µSv from ^{3}H and 0.03 µSv from ^{7}Be (UNSCEAR, 2000). These four (4) doses combined therefore entail that their contribution to radiation exposure from natural sources is considered as an exemption in terms of radiation protection management.

2.2.3 Terrestrial Radiation

Terrestrial or primordial radionuclides are initial radionuclides that have been around since the earth was made (4.5 billion years ago), and those radionuclide have not completely decayed to stability because of their long half-lives. There is a primordial radionuclide decay chain of products, they are ^{238}U, ^{232}Th, K^{40}, ^{87}Rb, and ^{235}U (UNSCEAR, 2000).

The levels of naturally occurring radionuclides are reported by UNSCEAR to differ in extremities in the environment. Fortunately, they are usually considered to be low, with global average concentrations of 33, 45 and 420 Bq/kg for ^{238}U, ^{232}Th and ^{40}K , respectively (UNSCEAR, 2008). The global population weighted against the annual effective dose rate is 2.03 mSv (UNSCEAR, 2008). However, in specific areas in the world, such as Guarapari, Brazil; Kerala, India; Ramsar, Iran; and Yangjiang, China, these levels are quite naturally high due to the geological and geochemical characteristics of the region (Mohanty, 2004), giving a significant effective dose level, as high as 131 mSv/a (Esmaili., 2002). These places are referred to as high natural background radiation (HNBR) areas. There is another situation where the amount of naturally occurring radionuclides has been changed by certain human activities. This

change can be intentional, as in uranium mines, or unintentional (uncontrolled release of radioactive material), as in oil and gas industries.

Table 2.1: **Uranium series 4n+2, half- life, and type of radiation its energy (Cember, 2009)**

		Energy (MeV)		
Nuclide	**Half life**	**Alpha[a]**	**Beta**	**Gamma(Photons)**
^{238}U	4.51×10^{9} yrs	4.18		
^{234}Th	24.10 d		0.193, 0.103	0.092 (0.04)
^{234m}Pa	1.175 min		2.31	1.0 (0.015)
^{234}Pa	6.66 h		0.5	Many (weak)
^{234}U	2.48×10^{5} yrs	4.763		
^{230}Th	8.0×10^{4} yrs	4.685		0.068 (0.0059)
^{230}Ra	1.622 yrs	4.777		
^{222}Em	3.825 d	5.486		0.51 (very weak)
^{218}Po	3.05 min	5.998 (99.978%)[c]	Energy not known (0.022%)[c]	0.186 (0.030)
^{218}At	2 s	6.63 (99.9%)[c]	Energy not known (0.1%)[c]	
^{218}Em	0.019 s	7.127		
^{214}Pb	26.8 min		0.65	0.352 (0.036)
^{214}Bi	19.7 min	5.505 (0.04%)[c]	1.65, 3.7 (99.96%)[c]	0.609 (0.295)
^{214}Po	1.64×10^{-4} s	7.680		
^{210}Tl	1.32 min		1.96	2.36 (1)
^{210}Pb	19.4 yrs		0.017	0.0467 (0.045)
^{210}Bi	5.00 d		1.17	
^{210}Po	138.40 d	5.298		0.802 (0.000012)
^{206}Pb	Stable			

Uranium has three forms of uranium isotopes, where ^{238}U exists in nature with a concentration in nature of 99.3%, whereas ^{235}U has a concentration in nature of 0.7% and ^{234}U has a concentration of about 5×10^{-3} % that exists in the environment. Actinium is the series that has ^{235}U as the parent radionuclide. Since the formation of earth

Uranium element has been part of the earth's existence and is thus found in soil and it is estimated to have average concentrations of 3 ppm (parts per million) by weight which is 74 mBq/g of soil (El-Gmal, 2007). Uranium chemically forms very stable compounds and with phosphorous. Phosphate-rich soil, therefore, contains uranium at concentrations much higher than average, from about 7 ppm to about 125 ppm medium-grade uranium ore contains about 1000 - 5000 ppm uranium, while the uranium concentration in high-grade ore is about 10,000 - 40,000 ppm (Cember, 2009).

Table 2.2: Thorium series 4n, half-life, type of radiation and amount of energy emitted in MeV (Cember, 2009).

		Energy (MeV)		
Nuclide	**Half life**	**Alpha[a]**	**Beta**	**Gamma(Photons)**
^{232}Th	1.39 10^{10} yrs	3.98		
^{228}Ra	6.7 yrs		0.01	
^{228}Ac	6.13 h		Complex decay scheme Most intense beta group is 1.11 MeV	1.59 (n.v.) 0.966 (0.2)
^{228}Th	1.91 yrs	5.421		0.084 (0.016)
^{224}Ra	3.64 d	5.681		0.241 (0.038)
^{220}Rn	52 s	6.278		0.542 (0.0002)
^{216}Po	0.158 s	6.774		
^{212}Pb	10.64 h		0.35, 0.59	0.239 (0.40)
^{2212}Bi	60.5 min	6.086	2.25 (66.3%)c	0.04 (0.034 branch)
^{212}Po	3.04×10^{-7} s	8.776		
^{208}Tl	3.1 min		1.80, 1.29, 1.52	2.615 (0.997)
^{208}Pb	Stable			

Thorium exists as six isotopes – ^{234}Th, ^{232}Th, ^{231}Th, ^{230}Th, ^{228}Th, and ^{227}Th. The isotopes of thorium are present in all the natural decay series. Thorium mostly comes in the tetravalent Th (IV) state. It is an insoluble element and has inhibited mobility (Chabaux, 2003). Thorium is a NORM that is ubiquitous in the environment, only it is

4 times the amount of the Uranium element that exists in the environment. ^{232}Th is the most abundant form of thorium isotope that exists on earth and it is also the parent radionuclide of the thorium radioactivity chain. The members of the thorium radioactivity chain share common characteristics. The parent radionuclide has a half-life value that is comparable to that of the earth's age (Cember, 2009).

Table 2.3: Actinium series 4n, half-life, type of radiation and amount of energy emitted in MeV (Cember, 2009).

		Energy (MeV)		
Nuclide	**Half life**	**Alpha[a]**	**Beta**	**Gamma(Photons)**
^{235}U	7.13 × 10^{8} yrs	4.39		0.18 (0.7)
^{231}Th	25.64 h		0.094, 0.302, 0.216	0.022 (0.7)
^{231}Pa	3.43 × 10^{4} yrs	5.049		0.33 (0.05)
^{227}Ac	21.8 yrs	4.94	0.0455	
^{227}Th	18.4 d	6.03		0.24 (0.2)
^{223}Fr	21 min		1.15	0.05 (0.40)
^{223}Ra	11.68 d	5.750		0.08 (0.24)
^{219}Em	3.92 s	6.824		0.267 (0.086)
^{215}Po	1.83 x 10^{-3} s	7.635		
^{211}Pb	36.1 min		1.14, 0.5	Complex spectrum, 0.065–0.829 MeV
^{211}Bi	2.16 min	6.619	Energy not known	
^{211}Po	0.52 s	7.434		0.88 (0.005)
^{207}Tl	4.78 min		1.47	0.87 (0.005)
^{207}Pb	Stable			

According to Cember, lead-206 (^{206}Pb) being the final stable nuclide of each the 3 radioactive series is an essential part to consider as this characterises the natural radioactive series. In the situation of the uranium radioactivity chain as shown in Table 2.1, ^{206}Pb is the final end product for ^{238}U, as shown in Table 2.3, actinium has ^{207}Pb as its final product and as shown in Table 2.2 ^{208}Pb is the final product for the thorium radioactive decay series chain. These four radioactive decay series, the three naturally

occurring ones and the artificially produced neptunium series, are often designated as the $4n$, $4n + 1$, $4n + 2$, and $4n + 3$ series. These identification numbers refer to the divisibility of the mass numbers of each of the series by 4. The atomic mass number of ^{232}Th, the first member of the thorium series, is exactly divisible by 4. Since all disintegrations in the series are accomplished by the emission of either an alpha particle of 4 atomic mass units or a beta particle of 0 atomic mass units, it follows that the mass numbers of all members of the thorium series are exactly divisible by 4. (Cember, 2009).

Table 2.4: Low atomic-numbered naturally occurring radioisotopes

NUCLIDE	ISOTOPIC ABUNDANCE (%)	HALF-LIFE (YRS)	PRINCIPAL RADIATIONS	
			PARTICLES (MeV)	GAMMA (MeV)
^{40}K	0.0119	1.3×10^{9}	1.35	1.46
^{87}Rb	27.85	5×10^{10}	0.275	None
^{138}La	0.089	1.1×10^{11}	1.0	0.80, 1.43
^{147}Sm	15.07	1.3×10^{11}	2.18	None
^{176}Lu	2.6	3×10^{10}	0.43	0.20, 0.31
^{187}Re	62.93	5×10^{10}	0.043	None

There exists several primordial radionuclides in nature other than thorium, uranium, and actinium series where there are elements whose half – lives are as long as uranium and thorium and have lower atomic numbers as shown in the above Table 2.4. According to Cember ^{40}K by virtue of the widespread distribution of potassium in the environment (the average concentration of potassium in crustal rocks is about 27 g/kg and in the ocean is about 380 mg/L) and in plants and animals, including humans (the average concentration of potassium in humans is about 1.7 g/kg) (Cember, 2009).

2.3 The equilibrium state

In the measurement of radionuclides in the natural decay series, the activity concentration of a parent radionuclide is usually estimated from its daughters and vice versa. Such measurements are based on the assumption of equilibrium conditions, where the activity concentrations of the parent and daughter radionuclides are equal in a secular equilibrium or can be calculated in a transient equilibrium (Debertin, 1988). A comprehension on the state of equilibrium is essential in the context of dose assessment due to NORM (Lombardo, 2008).

Equilibrium conditions are applied when the radionuclide cannot be directly identified by the detection method being used. In gamma spectroscopy, the activity concentration of ^{226}Ra is usually determined through gamma-rays emitted from its decay products ^{214}Pb and ^{214}Bi after achieving secular equilibrium (Al-Masri, 2003). This is more accurate than using the deconvolution or the activity ratio (^{238}U/^{235}U) (Dowdall, 2004) when measuring ^{226}Ra directly from its gamma peak at 186.1 keV that interferes with the 185.7 keV peak of ^{235}U. More examples of radionuclide measurement using equilibrium are given in Table 2.5

Table 2.5: Examples of radionuclides in equilibrium

Radionuclide of interest	Measured radionuclide	Typical delay time	Reference
^{238}U	^{234}Th and ^{234m}Pa	4 months	(Huy and Luyen, 2004; Lenka et al., 2009; Yücel et al., 2009)
^{226}Ra	^{214}Pb and ^{214}Bi	3 weeks	(Dowdall et al., 2004; Landsberger et al., 2013; Murray et al., 1987)
^{228}Ra	^{228}Ac	36 hours	(Lourtau et al., 2014; Xhixha et al., 2013)
^{228}Th ^{224}Ra	^{212}Pb and ^{208}Tl	3 weeks 2 days	(Awudu et al., 2012; Condomines et al., 2010)
^{227}Ac	^{227}Th and ^{223}Ra	3 months	(Köhler et al., 2000; Van Beek et al., 2010)
^{223}Ra	^{219}Rn	A minute	(Desideri et al., 2008; El Afifi et al., 2006)

The disadvantage of using equilibrium conditions in the measurement of radioactivity is the waiting time needed to achieve equilibrium, more so for relatively long-lived daughters. For instance, the measurement of ^{226}Ra through its decay products require at least three weeks of delay period to obtain secular equilibrium (Siegel, 2013).

Equilibrium state can be disrupted under certain conditions. This occurs when some members of the radioactive decay series are removed or added to the system, creating a condition of disequilibrium. This disequilibrium can occur naturally or technologically due to some human activities, such as in uranium mines, where uranium isotopes are separated from the rest of the primordial radionuclides in the uranium decay chain. In the environment, disequilibrium is controlled by the behaviour of individual radionuclides; physicochemical properties play a role in causing leachability and mobility of radionuclides (Cañete, 2008).

This disequilibrium has been prevalent in water sediment and NORM industrial sites. Once the equilibrium is disturbed, it requires days, weeks, months, thousands or even millions of years to be restored, depending on the half-lives of the radionuclides. Disequilibrium can be a serious source of error in the measurement of radionuclides in the decay series (IAEA, 2003).

Charette (2012) Stated that assuming equilibrium, which is not the case in reality, can lead to an erroneous estimate of the activity concentration of radionuclides of interest.

2.4 Radon and its Decay Products

Radon is a radioactive gas that is derived from the radioactive decay of Ra in three natural series as ^{222}Rn, ^{220}Rn, and ^{219}Rn. As a noble gas, radon is chemically inactive, and does not precipitate in solid phase, although it can compound with fluorine under special conditions (Chernick, 1962). Radon is transported from subsurface to the ground mostly through diffusion, which is proportional to the gradient of gas concentration in interstitial spaces; additionally advection mechanisms, caused by differences in pressure created by meteorological conditions also support Radon mobility (Anderson, 2001; Chauhan, 2013; Jacob, 1990). As radon is exhaled from the ground into the atmosphere and decays, its short lived progeny reacts with water vapour and trace gases, forming clusters with diameters from 0.5 to 5nm, which are then attached to aerosol particles (Michielsen, 2007; Porstendörfer, 1994; Porstendörfer, 1999). The concentration of radon is much higher in indoor air, where it is accumulated, than in open air, where it is diluted (UNSCEAR, 2006). In water, radon is soluble, and its solubility is sensitive to water temperature and salinity (Schubert, 2012).

Some of radon's isotopes are however of a less radiological relevance. ^{232}Th is significantly abundant in nature than ^{238}U and has a longer half-life. As a result the average rate of production of ^{220}Rn in the earth is about the same as that of ^{222}Rn. However the shorter half-life (56seconds) of ^{220}Rn as compared with 3.82 days for ^{222}Rn gives a higher probability to decay prior to converting to airborne. The additions of ^{220}Rn daughters to lung dose are negligible compared with ^{222}Rn. Actinium series produces ^{219}Rn which has a half-life of 4 seconds renders its contribution to airborne Radon insignificant (Turner, 2007).

2.4.1 Radiological Effects of Radon

^{222}Rn exposure in indoor environments has been given a lot of attention (IAEA, 2015). This is because of available data relating health risks to exposure levels and the presence of ^{222}Rn in all buildings and closed spaces (Darby, 2005). Inhalation of ^{222}Rn and its short-lived progeny is the second main cause of lung cancer (WHO, 2009). The health risk that is commonly attributed to ^{222}Rn is actually associated with its short-lived progeny radionuclides ^{218}Po, ^{214}Pb and ^{214}Bi that are produced in air; Most of inhaled ^{222}Rn gas is exhaled from the lungs before it decays, due to its relatively long half-life of 3.8 days (UNSCEAR, 2006). Based on the review of recent epidemiological studies on the association between exposure to ^{222}Rn and its progeny and lung cancer, the ICRP has announced that the risk from exposure due to the inhalation of ^{222}Rn progeny is double that of the current estimation (ICRP, 2010). These epidemiological studies included residential and occupational exposures and observed a significant association with the risk of lung cancer at average annual ^{222}Rn concentration of approximately 200 Bq/m^3 (ICRP, 2010).

^{222}Rn decays into a series of short-lived daughters, two of which, ^{218}Po and ^{214}Po, are alpha emitters. When an alpha particle is ejected in the lungs, it deposits all of its energy locally within a small thickness of adjacent tissue due to its high electrical charge and relatively slow speed because of its great mass. An alpha particle from ^{214}Po, for example, deposits its 7.69 MeV of energy within about 70 μm. A 1-MeV beta particle from ^{214}Bi, on the other hand, deposits its energy over a much larger distance of about 4000 μm. The dose to the cells of the lung from the beta (and gamma) radiation from radon daughters is very small compared with that from the alpha particles. The radon problem, technically, is that of alpha-particle irradiation of sensitive lung tissue by the short-lived daughters of radon and the associated risk of lung cancer. The health hazard

from radon is thus closely related to the air concentration of the potential alpha-particle energy of the short-lived daughters (Cember, 2009; UNSCEAR, 2000).

2.5 Biological effects of exposure due to NORMs

2.5.1 Effects at cellular level due to exposure of NORMs

NORMs contribute majority (more than 90 %) of the average annual effective dose of ionizing radiation to individuals and ionizing radiation has a harmful effect on the human cell. Ionizing radiation is divide into direct and indirect ionizing radiation. Most of the particulate types of radiation are directly ionizing i.e. individual particles with sufficient kinetic energy can directly disrupt the atomic structure of the absorbing medium through which they pass producing chemical and biological damage to molecules (Cember, 2009). In contrast, electromagnetic radiations, namely, X and γ rays, are indirectly ionizing because they do not produce chemical and biological damage themselves but produce secondary electrons (charged particles) after energy absorption in the material (Kiefer, 1990).

2.5.2 Mechanisms of ionizing radiation damage

The damage caused by ionizing radiation begins at the microscopic level cellular level where the incident radiation is absorbed by the cell and the possibility to harm the critical targets of the cells are high, and ultimately it can lead to the damaging of the DNA which is responsible for the death, mutation of a cell, and eventually lead to cancer. Cell erosion can be understood through two situations (UNSCEAR, 2008).

2.5.3 Ionizing radiation

2.5.3.1 Direct ionizing radiation

The DNA structure can be affected when exposed to radiation resulting in the ionization of atoms that is part of the DNA molecule. This kind of radiation exposure is called direct ionizing radiation as the radiation directly interacts with the DNA. This mechanism has a low probability of occurring due to its nano-size (the DNA helix has a diameter of 2nm). For direct ionizing radiation to occur the generation of the radiation must produce ionization within a few nanometres of the DNA helix. (Hall, 1994).

2.5.3.2 Indirect ionizing radiation

In the second scenario, the incident radiation is exposed to the non-critical targets of the molecules e.g H_2O, this leads to the formation of free radicals which are very chemically reactive due to their unpaired state of electrons. These free radicals consequently leads to harm of the structure of the DNA as shown in Figure 2.1. The unpaired molecules have the ability to diffuse some distance in the cell, thus, damage from indirect action is much more common than damage from direct action, especially for radiation that has a low specific ionization (BIER, 2006).

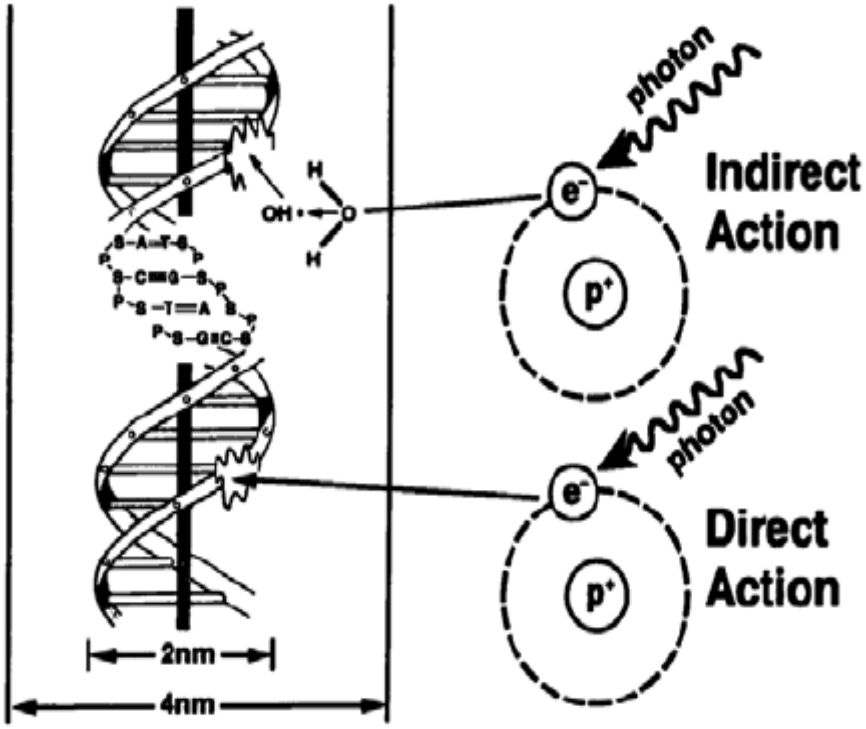

Figure 2.1: Mechanism of radiation damage by direct and indirect ionizing radiation (Hall., 1994).

When the DNA interacts with incident photons, either through direct or indirect radiation as a result of incident radiation, the destruction is brought about by the damage of the DNA molecule strands that is responsible for the formation of the double helix structure that form as walls of the DNA molecule. The damage usually involves only one of the two strands of DNA breaking apart thus being able to repair itself. The non-damaged strand is uniquely able to be used by the cell as a template to form another strand to take over the place of the damaged strand. If both strands are damaged the cell can potentially erroneously recombine the breaks and form dicentric chromosomes and centric rings which can result in the mutagenetic effects (cancer) (UNSCEAR, 2000).

2.6 Radiolysis of water

2.6.1 Ionization

$$\text{Radiation} + \text{H-O-H} \rightarrow H_2O^+ + e^- \quad (1)$$

$$\rightarrow H^+ + OH^- \quad (2)$$

Radiolysis of water is the splitting apart of water by radiation. Water is the major constituent of the cell. As such, the majority of the interactions of radiation in cells will be with water. Free radicals are neutral (uncharged) atoms or molecules with unpaired electrons. They are extremely reactive and within a microsecond of their formation they may react with some molecule (the target) and damage it, or they may react with the molecule to produce a new radical species which then proceeds to damage other molecules (Glass, 1991). Equation (1): shows water molecules becoming ionized when interacting with radiation and results in an ionized water molecule and an electron. Equation (2): shows a hydrogen positive ion and a hydroxide ion.

2.6.2 Free radicals

$$\text{Radiation} + \text{H-O-H} \rightarrow H^o + OH^o \quad (3)$$

$$RH + OH^o \rightarrow R^o\, H_2O \quad (4)$$

When many free radicals exist, orbital neutrality can be achieved by hydrogen radical dimerization (H_2), the production of toxic hydrogen peroxide (H_2O_2) and also the radical can be transferred to an organic molecule in the cell (Glass, 1991). Equation(3): Radiation interacting with water molecules to form a hydrogen radical and a hydroxyl radical. Equation (4): Shows a generic equation of a hydrogen atom reacting with a hydroxyl radical giving a product of a water molecule coupled with a radical.

2.6.3 Hydrogen peroxide

$$OH^{o} + OH^{o} \rightarrow H_2O_2 \quad (5)$$

$$O_2 + e^{-} \rightarrow O_2^{-} \quad (6)$$

$$O_2^{-} + H^{+} \rightarrow HO_2 \quad (7)$$

$$HO_2 + H^{o} \rightarrow H_2O_2 \quad (8)$$

Another radiolytic product of interest is hydrogen peroxide. Hydrogen peroxide has the potential to be damaging to cell components. It is much longer lived than free radicals and can travel substantial distances in the cell, even across membrane, to attack its target. Nevertheless, it is readily broken down by a variety of enzymes present in most healthy cells. As such, damage produced by hydrogen peroxide is of limited consequence (Glass, 1991). Equation (5) shows 2 separate hydroxyl radicals paring to form hydrogen peroxide. Equation (6) shows a dioxygen atom reacting with an electron and it becomes ionized. Equation (7) shows an ionized dioxygen atom and reacts with a hydrogen ion and they pair to form water. Equation (8) shows water pairing with a free radical to form hydrogen peroxide.

2.7 Biological Effects of Radiation

The biological consequences which occurs in the human body due to exposure from ionizing radiation is extremely harmful and fatal. When ionizing radiation interacts with the human cell it induces alterations in the DNA structure within the cell. The incident radiation damages the cells of human body and ultimately harm the tissue and organs of the body (Kiefer, 1990).

The complex types of DNA damage produced by radiation can be broadly classified as single-strand breaks, double-strand breaks, and base damages. These structural changes

and errors in their repair can lead to gene mutations and chromosomal alterations. A great deal is understood about the molecular details of DNA damage repair and misrepair and its relation to potential tumor induction and other adverse health effects. Intricate controls exercised by molecular checkpoint genes at specific stages of the cell reproductive cycle appear to recognize and react to the management and repair of damaged DNA (UNSCEAR, 2010).

2.7.1 Stochastic Effects

Stochastic effects are characterized by no known threshold level of radiation exposure, and the effects are associated with exposures to low levels of radiation over a long period of time and occurrence of these effects are statistical in nature. There exists no amount of dose dependent on its severity, however the probability of the effect increases as the doses of radiation of exposure increases. The induction of cancer and genetic defects are attributed to stochastic effects (Hall, 1994).

2.7.2 Deterministic Effects

Deterministic effects are characterised by the existence of a dose threshold and there is a causal relationship between the dose and the effect. The biological effects develop early (and/or late) in the exposed person due to a high dose of radiation received over a short span of time. Severity increases with the magnitude of the radiation dose as could be expected. The biological effects of radiation can be quantified in terms of the dose-response relationship that is the severity of the effect is dose dependent. Acute radiation syndrome (ARS), cutaneous radiation syndrome (CRS), hypothyroidism, and cataracts are associated with deterministic effects (Turner, 2004).

2.7.3 Late Somatic Effects

Biological effects induced by radiation is either exposed at a high dose in short span of time or at a low dose over long period of time. These effects may appear to be visible after a long time in the exposed person (victim). These changes are what is called late somatic effects and compared to genetic effects which appear in the children of the exposed person, the late somatic effects may appear in the victim instead (Turner, 2004).

2.7.4 Cancer

The probability of getting cancer is dependent on many factors such as the amount of dose, the duration of the exposure to the dose, the distance from the source that is emitting the dose, even as far as your body weight, age, sex and your genetic background (WHO, 2009). Additional factors, such as exposure to other carcinogens and promoters, are also important. Cancer causes almost 20% of all deaths in the United States. The relatively small contribution made by low levels of radiation to this large total is not statistically evident in epidemiological studies. In addition, radiogenic cancers are not distinguishable from other cancers as stated in the BEIR VII Report (BIER, 2006).

Table 2.6: Estimated number of cases and deaths increasing for solid tumors and leukemia for both female and male

	All Solid Cancers		Leukemia	
	Male	Female	Male	Female
Excess cases	800	1,300	100	70
Number cases without dose	45,500	36,900	830	590
Excess deaths	410	610	70	50
Number deaths without dose	22,100	17,500	710	530

At doses less than 40 times the average yearly background exposure (100 mSv), statistical limitations make it difficult to evaluate cancer risk in humans. Therefore, cancer risk at low doses can at present only be best estimated by extrapolation from human data at high doses, where excess incidence is statistically detectable. Probably the most reliable risk estimates for cancer due to low linear energy transfer (LET) radiation are those for leukemia and for the thyroid and breast. The minimum latent period of about 2 years for leukemia is shorter than that for solid cancers. Excess incidence of leukemia peaked in the Japanese survivor population around 10 years post-exposure and decreased markedly by about 25 years. These observations are consistent with leukemia experience from other sources, such as patients treated for ankylosing spondylitis and for carcinoma of the uterine cervix. Solid tumors induced by radiation require considerably longer to develop than leukemia. Radiogenic cancers can occur at many sites in the body. As an example, Table 2.6 gives a summary from the BEIR VII Report for lifetime risks for all solid cancers and for leukemia. The Committee considered a *linear-no-threshold* model as the most reasonable for describing solid cancers and a *linear-quadratic* model for leukemia (BIER, 2006).

2.8 Regulations on NORM

The current radiological protection system is recent and is developed for artificial radionuclides. The concept of exemption, for example, is mainly designed for artificial sources of radiation in planned exposure situations, where the source of exposure is introduced deliberately (ICRP, 2007). Recommendations and policies for NORM are included in general guidance with other radionuclides with no complete guidance for controlling different situations of NORM this includes Namibia (IAEA, 2014; ICRP 2007) This has led to difficulties in regulating NORM, because scenarios of exposure to NORM are often quite different from those to artificial radionuclides (Michalik, 2009). A special case of NORM concerns radon in dwellings and workplaces, and this is treated separately.

Generally, exposure to natural sources, including NORM, is considered to be an existing exposure situation, as the source already existed when the decision to regulate was made; with the potential to be subject to the requirements of a planned exposure situation because human intervention and industrial processes could change its distribution and rate of exposure (IAEA, 2014; ICRP, 2007). This can create confusion among those who use the standards (Hedemann-Jensen, 2010). According to Haridasan (2015) identifying a situation as either an existing or a planned exposure, and accordingly using appropriate reference levels or dose constraints, is one of the main radiation protection challenges. The IAEA (2014) also recognised the interference between the two situations and stated, some exposures due to natural sources may have some characteristics of both planned exposure situations and existing exposure situations. The IAEA (2014) has laid downs a criterion to solve the predicament where exposure to natural sources should be treated as a planned exposure situation:

(1) If the activity concentration of any radionuclides in the ^{238}U and ^{232}Th decay series exceeds 1 Bq/g, or 10 Bq/g in the case of 40K

(2) Public exposure due to discharge or waste from the situation outlined above

(3) Exposure due to ^{222}Rn and ^{220}Rn and their decay products in which NORM is controlled as a planned exposure situation

(4) Exposure due to ^{222}Rn and its decay products where its annual concentration in the workplace remains above the reference level that is proposed by the relevant regulatory authority, after applying reduction measures.

The values of activity concentrations, that is, 1 and 10 Bq/g, were selected as the optimum boundaries between the ubiquitous unmodified concentrations of the nominated radionuclides in soil and the activity concentrations in ores, mineral sand, industrial residues.

2.9 Radiation detection and measurement

Humans do not have any organic senses that can detect ionizing radiation. As a consequence of this deficiency, they must rely entirely on instruments for the detection and measurement of radiation fields in environments. Instruments used in the practice of health physics have a multi-purposes. It is logical, therefore, to find multiple types of instrument types. We have, for example, instruments such as the Geiger Muller (GM) counter and scintillation counter, which measure particles; film badges, pocket dosimeters, and thermoluminescent dosimeters, which measure accumulated doses over a period of time; and ionization-chamber type instruments, which measure dose and dose rate. In each of these categories, one finds instruments designed specifically for

the measurement of a certain type of radiation, such as low-energy X-rays, high-energy gamma rays, fast neutrons (Cember, 2009). It is an important requirement of detector that comes into contact with the incident radiation such that the ability of the instruments response is proportional to the radiation effect that is being determined. For the detector to respond and interact with the incident radiation it should undergo one of the processes:

1. Photoelectric effect
2. Compton scattering
3. Pair production

There are different instrument types, and are all necessary the operating principles for most radiation-measuring instruments are relatively few. The basic requirement of any such instrument is that its detector interacts with the radiation in such a manner that the magnitude of the instrument's response is proportional to the radiation effect or radiation property being measured. Some of the physical and chemical radiation effects that apply to radiation detection and measurement for health physics purposes are listed in Table 2.7 below (Cember, 2009).

Table 2.7: Radiation effects used in the detection and measurement of radiation (Cember, 2009).

Effect	Type of instrument	Detector
Electrical	1. Ionization chamber 2. Proportional counter 3. Geiger counter 4. Solid state detector	1. Gas 2. Gas 3. Gas 4. Semiconductor
Chemical	1. Film 2. Chemical dosimeter	1.Photographic emulsion 2. Solid or liquid
Light	1. Scintillation counter 2. Cerenkov counter 3.Opticoluminiscent dosimeter	1. Crystal or liquid 2. Crystal or liquid 3. Crystal
Thermoluminescence	Thermoluminescent dosimeter	Crystal
Heat	Calorimeter	Solid or liquid

One of the aims in this project is to detect gamma rays being emitted by the naturally occurring radioactive materials (^{238}U, ^{232}Th and ^{40}K) in the soil, then they are grouped according to their energies and then calculating the activities of the radionuclides in units of Becquerel (Knoll, 2000). There are different types of detectors for detecting ionizing radiations as described in the below sub sections.

2.9.1 Ionization Chamber Counter

If a detector is exposed to a flux of constant radiation running through it, where the supply voltage is varied accordingly, certain regions that are relevant in radiation measurement can be found as shown in Fig 2.2.

The voltage of the chamber is changed to a higher value from zero to low voltage values, the initial region is found and is identified as ionization chamber region. If the

chamber has polarity electrical difference then the positively charged ions tend to be collected to the cathode located on the outer side, whereas the ions that are negatively charged will be collected by the anode which is located at the centre of the chamber. When the voltage is set to low voltages, then there is usually a range of voltage ample to gain ions prior to a fraction of some of those ions can recombine, however that low voltage collecting the ions is not sufficient enough to stimulate the ions to accelerate sufficiently to lead to secondary ionization by impact collision. The exact value of this voltage is dependent and it is a function of the type of gas, the gas pressure, and the size and geometric arrangement of the electrodes. In this region, the number of electrons collected by the anode will be equal to the number produced by the primary ionizing particle. The pulse size, accordingly, is not dependent on the voltage, and will depend only on the number of ions produced by the primary ionizing particle during its passage through the detector. The amplitude of the signal is proportional to the quantity of energy deposited in the active region of the detector. Therefore, an ionization chamber in which the average current generated by the radiation is measured is used mainly to measure radiation dose (Cember, 2009).

2.9.2 Proportional Counter

The pulse value from the GM counter working under the ionization chamber region is dependent on the amount of ions formed in that region allowing the counter to differentiate the radiation types. For instance, consider a particle running across the tube, forming 105 ion pairs which is equal to 1.6×10^{-14} C. Consider the counter to have a capacitance of 10 pF then the voltage pulse will be estimated to (Knoll, 2000).

$$V = \frac{Q}{C} \tag{12}$$

$$= \frac{1.6 \times 10-14}{10 \times 10-12} \quad (13)$$

$$= 1.6 \times 10^{-3}\ \text{V} \quad (14)$$

2.9.3 Geiger Muller Counters

In the proportional region the high voltage continues to increase beyond the proportional region and till it causes the avalanche to have an extension across the anode of the chamber. When it occurs, the last portion of the proportional region is reached continuing to the GM region. This leads to the pulses is uniform. When it is working in GM region, usually the difference cannot be single out between the different radiation types. However a higher output value more than 0.25 voltage that emanates from the amplification of the high gas in the counter, means the exiting of the amplifier or the possibility of faulty counter (Cember, 2009).

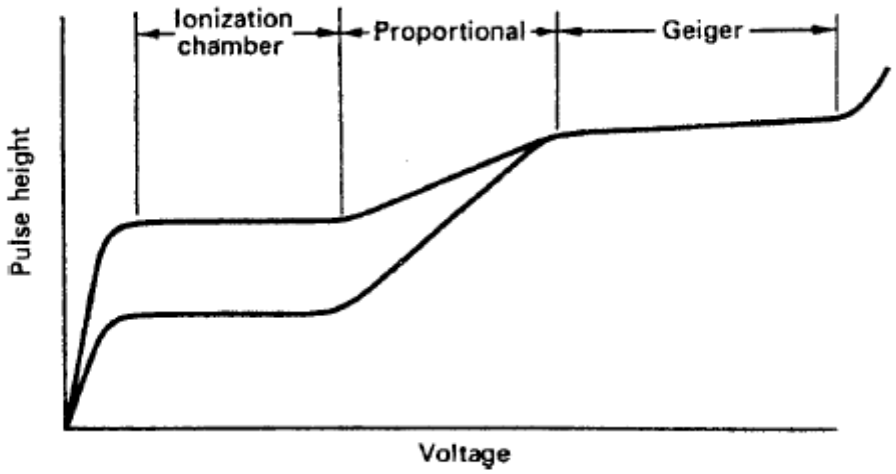

Figure 2.2: The behaviour of a curve of the pulse height versus the voltage applied across the anode in a gas chamber and going through different regions

2.9.4 Nuclear Spectroscopy

Nuclear spectroscopy is the analysis of radiation sources or radioisotopes by measuring the energy distribution of the source. A spectrometer is an instrument that separates the output pulses from a detector, usually a scintillation detector or a semiconductor detector, according to size. Since the size distribution is proportional to the energy of the detected radiation, the output of the spectrometer provides detailed information that is useful in identifying unknown radioisotopes and in counting one isotope in the presence of others. This technique has found widespread application in X-ray and gamma-ray analysis using NaI(TI) scintillation detectors and HPGe (high-purity germanium) semiconductor detectors, in beta analysis using liquid scintillation detectors or plastic scintillation detectors, and in alpha analysis using semiconductor detectors. Nuclear spectrometers are available in two types, either a single-channel instrument or a multichannel analyser (MCA) (Cember, 2009).

The spectrometer is a singular channel type and it is composed of a detector, pulse selector, linear amplifier, and a display device, Fig. 2.4. The pulse height selector is an electronic slit which may be adjusted to pass pulses whose amplitude lies between any two desired limits of maximum and minimum. The output from the pulse-height analyser is a logic pulse to a scaler or to a count ratemeter. The main use of the single-channel analyser is to discriminate between a desired radiation and other radiations that may be considered noise. Thus, the single-channel spectrometer is used to measure one radiation in the presence of another or to optimize the signal-to-noise ratio when a low-activity source is being measured in the presence of a significant background (Cember, 2009).

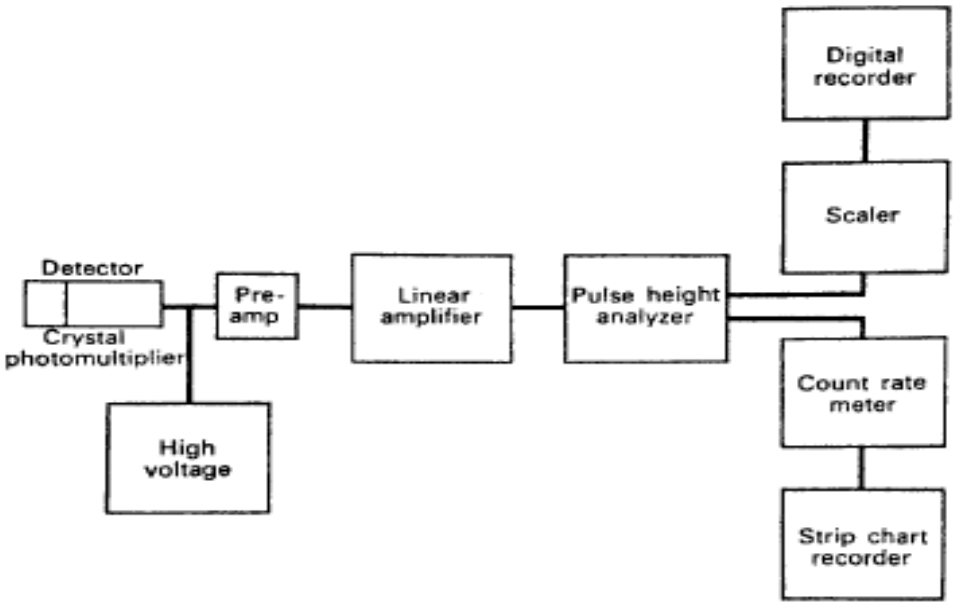

Figure 2.3: Block diagram of a singled-channel gamma spectrometer

The above figure shows the spectrometry having a multichannel analyser which has the function of changing from analog to digital information waves. The multichannel analyser (MCA) consists of a computer component of which stores the data information from the analog-to–digital–converter (ADC). The analog-to-digital-converter is able to give a logic output pulse that is saved under a specific channel number (Ahmed, 2007). Cember is quoted describing the process saying the address is determined by the number of clock pulses that were counted during the discharge of the capacitor. Majority of the multichannel analysers are built with the number of channels varying by a factor of 2 over the range of 128–16,384, each with a storage capacity of 10^5–10^6 counts per channel, and clock frequencies ranging from 4 to 100 MHz (Cember, 2009).

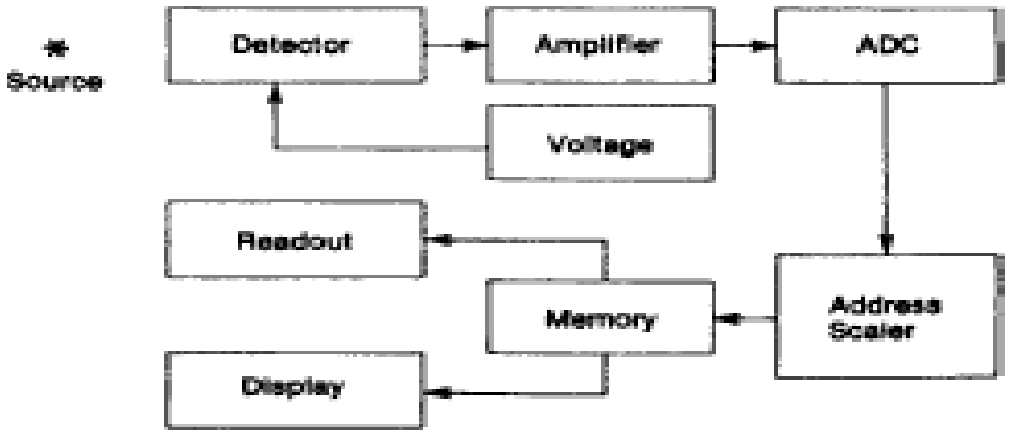

Figure 2.4: Block diagram of a multichannel analyser

Nuclear spectroscopy is the ability to find the position of the energy of the line of the spectra out the rest of the absorbed particles or gamma photons. Hence, knowing the resolution of the detector is essential, as it can be able to differentiate the spectral lines if they happen to be near each other and thus separate them. Cember described the definition of the resolution as the ratio of the full width at half maximum (FWHM) of the full-energy peak (Cember, 2009). If the FWHM is ΔE, then smaller the energy spread, ΔE, the better is the ability of a detector to separate full-energy peaks that are close together (Cember, 2009).

$$\text{Percent (\%) resolution} = \frac{\Delta E}{E} \times 100\% \qquad (15)$$

The resolution of a given detector is a function of energy and improves with increasing energy (Cember, 2009).

2.9.5 NORM Measurement

Germanium (Ge) detectors are the most common gamma detectors for measuring activity concentration. Germanium detectors a have higher gamma energy resolution, which enables them to distinguish gamma emission for different radioisotopes. The higher atomic number of germanium compared to the previously-used silicon (Si) detectors also makes it applicable for a wide range of energy (Gilmore, 2008). There exists several types of high-purity germanium (HPGe) detectors. These detectors have different crystal configurations to fit particular applications. The coaxial HPGe detector has been widely utilised in numerous environmental studies (Alghamdi and Aleissa, 2015; De Corte et al., 2005; El-Daoushy and Hernández, 2002; Kaste et al., 2006; Lenka et al., 2009; Mauring et al., 2014; Putyrskaya et al., 2015; Scholten et al., 2013; Siegel, 2013; Van Beek et al., 2010; Yücel et al., 2010). Lenka et al. (2009) used a coaxial HPGe detector to measure ^{238}U in soil through the 63 keV gamma peak of its daughter radionuclide ^{234}Th.

2.9.6 High Purity Germanium (HPGe) detectors

HPGe detectors are detectors called semiconductors consisting of diodes (p-i-n structure) of which the intrinsic region is susceptible to react when exposed to ionizing radiation. Under reverse bias, an electric field passes thorough the depleted region. When photons interact with the material within the depleted volume of a detector, charge carriers (hole and electrons) are produced and drifted by the electric field to the P and N electrodes. This charge, which is in proportion to the initial energy deposited in the detector by the incoming photon, is changed into a voltage pulse by an integral charge sensitive preamplifier (Knoll, 2000).

Germanium detectors have a low band gap, hence why they are cooled down by using liquid nitrogen gas as it has properties to lower the heat that is produced by the "charge carriers" to a needed level. If the liquid nitrogen is not used the leakage current induced noise will damage the energy resolution of the HPGe detector. The detector is connected to a chamber of which it is connected to the LN_2 dewar.

The sensitive detector surfaces are thus protected from moisture and condensable contaminants. The energy resolution of these detectors is very high, but because of their small volume, their sensitivity is low and it may take several minutes to record a spectrum. Arrangement of p-type and n-type semiconductor detectors is shown in the following figures (Knoll, 2000).

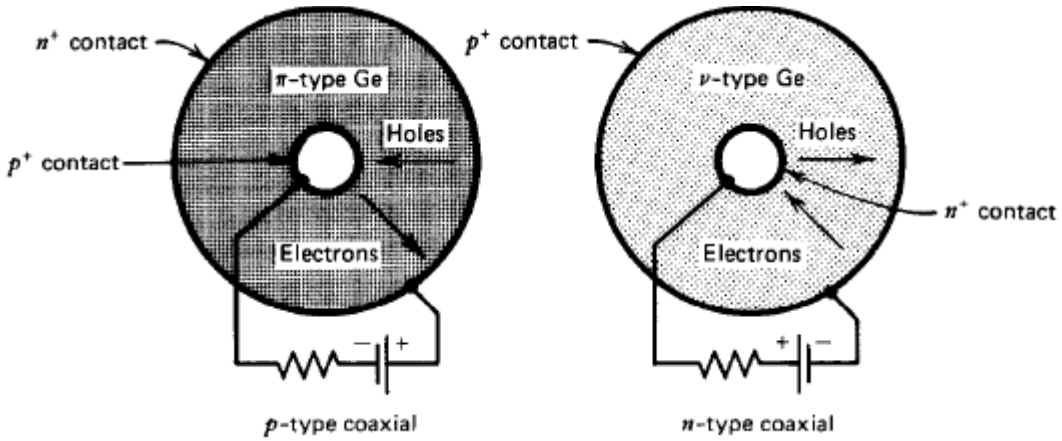

Figure 2.5: (a) - p type coaxial type and 2.6 (b) - n type coaxial type

2.10 Studies done on NORM

2.10.1 Measurements of NORM

NORM such as ^{238}U, ^{232}Th and ^{40}K are present in soil. The quantity present determines the degree of radiation exposure. The unstable radionuclides emit radiation and contribute significantly to natural background radiation. It is scientifically established that it is not desirable for human beings to live in an area with known high background radiation (mean annual effective dose equivalent greater than 1mSv). There have been many studies done to determine the concentrations of naturally occurring radionuclides in soil and the levels of the associated radiation exposures in different parts of the world.

Shanthi et al., (2010) used a gamma spectroscopy with NaI (Tl) detector to assess the concentration of natural radionuclides (^{226}Ra, ^{232}Th and ^{40}K) in the soil samples and 28 sample points were determined in southwest India (Kanyakumari district).The mean activity concentrations for ^{232}Th and ^{40}K are greater than the world average values reported by United Nations Scientific Committee on Effects of Atomic Radiation for areas of normal background radiation. Radiological indices were estimated for the radiation of the natural radioactivity of all soil samples. The estimated mean total absorbed dose in air from activity concentration of (^{226}Ra, ^{232}Th and ^{40}K) in high background radiation areas (HBRAs) is 200 ± 30 nGy/h and in low background radiation areas (LBRAs) is 29 ± 14 nGy/h. Annual outdoor effective dose was also calculated for HBRA and LBRA. Also the representative level index, which resulted from the natural radionuclides in the soil samples were also estimated and given.

Samreh, (2014) assessed the activity concentrations of ^{238}U, ^{232}Th, ^{40}K, in 50 soil samples of Bethlehem Province, West Bank, Palestine. Gamma-ray spectroscopy was used to perform the measurements using an HPGe detector. On one hand, the activity concentrations of natural radionuclides were found to vary from 12.7 to 122.3 Bq/kg with an average value of 41.4 Bq/kg for ^{238}U, from 2.0 to 32.2 Bq/kg with an average value of 19.5 Bq/kg for ^{232}Th, and from 12.0 to 183.8 Bq/kg with an average value of 113.3 Bq/kg for ^{40}K. On the other hand, the activity concentrations of the artificial ^{137}Cs radionuclide were found to be between 1.0 and 12.2 Bq/kg, with an average value of 2.8 Bq/kg. The variations of the assessed radiological hazard parameters indices Ra_{eq}, D_r, H_{ex}, and I_γ of natural radionuclides were found to be as follows: 16–148, 7–65, 0.04–0.4, and 0.11–1.00, respectively. The results were found to be comparable to or lower than similar reported data worldwide. Accordingly, the investigated soil zones can be considered to have normal levels of natural background radiation.

According to El-Gmal, (2007), sediment samples were collected along the Upper Egypt Nile River region starting from Aswan in the south to the north of El-Minia Governorate. Gamma radiation measurements were performed using high resolution HPGe detector with low background PC multichannel spectrometer by (El-Gmal, 2007). The results of the gamma measurements of the alluvial sediments found the presence of the natural long-lived radioisotopes ^{238}U, ^{232}Th and ^{40}K. The ranges of their activity concentrations were 3.83 ± 1.54 - 34.94 ± 4.01, 2.88 ± 1.07 - 30.10 ± 1.83 and 112.31±4.77 - 312.98±12.24 Bq/kg, respectively. The measured activity concentrations differ widely as their presence in the Nile River depends on the environmental situation such as the presence of dams, barrages and sediments type. Absorbed dose rates have been estimated for each location with range 12.71 ± 0.96.38.17 ± 1.55 nGy/h.

According to Murty, (2008), the concentrations of primordial radionuclides in soil samples were also carried out in Botswana these measurements were made by gamma spectrometry employing a HPGe detector. The activity of ^{226}Ra was found to vary in the range 6.1 – 97.4 Bq/kg with a mean value of 34.8 Bq/kg, while for ^{232}Th the values were in the range 7.4 – 110.0 Bq/kg with a mean value of 41.8 Bq/kg and ^{40}K varied between 33.5 Bq/kg and 1085.7 Bq/kg with a mean value of 432.7 Bq/kg in surface soils. The mean value of the annual effective dose was 0.07 mSv which is less than the recommended limit of 1.0 mSv.

Studies on the radionuclide distribution and the radiation level of the primordial radionuclides ^{238}U, ^{232}Th and ^{40}K in the soils of the coastal areas of Southern Nigeria have also been carried out (USNCEAR,2000). Soil samples were analysed for the radioactivity concentrations of these naturally occurring radionuclides using an HPGe detector. The mean activity of the radionuclides were found to be 283.28, 34.54 and 9.17 kBq/kg for ^{40}K, ^{226}Ra (a daughter of ^{238}U) and ^{232}Th. The mean absorbed dose rate in air due to these NORM was found to be 33.655 ± 3.409 nGy/h, which is far less than the world average value of 59 nGy/h reported for normal background areas (UNSCEAR, 2008).

There are numerous causes for these elevated exposure levels. The monazite sand deposits (which have high levels of thorium) that are found at Guarapari in Brazil, at Yangiang in China and in the states of Kerala and Madras in India are some of the causes for the high exposure levels. Volcanic soils such as in Mineas Gerais in Brazil, Niue Island in the Pacific and in some parts of Italy are also causes of high exposure levels. In the areas of Ramsar and Mahallat in Iran, the elevated levels of radioactivity are due to ^{226}Ra deposited in the area from waters flowing from hot springs (UNSCEAR, 2000).

At the international high-energy stereoscopic system (HESS) project in Namibia, concentrations of the natural radionuclides ^{238}U, ^{232}Th and ^{40}K in soil samples have been determined using an HPGe detector. The samples were found to vary from 10.8 ± 1.4 to 26.4 ± 1.8 Bq/kg for ^{238}U, for ^{232}Th, the values varied from 12.8 ± 2.4 – 52.3 ± 3.7 Bq/kg and from 212.1 ± 12.1– 683.8 ± 27.1 Bq/kg for ^{40}K. The corresponding annual effective dose is 0.06 ± 0.01 mSv, which is less than the limit of 1.0 mSv recommended for the public by the ICRP. The radioactivity in the four major towns in northern Namibia have also been (Oyedele, 2008), using gamma-ray spectrometry with the objective of providing baseline data on the radiation level in the region. The average concentrations of radionuclides in the towns vary from 7.5 ± 2.3 to 14.2 ± 3.3 Bq/kg for ^{238}U, 5.8 ± 2.6 to 24.9 ± 6.1 Bq/kg for ^{232}Th and 52.1 ± 28.7 to 380.1 ± 112.9 Bq/kg for ^{40}K. These concentrations were used to calculate the mean absorbed dose rate and the mean annual effective dose in the region. The low value of 21 ± 16 μSv obtained for the mean annual effective dose indicates that the region has normal background radiation (Oyedele, 2006).

In this study the samples in the study area will be analysed using direct gamma spectrometry and analysis through non-destructive methods for the measurement of gamma rays for soil samples using a Germanium semiconductor detector. Based on the reviews of the studies done, most of the studies used an HPGE detector which will be used in this case as well over other detectors. A Germanium detector will be utilised because it has a high energy resolution which is important for qualitative and quantitative analysis of complex gamma spectra from samples which have long-lived radionuclide content. The downside of NaI detectors is that a larger volume crystal is needed to maintain a high efficiency for higher energy gammas. In addition to its advantages is its crystal property of having a high atomic number in comparison to

Silicon detectors, which only needs a smaller volume to attenuate gamma photons and deposit their energy within the detector crystal. Which will give opportunity for a more efficient separation of close gamma lines and thus removing ambiguity in terms of qualitative analysis (Knoll, 2000). The activity concentrations of the naturally occurring radioactive materials in the samples were measured utilising a High Purity Germanium detector. The gamma spectrometry has an n-type of HPGe detector and its geometry; coaxial on end open, one end closed (end facing detector window). The gamma spectrometry system was connected to a computer operated multi-channel analyser. The detector was operating at relative frequency of 25% with an energy resolution of 2.0 keV at gamma ray energy of 1332.5 keV of ^{60}Co. The radionuclides were identified and using their gamma ray energies that they emitted and their quantitative analysis was done using gamma ray spectrum analysis e.g like GENIE 2000 software.

CHAPTER THREE

MATERIALS AND METHODS

In this chapter, the locations and sizes of the four study areas will be analysed and described, including their soil content, mineralogy, geological aspects and their demographics characteristics in detail. Additionally, the sampling collection method applied, sample preparation and the radio analytical methods used are described. Determination of activity concentrations of the natural radionuclides are also described in detail using mathematical models.

3.1 Description of the study area

The study area is located in the Erongo region, with four sub-study areas namely; Arandis, Walvis Bay, Swakopmund, and Henties Bay, along the western coastal stretch (between Walvis Bay – Henties Bay) of the Republic of Namibia as shown in Figure 3.2 The coastal area is found in the Erongo region of the country (Figure 3.1) which is well known for its mass fishing, sky diving, sand diving, camel riding, deep water harbour, large scale uranium mining, tourism, and many other activities. This region is named after the Erongo Mountain, known geological landmark in this part of the country.

The region has a geology that consists of uranium deposits and these deposits of the Namib desert come from 2 different types of mineralization, known as primary uranium mineralization in coloured granite marble, called alaskite which is commonly found in both the Rössing uranium mine and Husab uranium mine. The other type is the mineralization of uranium in calcrete which is found in the Langer Heinrich uranium mine. Secondary mineralization happens when the rocks are weathered. Alaskites which contain uranium have invaded sediments of the Khan and Rossing formations

for hundreds of millions of years. Alaskite content is called uraninite (UO_2) (Johnston, 1978; Jacob, 1974).

Betafite whose chemical formula is U(Nb, Ti)$_2O_6$(OH) is ubiquitous in the Khan formation, and calcrete contains content of secondary uranium deposits which formed the valleys of the palaeo of ancient rivers that drifted in a westerly direction about 20 to 80 million years ago. Calcrete mineral (carnonite) is the majority of the content in the uranium deposit and its chemical formula is $K_2(UO_2)_2(VO_4)_23H_2O$. The mineral is formed in the form of thin films of cracks and it coats the sediment grains in the fluvial streams. All the above mentioned types of mineralisations make it possible for open pit mining techniques. (NUA, 2019; Johnston, 1978).

The Erongo region is next to the Atlantic Ocean, and shares borders with the following regions; the north Kunene, the east Otjozondjupa , the south east Khomas and the south Hardap region as shown in Figure 3.1. There are a 6 (six) towns in the region namely; Usakos, Arandis, Henties Bay, Swakopmund, Walvis Bay and Wlotzkasbaken as shown in Figure 3.2.

Four of the above mentioned towns (Henties Bay, Walvis Bay, Swakopmund, and Arandis) are of interest to this study in this project. The main reason these towns are of interest is due to their close proximity to the uranium mines and how the mining activities can have an effect on the health of the residences in these town, hence a radiological assessment is needed.

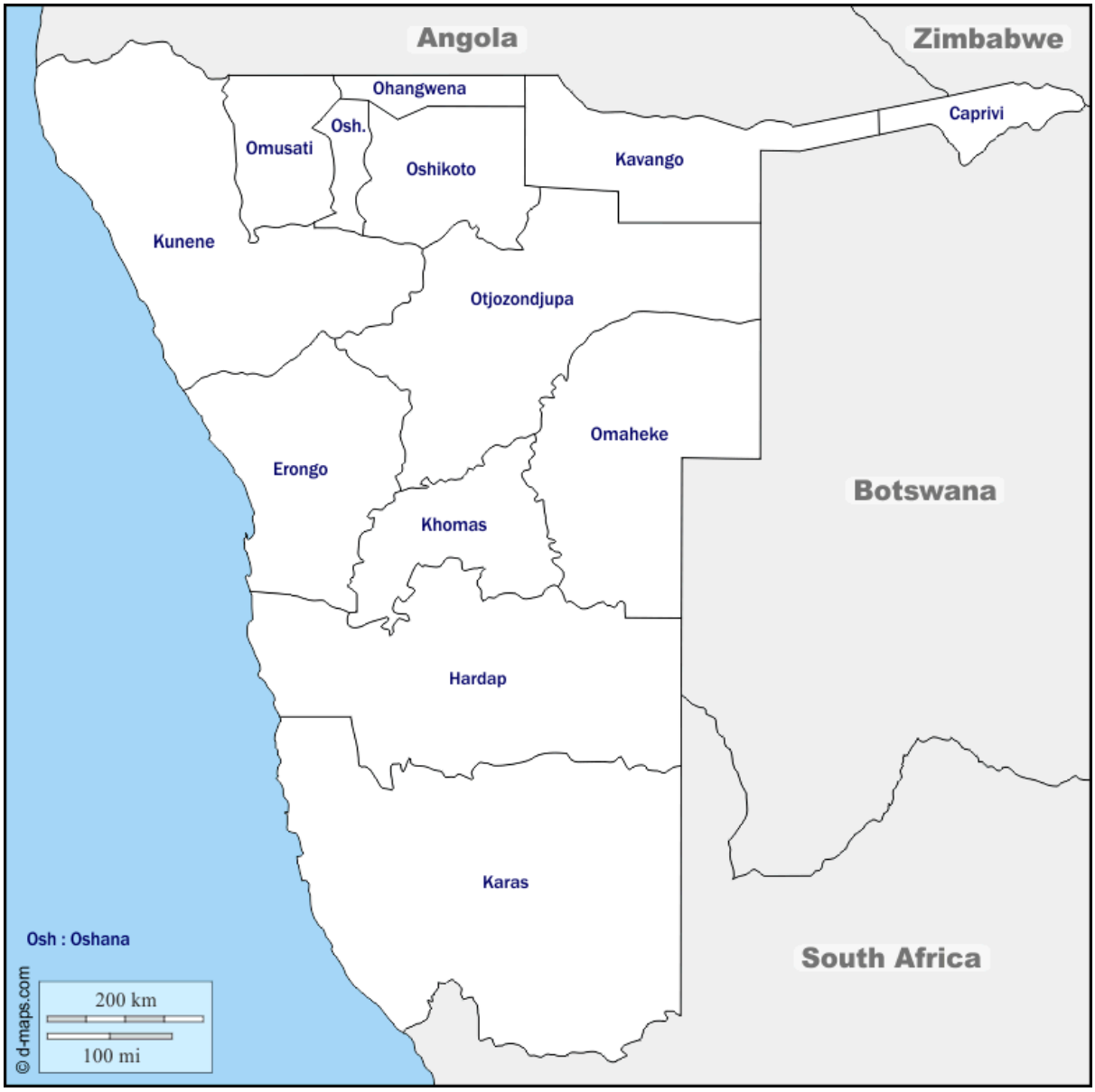

Figure 3.1: **Map showing the 12 regions of Namibia**

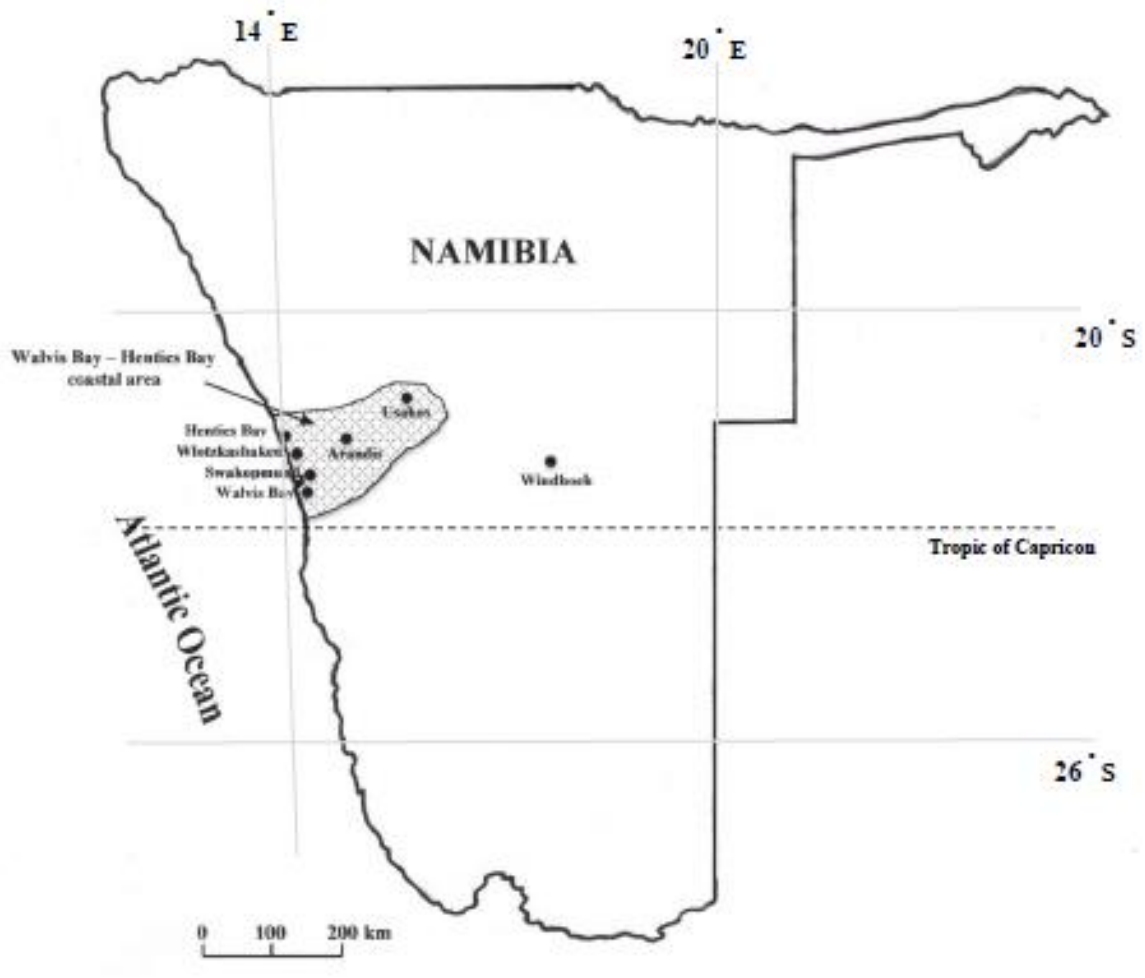

Figure 3.2: **Map showing the boundary lines which includes all the towns in the region of Erongo**

The largest town of the region is called Walvis Bay and it is centrally located at latitude 22° 57′ 22′′ S and longitude 14° 30′ 29′′ E. It is positioned in the northern direction of the Tropic of Capricorn and it lies in the Kuiseb River delta. A portion of Walvis Bay lies below sea level (about 1.2 meters) and is safeguarded by a dike against flooding. The towns harbour serves is the country's principal port. Walvis Bay has more than 85 000 people living in it alone and is the most occupied town in the coastal area. It is one of the most common holiday and tourist destinations both locally and internationally. The town is the home of sea vessels due to its nature of deep water harbours,

safeguarded by the Pelican Point sand spit. The towns harbour is the only one of its scale along the country's coastline. (Municipality of Walvisbay, 2019).

Swakopmund was founded in 1892, and it is the capital town of Erongo region, and it is located at latitude 22° 41′00′′ S and longitude 14° 32′ 00′′ E. The name of the town Swakopmund in German means "Mouth of the Swakop" as the town is situated at the mouth of the Swakop River that runs through Swakopmund. In the colonial era the administration in charge made an exodus from Windhoek to Swakopmund due to cooler conditions. The town has a capacity of more than 44 000 people (2011) and has land area of 193 km^2. It is one of the most popular holiday and tourist destinations in the country. Many people who work at the uranium mines live in Swakopmund (Green, 2019).

The town of Arandis is located at latitude 22° 25′00′′ S and longitude 14° 58′ 00′′ E. It is about 65 km north-east of Swakopmund and located about 14 km from the Rossing Uranium Mine, which has one of the highest scale open cast uranium mines on earth. Rossing mine currently produces about 7.7% of uranium yellow cake out of the total of the rest of the earth's uranium. Arandis was first established in 1976 and later on it further developed by the Rossing mine to for reasons of sheltering its workers and their families. The minewas in charge of the town from the 1970's till the early 1990's until the government took was handed the town in the form of a gift for having attained political independence. In 1995, the town of Arandis was recognised as a town and it has approximately 7 000 residents to date (Arandis Town Council, 2010).

The town of Henties Bay is located at latitude 22° 07′ 06′′ S and longitude 14° 16′ 57′′ E. It is located more than 80 km in the northern direction of Swakopmund and it's considered a holiday destination for many Namibians and tourists. The seal colony of

Cape Cross is about seventy (70) km to the northern direction. The name in English is literally “Henty's Bay”, in the Afrikaaners language (Afrikaans) it is “Hentiesbaai” in the German language it is “Hentiesbucht”. It is a coastal town in the Erongo Region, of Namibia and it has about 3,300 inhabitants and owns 121 km^2 of land. It is known for its intense fishing activities. In fact, Henties Bay is one of the foremost angling destinations for many anglers flocking to the coast throughout the year. The town is nestled between the Atlantic Ocean and the Namib Desert (Henties Bay Tourism Association, 2019).

3.2 Climate of the area

The Erongo region mostly lies in the Namib Desert, the coastal lowland lying western region of Namibia. The areas in question forms part of the central four features which have a dominant effect on the climate of the Namib Desert. The Benguela Upwelling System, the Great Escarpment, and the absence of topographical features on the wide plains. These pervasive features make the Namib one of the more climatically stable places in the world. This is re-enforced by the climatic characteristics in general of the western part of southern Africa, particularly in winter when high pressure systems dominate (Besler, 1994).

An anticyclonic, high-pressure cell runs stretches across the Atlantic Ocean drives west winds up to the escarpment that prevents air masses that come from the east from penetrating the Namib. As a coastal desert, the Namib is strongly influenced by the Benguela current, which is characterised by cool, upwelling water. The water cools the overlying atmosphere, resulting in a stable temperature inversion layer. This layer prevents moist air that originates from the Atlantic Ocean from rising and forming rain clouds, although they do form fog clouds at lower levels. The westerly winds and the

temperature inversion subside can rain clouds that have managed to cross this far across the continent from the Indian Ocean penetrate the desert to bring patchy thundershowers. During May to July (winter season), the Atlantics high-pressure cell's influence becomes weak and east winds (also called berg winds) reach the Namib, but during this time of year its atmosphere is extremely dry and it rarely bears any rain due to effect of the strong high pressure system on the continent (Taljaard, 1979).

The Central Namib is essentially a flat plain with a gradual 1% gradient in elevation from the coast up to the foot of the escarpment. Despite several river valleys, Inselbergs, and dunes, there are no major landscape features that would influence the macro-climate between the ocean and escarpment. This plain topography makes the Namib unique among deserts of the world (Taljaard, 1979). A steady gradients develop across the Namib from west to east affecting rainfall, fog, humidity, temperature, and wind patterns.

3.3 Rainfall

Rainfall is variable and it does not have a strict pattern over many years. Most rain falls in late summer between January to April (73%), while some rain falls in winter (22%), with the driest phase in early summer, September to December (5%). There is a strong west-east gradient of increasing rainfall across the Namib. The eastern zone gets some rain in most years (average 87 mm), while rain gets less towards the coast (average 15 mm) as well as more sporadic over space and time. Wet years of >100 mm (maximum 115 mm) are very rare coastward of the middle zone and have been recorded only in 1934, 1976 and 1978 (Walter, 1936; lancaster, 1984).

3.4 Geological study of the area

The onshore coastal geology of the Erongo region consists of old crystalline rocks that form the basement to the Permo-Triassic Karoo Sequence and young deposits of the Namib Dessert. The crystalline basement in the Erongo region is presented by rocks of the Abbabis Complex and the Nosib and Swakop Groups of the Damara Sequence that comprises mostly a thick pile of metasedimentary rocks as shown in Figure 3.3. Based on stratigraphy, structure and metamorphic grade, the Damara Orogen is subdivided into zones, that comprise of the Central Zone, the Northern Zone and the Southern Kaoko Zone. The Nosib Group is predominantly siliciclastic and is subdivided into the lower Etusis and upper Khan Formation, which generally have an interfingering relationship. The Etusis Formation consists predominantly of pinkish to buff-coloured, medium- to coarse grained meta-arkoses and micaceous to feldspathic quartzites and paragneisses. Conglomerate, mica schist, calc-silicate bearing quartzite and marble occur locally the Khan Formation is predominantly made up of massive to bedded, greyish-green-calc-silicate rocks. Layers of meta-conglomerate also occur locally. A unit of interbedded amphibolite and biotite schist is present near the Rössing Dome (Schreiber, 1996).

The Swakop Group is subdivided into the Rössing, Chuos, Arandis, Karibib and Kuiseb Formations. A bluish-grey dolomitic marble, minor quartzite, metaconglomerates, schist, gneiss and calc-silicate rocks are evident in the Rössing Formation. Bulk of the Chuos Formation consists of dark-grey to greenish-grey diamictites. Subordinate interbedded quartzite and marble occur within pebble-bearing schists. The Arandis Formation contains schists, calc-silicate rocks and marbles. A marble-dominated Karibib Formation is widely distributed and underlies large parts of the flat, poorly exposed coastal region. Also, the study area is home to many uranium mines such as

Rössing Uranium, Langer Heinrich Uranium, Reptile Uranium Mine, Tjrekkope, Uranium Inc. and Valencia Uranium Project (CZM, 1999).

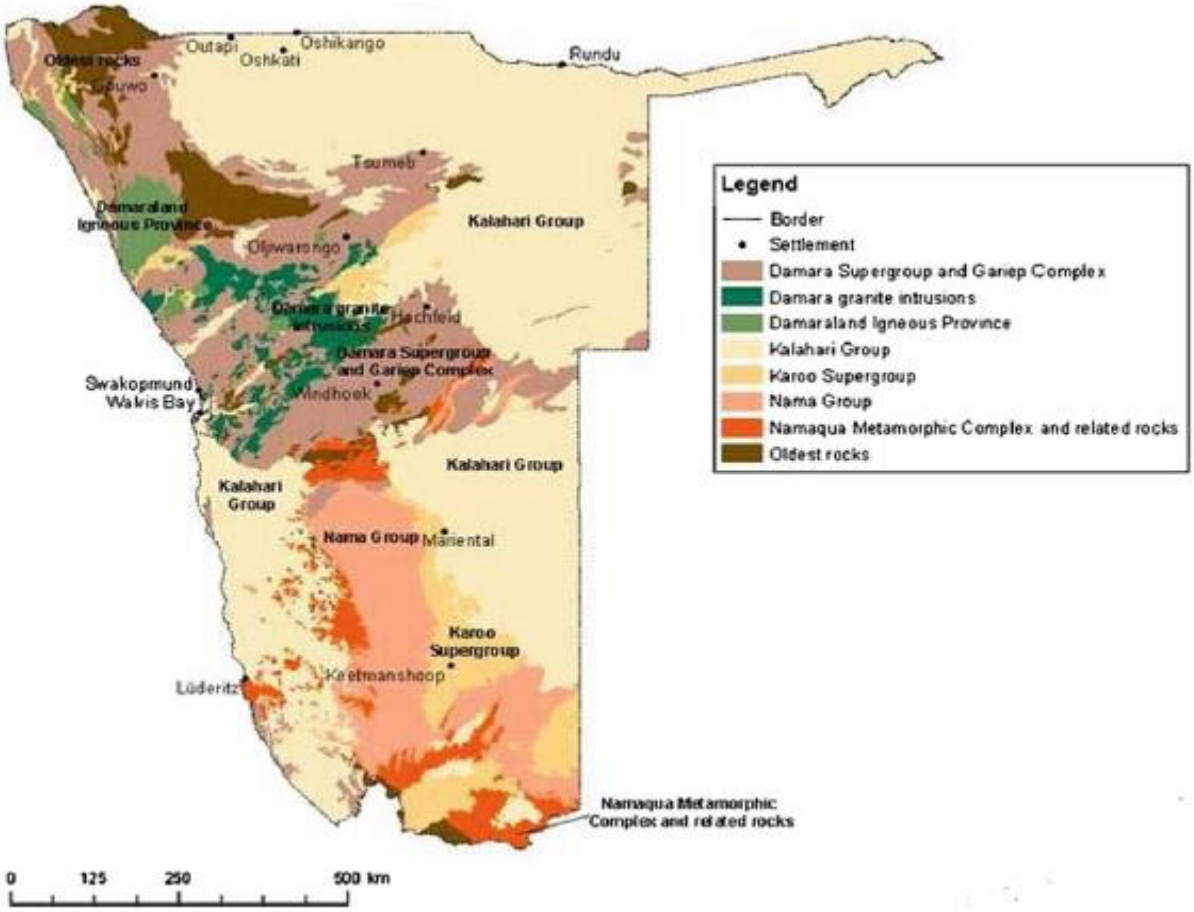

Figure 3.3: Geological map of Namibia

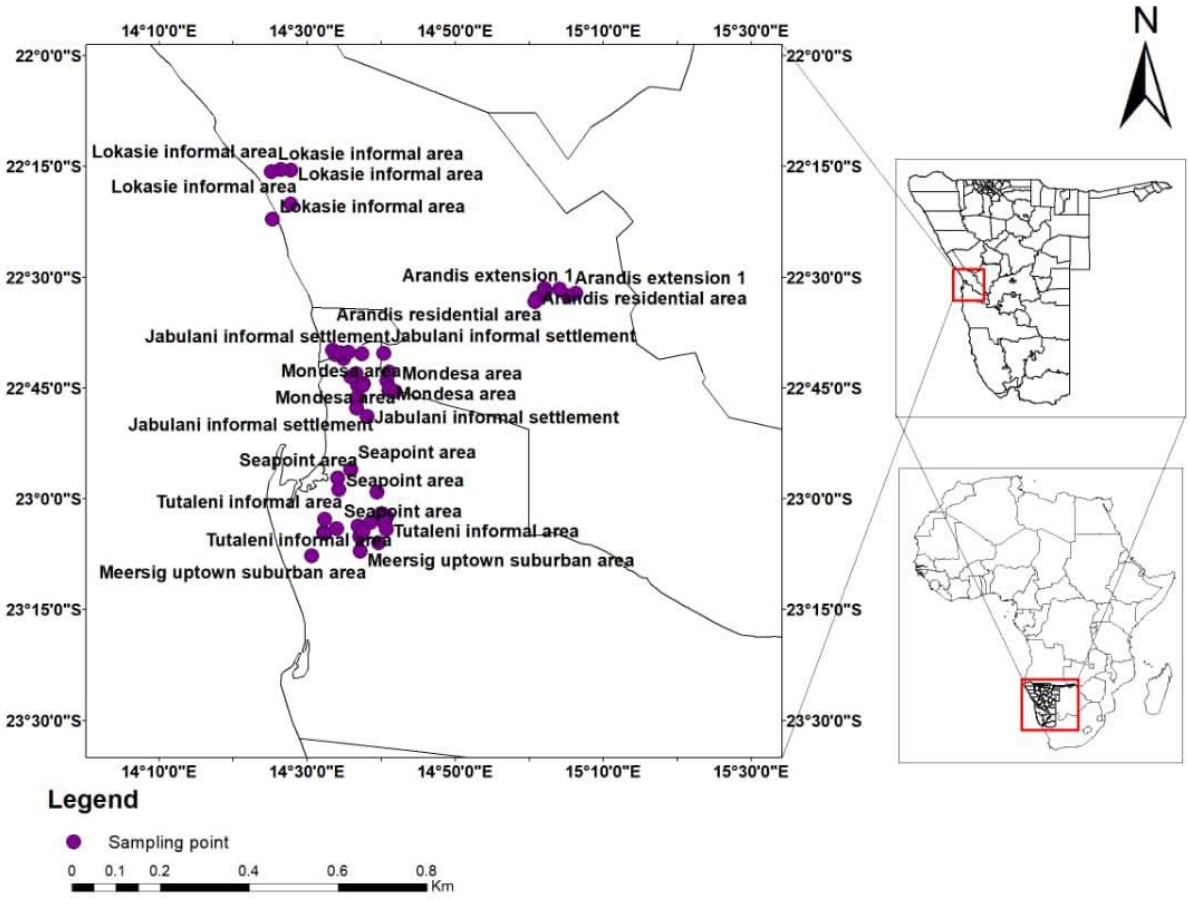

Figure 3.4: Layout of the Erongo region showing the sampling points

3.5 Sample Collection

3.5.1 Soil Sampling

Sampling was done in each of the four towns within the Erongo region; Walvis Bay, Arandis, Henties Bay and Swakopmund. The selection of the sampling points was based on the residential areas occupied by people who live in close proximity to the Uranium mines. A total of 80 soil samples were collected from the designated areas of the four towns, GPS coordinates of each sample was recorded as shown in Tables 3.1 to 3.4.

Random sampling is when any sample has the same probability of being included in the defined boundaries of the area of interest (IAEA, 2005). Soil sampling points were then chosen using the above mention method of utilising a random selection procedure. Each sampling point was chosen arbitrarily. The soil samples were each collected using a hand tool and were taken at a depth of 10 cm. At each sampling location, soil samples were collected and placed in labelled plastic bags. The samples were then transported to Windhoek, the capital city of Namibia to finally fly the samples to Ghana.

Table 3.1: Location of the soil sample area in Walvis Bay and their coordinates

Sample ID	Description of sampling location	Coordinates
M1	Meersig uptown suburban area	S22^{0}58’38.946 E14^{0}29’18.984
M2	Meersig uptown suburban area	S22^{0}58’40.101 E14^{0}29’20.174
M3	Meersig uptown suburban area	S22^{0}58’57.972 E14^{0}29’9.54
M4	Meersig uptown suburban area	S22^{0}58’54.438 E14^{0}28’55.002
M5	Meersig uptown suburban area	S22^{0}58’42.45 E14^{0}28’54.45
N1	Narraville residential area	S22^{0}56’45.912 E14^{0}32’29.274
N2	Narraville residential area	S22^{0}56’42.798 E14^{0}32’39.486
N3	Narraville residential area	S22^{0}56’50.418 E14^{0}32’33.114
N4	Narraville residential area	S22^{0}56’59.592 E14^{0}32’45.558
N5	Narraville residential area	S22^{0}57’12.288 E14^{0}32’44.28
S1	Seapoint area	S22^{0}56’16.14 E14^{0}31’19.512
S2	Seapoint area	S22^{0}56’10.482 E14^{0}31’16.65
S3	Seapoint area	S22^{0}56’6.828 E14^{0}31’18.486
S4	Seapoint area	S22^{0}56’0.18 E14^{0}31’29.238
S5	Seapoint area	S22^{0}55’54.048 E14^{0}31’17.67
T1	Tutaleni informal area	S22^{0}55’41.604 E14^{0}31’54.168
T2	Tutaleni informal area	S22^{0}55’44.448 E14^{0}31’58.494
T3	Tutaleni informal area	S22^{0}55’46.626 E14^{0}32’1.902
T4	Tutaleni informal area	S22^{0}55’49.998 E14^{0}31’56.748
T5	Tutaleni informal area	S22^{0}55’54.642 E14^{0}31’58.008

Table 3.2: Location of the soil sample area in Swakopmund and their coordinates

Sample ID	Description of sampling location	Coordinates
TM1	Tamariskia urban area	S22^{0}39'246 E14^{0}32'27.294
TM2	Tamariskia urban area	S22^{0}39'33.906 E14^{0}32'28.938
TM3	Tamariskia urban area	S22^{0}39'32.100 E14^{0}32'33.222
TM4	Tamariskia urban area	S22^{0}39'33.876 E14^{0}32'3220.37
TM5	Tamariskia urban area	S22^{0}39'26.664 E14^{0}32'23.34
MD1	Mondesa area	S22^{0}39'29.85 E14^{0}32'52.5
MD2	Mondesa area	S22^{0}39'22.932 E14^{0}32'54.408
MD3	Mondesa area	S22^{0}39'37.734 E14^{0}32'54.24
MD4	Mondesa area	S22^{0}39'35.928 E14^{0}32'54.69
MD5	Mondesa area	S22^{0}39'38.37 E14^{0}32'58.86
TW1	Tulinawa informal settlement	S22^{0}39'11.844 E14^{0}33'11.13
TW2	Tulinawa informal settlement	S22^{0}39'8.37 E14^{0}33'4.398
TW3	Tulinawa informal settlement	S22^{0}39'4.968 E14^{0}33'2.532
TW4	Tulinawa informal settlement	S22^{0}39'6.948 E14^{0}33'8.544
TW5	Tulinawa informal settlement	S22^{0}39'6.876 E14^{0}33'15.102
JB1	Jabulani informal settlement	S22^{0}39'43.806 E14^{0}32'28.116
JB2	Jabulani informal settlement	S22^{0}39'52.152 E14^{0}32'27.714
JB3	Jabulani informal settlement	S22^{0}39'58.692 E14^{0}32'36.528
JB4	Jabulani informal settlement	S22^{0}40'2.028 E14^{0}32'324.03
JB5	Jabulani informal settlement	S22^{0}40'1.47 E14^{0}32'50.07

Table 3.3: Location of the soil sample area in Arandis and their coordinates

Sample ID	Description of sampling location	Coordinates
AR1	Arandis residential areas	S22^{0}25'9.216 E14^{0}58'27.768
AR2	Arandis residential areas	S22^{0}25'27.276 E14^{0}58'27.276
AR3	Arandis residential areas	S22^{0}25'11.13 E14^{0}58'29.31
AR4	Arandis residential areas	S22^{0}25'10.56 E14^{0}58'21.576
AR5	Arandis residential areas	S22^{0}25'11.124 E14^{0}58'21.63
AR6	Arandis police station	S22^{0}25'10.752 E14^{0}58'37.422
AR7	Arandis police station	S22^{0}25'9.132 E14^{0}58'40.98
AR8	Arandis park	S22^{0}25'9.238 E14^{0}58'43.302
AR9	Arandis park	S22^{0}25'2.772 E14^{0}58'41.664
AR10	Arandis park	S22^{0}24'57.905 E14^{0}58'40.906
AR11	Arandis extension 1	S22^{0}24'55.044 E14^{0}58'46.074
AR12	Arandis extension 1	S22^{0}24'57.45 E14^{0}58'50.616
AR13	Arandis extension 1	S22^{0}24'58.26 E14^{0}58'53.148
AR14	Arandis extension 1	S22^{0}24'48.582 E14^{0}58'49.434
AR15	Arandis extension 1	S22^{0}24'50.694 E14^{0}58'43.074
AR16	Arandis residential area	S22^{0}24'45.156 E14^{0}58'36.372
AR17	Arandis residential area	S22^{0}24'45.12 E14^{0}58'24.246
AR18	Arandis residential area	S22^{0}24'48.33 E14^{0}58'24.648
AR19	Arandis residential area	S22^{0}24'52.674 E14^{0}58'17.904
AR20	Arandis residential area	S22^{0}24'55.542 E14^{0}58'16.608

Table 3.4: Location of the soil sample area in Henties Bay and their coordinates

Sample ID	Description of sampling location	Coordinates
HB1	Suburban area	S22^{0}79'0.672 E14^{0}17'4.98
HB2	Suburban area	S22^{0}71'4.094 E14^{0}17'1.938
HB3	Suburban area	S22^{0}72'1.534 E14^{0}17'0.976
HB4	Suburban area	S22^{0}71'4.484 E14^{0}16'53.118
HB5	Suburban area	S22^{0}71'5.396 E14^{0}16'45.744
HB6	Suburban area	S22^{0}73'2.688 E14^{0}17'2.868
HB7	Suburban area	S22^{0}73'9.426 E14^{0}17'10.638
HB8	Suburban area	S22^{0}74'1.652 E14^{0}17'2.41
HB9	Suburban area	S22^{0}75'1.252 E14^{0}17'23.532
HB10	Suburban area	S22^{0}75'8.992 E14^{0}17'28.38
HB11	Lokasie informal area	S22^{0}75'81.056E14^{0}17'41.958
HB12	Lokasie informal area	S22^{0}75'3.646 E14^{0}17'46.224
HB13	Lokasie informal area	S22^{0}75'6.37 E14^{0}17'54.414
HB14	Lokasie informal area	S22^{0}75'0.97 E14^{0}17'45.804
HB15	Lokasie informal area	S22^{0}74'7.256 E14^{0}17'40.386
HB16	Lokasie informal area	S22^{0}72'.472 E14^{0}17'13.632
HB17	Lokasie informal area	S22^{0}70'.198 E14^{0}17'28.356
HB18	Lokasie informal area	S22^{0}65'2.518 E14^{0}17'28.506
HB19	Lokasie informal area	S22^{0}64'8.072 E14^{0}17'20.538
HB20	Lokasie informal area	S22^{0}65'3.79 E14^{0}17'12.618

Figure 3.5: S**oil samples heated in an oven**

All the soil samples weight were recorded and were placed in an oven that is thermostatically controlled and each individual sample was placed in an open tray and placed in the oven where they were heated at a temperature of 105 °C for 3 hours to remove any water molecules and after heating the sample weight is taken and the samples are heated again and weight is recorded this is done until the mass remains constant as shown in Figure 3.5.

Figure 3.6: Sample preparations at the gamma laboratory at GAEC

The Figure above shows each sample being sieved with a mesh size pore and transferring to polythene cylindrical containers, after having undergone grinding using a ball mill.

3.5.2 Sample preparation for direct gamma spectrometry

A total number of twenty eight composite (28) soil samples were made from the 80 samples collected from the 4 towns for analysis. They comprised of 7 soil samples each from towns Walvis Bay, Arandis, Henties Bay and Swakopmund within the Erongo region of Namibia. In the laboratory, each of the soil samples was air-dried on trays for 7 days and then oven-dried at a temperature of 105^{o}C for between 3 and 4 h and. The

samples were then grinded into fine homogenous powder using a ball mill and sieved through a 500µm mesh size pore and transferred into polyethylene cylindrical containers as shown in Figure 3.6. These cylindrical containers, containing the samples, were completely sealed and stored for 1 month to allow the short-lived daughters of ^{238}U and ^{232}Th decay series to attain equilibrium with their long-lived parent radionuclides (ASTM, 1983; 1986). The sealed samples were weighed and each counted using a high purity germanium detector.

3.5.3 Instrumentation and calibration

Direct gamma spectrometry analysis without pre-treatment (non-destructive) was used for the measurement of gamma rays from the soil samples using a High Purity Germanium detector (HPGE). The gamma spectrometry system consists of HPGE detector coupled to a computer based multi-channel analyser (MCA). The relative efficiency of the detector is 40 % with energy resolution of 2.0 keV at gamma ray energy of 1332 keV of ^{60}Co. The identification of individual radionuclides was performed using their characteristic gamma-ray energies and the quantitative analysis of radionuclides was performed using the Genie 2000 gamma acquisition and analysis software. The detector is housed in a 100 mm passive shielding of lead lined with copper, cadmium and plexiglass (3mm each) to reduce the background radiation. The detector is cooled in liquid nitrogen at a temperature of -196 °C (77 k). In order to determine the background distribution in the environment around the detector (quality control), ten (10) empty Marinelli beakers were thoroughly cleaned using nitric acid and counted for 36000 s in the same geometry as the samples. The background spectra were used to correct the net peak area of gamma rays of measured isotopes. The background spectra were also used to determine the minimum detectable activities of radionuclides at each photo peak for the detector.

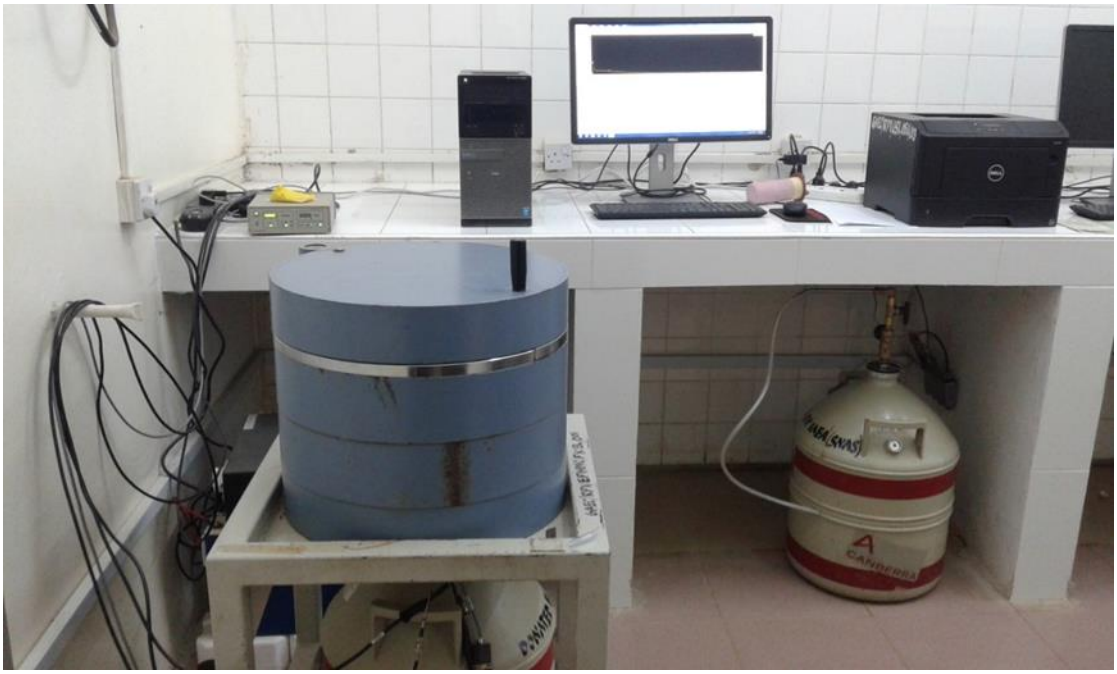

Figure 3.7: Gamma spectrometry system with Germanium coaxial detector

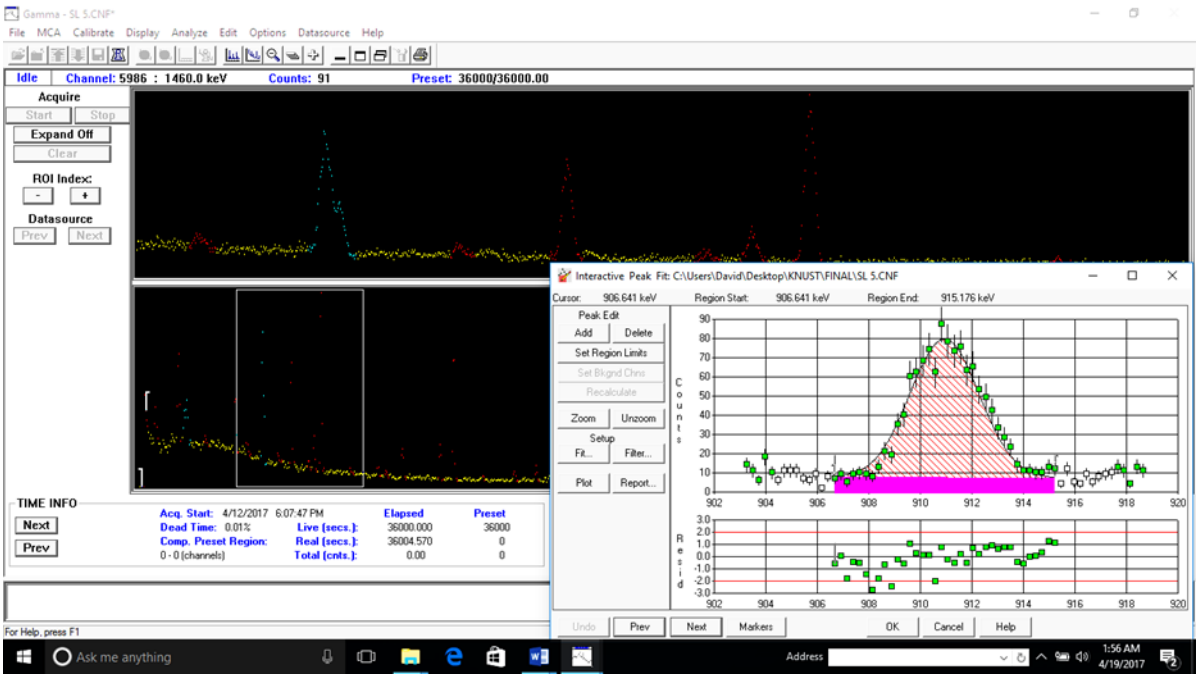

Plate 3.8: Genie 2000 gamma acquisition and analysis software interface

3.5.4 Calibration of the gamma ray spectrometry

Calibration is the process of determining an instruments response relative to a set of already known radiation values (from a standard radiation source) which already includes the range of that instrument, and changing the settings of that instrument to render a correct and appropriate response (Martin, 2006). The most relevant parameters in gamma ray spectrometry is energy and efficiency calibrations, and henceforth forms part of this analytical technique for both analysis (qualitative and quantitative) of radionuclides in the samples being analysed.

3.5.5 Energy Calibration

With energy calibration, it is possible to identify radionuclides in a gamma spectrum. The detector energy calibration (the aim is to find the channel number of multichannel analyser in relation to gamma-ray energy) was made by counting standard radionuclides with known activities with defined energies within the energy range between 60 – 2000 KeV (IAEA, Measurement of Radionuclides in Food and Environment , 1989). In simpler terms the identification of the radionuclides of interest found by matching the energies of the principal gamma rays found in the spectrum to the energies of the gamma rays emitted by the radionuclides in the standard reference sample. The calibration standard of the gamma detector was counted for 10 hours (36 000 s) to produce well defined photo peaks. The channel number corresponding to the centroid of each full energy event on the MCA was recorded and plotted to obtain a calibration curve. The linear curve found from data points shows that the system is operating efficiently (IAEA, 1989). The following is the formula relating the energy and the channel number as:

$$E = A_0 + A_1CN \quad (1)$$

Where E is the energy, CN is the channel number for a given radionuclide. A_0 and A_1 are calibration constant for a given geometry. The graph of the energy against channel number is in Chapter 4, Figure 1.

3.5.6 Efficiency calibration

The IAEA reference materials IAEA-RGU-1(U-ore), IAEA-RGTh-1 (Th-ore) and IAEA-RGK-1 (K-ore) with densities (1.33 ± 0.03) similar to the sludge and oil based mud samples to be measured were prepared into same cylindrical containers as that of samples for the efficiency calibration of the gamma system.

The efficiency of the detector refers to the ratio of the actual events registered by the detector to the total number of events emitted by the source of radiation (IAEA, 1989). An accurate efficiency calibration of the system is necessary to quantify radionuclides present in the sample. The standard was counted on the detector for 10 hours. The net counts for each of the full energy events in the spectrum was determined and their corresponding energies used in the determination of the efficiencies. The standard was in a sealed polythene container of the same geometry as the soil samples. Using equation (1) and known concentrations from the certificate, counting efficiency for each photopeak was calculated and used to estimate the efficiencies for photo peaks of natural radionuclides measured and quantified in the soil samples. The efficiency calibration was performed by acquiring a spectrum of the standard until the count rate of the total is calculated with statistical uncertainty of less than 5 % at confidence level of 95%. Performing an efficiency calibration on the detector improves the sensitivity of the instrument and gives a strong sense of reliability for the results obtained.

The expression used to determine the efficiencies is given as follows (IAEA, 1989)

$$\eta(E) = \frac{N_T - N_B}{P_E A_{STD} T_{STD}} \quad (3.1)$$

Where;

η (E) - is the efficiency of the detector,

N_T - is the total counts under a photopeak,

N_B - is termed as the background count

P_E – is the gamma emission probability for energy E,

A_{STD} is the activity (Bq) of the radionuclide in the calibration standard at the time of calibration,

T_{STD} is the counting time of the standard

3.5.7 Calculation of activity concentrations

To obtain the specific activity concentration of natural radionuclides in the soil samples, the following expression was used:

$$A_{SP} = \frac{N.e^{\lambda Td}}{\eta P.M.Tc} \quad (3.4)$$

Where;

A_{sp} is the specific activity in Bq/kg,

N is the background corrected net peak area,

η (E) is the absolute detection efficiency,

P is the gamma ray yield,

Tc is the counting time of the sample,

λ is the decay constant of individual radionuclides,

Td is the time between sampling and time of counting.

Some of the errors identified for the quantification of the uncertainty in the determination of the specific activity concentrations include the following: Net peak area, detection efficiency and sample mass.

The overall uncertainty in the determination of the activity concentrations was obtained using equation:

$$dA_{sp} = A_{sp} * [(\frac{dN}{N})^2 + (\frac{d\eta}{\eta})^2 + (\frac{dM}{M})^2]^{\frac{1}{2}} \quad (3.5)$$

dN is determined from the uncertainty in the integration of the peak area of each full energy event.

dM is the standard uncertainty on the weighing balance used to weigh the samples which was noted to be 0.0001kg.

dη is the uncertainty in the efficiency calibration of the counting system.

3.5.8 Calculation of external absorbed dose rate and annual effective dose

The external gamma dose rate from the soil samples was determined from the activity concentrations of the relevant radionuclides from equation (3.6) (UNSCEAR, 2008).

$$D\ (nGy/h) = 0.462A_U + 0.0417A_K + 0.604A_{Th} \quad (3.6)$$

Where;

A_U, A_K, and A_{Th} are the activity concentrations of ^{238}U, ^{232}Th and ^{40}K respectively. Table 3.5 shows the dose conversion factors of A_U, A_K, and A_{Th}

Table 3.5: Activity to dose rate conversion factors (UNSCEAR, 2000)

Radionuclide	**Dose Coefficient (nGy/h/ Bq/kg)**
A_U	0.462
A_K	0.0417
A_{Th}	0.604

To estimate the annual external effective dose, we must take into account; (1) The conversion coefficient from absorbed dose in air to effective dose (D), (2) The outdoor occupancy factor of 0.2 which assumes an average duration of time someone is outdoors (4.8 hours/day) and, (3) The annual estimated average effective dose equivalent received by a member is calculated using a conversion factor (F) of 0.7 Sv/Gy (UNSCEAR, 2008).

The annual effective dose equivalent are determined as follows;

$$H_E = D \times T \times F \qquad (3.7)$$

H_E (mSv/a)= Absorbed Dose rate(nGyh-1)× 8760h×0.5 × 0.7 Sv/Gy where D is the calculated dose rate in (Gy/h), T is the outdoor occupancy time (24 h × 365days × 0.2 = 1752 h/y) and F is the conversion factor (0.7 Sv/Gy). The results obtained were used to calculate the average effective dose equivalent rate for each geographical area for each of the four towns. Tables (A and B) shows the range (in parenthesis) of the effective dose rate for the samples collected in each area and the average effective dose rate in each area.

3.5.9 Determination of external (H_{ex}) hazard index

The main aim behind external hazard indices is to keep external annual gamma radiation dose from building materials to less than 1.5 mGy/yr or $H_{ex} \leq$ unity.

In this current study, H_{ex} was calculated using equation (3.8), as formulated by (Mathew, 1985).

$$H_{ex} = \frac{A_{Ra}}{370} + \frac{A_{Th}}{259} + \frac{A_K}{4810} \tag{3.8}$$

Where; A_{Ra}, A_{Th} and A_K represent the measured activity concentrations in Bq/kg for ^{238}U, ^{232}Th and ^{40}K, respectively. , the value of H_{ex} must be less than unity.

3.5.10 Determination of internal hazard index

The calculation of internal hazard index was based on the fact that radon and its daughters are also hazardous to the respiratory organs (Mathew, 1985). The H_{in} is calculated using equation (3.9).

$$H_{in} = \frac{A_{Th}}{259\ (Bq/kg)} + \frac{A_{Ra}}{180\ (Bq/kg)} + \frac{A_k}{4810\ (Bq/kg)} \tag{3.9}$$

Where; A_{Ra}, A_{Th} and A_K represent the measured activity concentrations in Bq/kg for ^{238}U, ^{232}Th and ^{40}K, respectively. , the value of H_{in} must be less than unity. The values; 259 Bq/kg, 180 Bq/kg, and 4810 Bq/kg are assumed to produce the same gamma dose rate.

3.5.11 Determination of Radium equivalent activity

The radionuclides of ^{238}U, ^{232}Th and ^{40}K are in-homogeneously distributed in soil. This is due to disequilibrium between ^{238}U and its daughters. The radionuclide concentrations have been defined in terms of radium equivalent activity (Raeq) in

Bq/kg. The radium equivalent activity is used to assess the hazards associated with materials that contain ^{238}U, ^{232}Th and ^{40}K in Bq/kg as defined by (Mathew, 1985). Which is determined by assuming that 370 Bq/kg of ^{226}Ra or 259 Bq/kg of ^{228}Ra or 4810 Bq/kg of ^{40}K produce the same gamma dose rate (Nasim, 2012). The Ra_{eq} of a sample in Bq/kg can be achieved using the following relation:

$$Ra_{eq} = A_U + 1.43A_{Th} + 0.077A_K \quad (4.0)$$

Where; A_U, $1.43A_{Th}$, $0.077A_K$ are activity concentrations in Bq/kg, respectively

3.5.12 Determination of Excess lifetime cancer risk

According to (UNSCEAR, 2008), to determine the lifetime cancer risk as described by the following equation (4.0)

$$LCR = H_E \times DL \times RF \quad (4.1)$$

Where;

H_E, is the total annual effective dose obtained from equation (3.7)

DL is the expected life of a person to be in existence (51.62 years)

RF is the risk factor, fatal cancer risk/ Serviet

According to the (IRCP, 60 report) 0.05 is designated for the public.

CHAPTER FOUR

RESULTS AND DISCUSSIONS

The ultimate objective of this study is to determine the radiological doses of the members of the public living in the four areas.The research focus is on the determination of the levels and the distribution of the naturally ocurring radionuclides of ^{266}Ra/ ^{228}Ra decay series as well as ^{40}K within the major four towns of the Erongo region. Therefore this section will deal with the results, analysis and discussions of the four towns from the 28 represenatives samples from the four towns (that were counted). In addition the mean activity concentrations of the four towns will be compared to the internationally accepted reference values and published work on previous studies from other countries. This section will also include the results of the absorbed dose rates, annual effective dose equivalent and the radiological hazard indices along with their graphs as presented in the following subsections. It will also include the estimation of the lifetime cancer risks for younger and to middle aged people who live in each of the communities under this study. This work is in the domain of existing exposure situation for which reference levels are applicable. This will enable this study to ascertain the radioactivity levels that exist in soil.

4.1 Quality control and validation of gamma spectrometry technique

Prior to the analysis, the gamma detector was calibrated for energy and efficiency and results are presented in Figures 4.1 and 4.2.

Analytical quality control procedures which were carried out for the gamma spectrometry systems was necessary in order to authenticate the quality and reliability

of measurements.

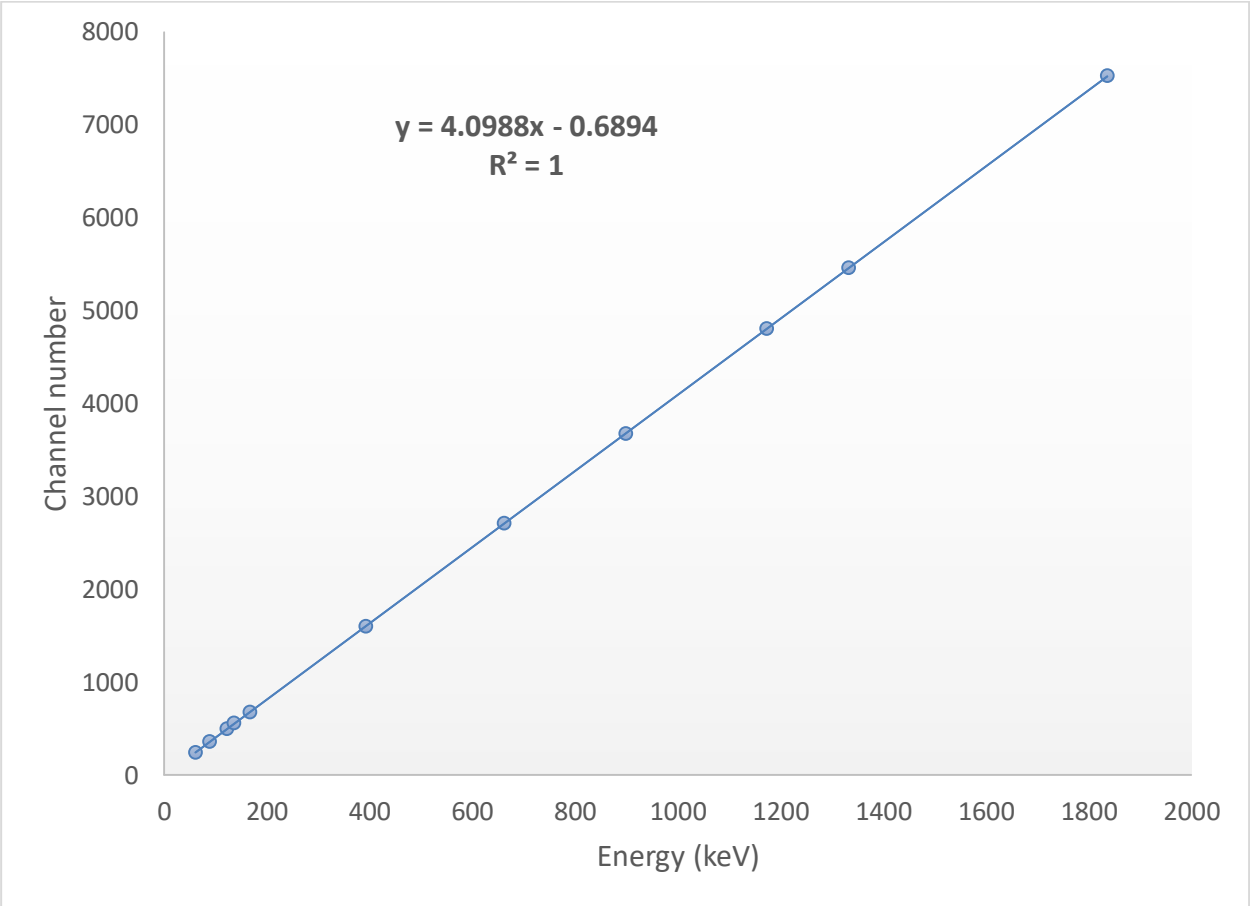

Figure 4.1: Energy calibration curve for gamma spectrometry system

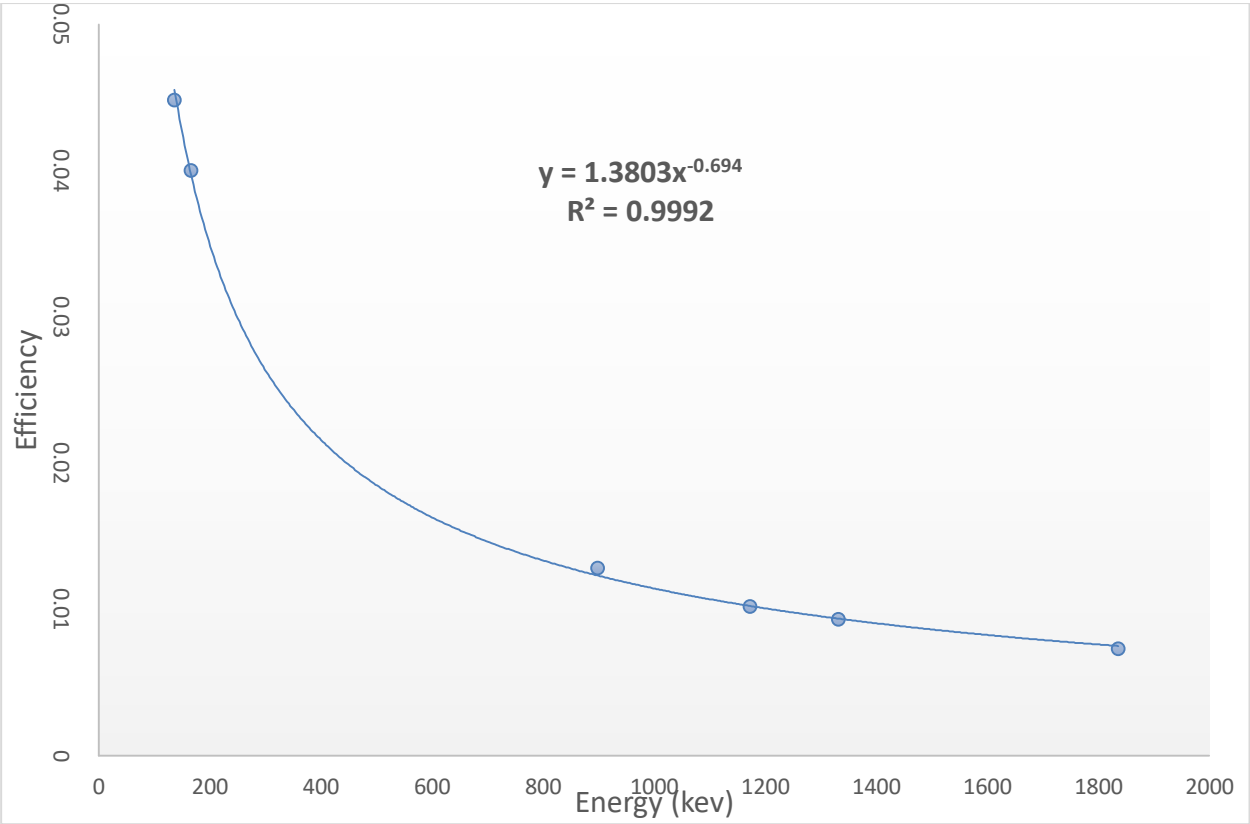

Figure 4.2: Efficiency calibration curve for waste water samples in 1L marinelli beaker geometry of HPGe detector

The IAEA reference materials IAEA-RGU-1(U-ore), IAEA-RGTh-1 (Th-ore) and IAEA-RGK-1 (K-ore) with mean densities (1.33 ± 0.03 g/cm^3) similar to the mean densities of solid matrix samples to be measured were prepared 0.5L Marinelli beakers of the same type as that of solid matrix samples were used to estimate the efficiencies for photo peaks of natural radionuclides measured and quantified in the samples.

For liquid matrix samples, a multi-gamma certified cocktail standard (^{241}Am, ^{109}Cd, ^{57}Co, ^{139}Ce, ^{113}Sn, ^{85}Sr, ^{137}Cs, ^{60}Co and ^{88}Y,) uniformly distributed in solid water with volume and density of 1000cm^3 and 0.98 gcm^{-3} respectively was used for efficiency calibration of the gamma system. The standard radionuclides provided by Deutscher Kalibriedienst was used for the energy and efficiency calibrations are shown in the

Appendix 1. Summing-up coincidence corrections were made for certified gamma cocktail in 1L marinelli geometry.

The accuracy and precision of analytical procedures used in this study for the gamma spectrometric technique was also validated with the analysis of IAEA SRMs (IAEA381 and IAEA375) under the same experimental conditions as the samples. The sensitivity of the method used in this work was in good agreement with the reference values for IAEA SRMs as shown in Tables 4.1

Table 4.1: Analysis of reference material via gamma spectrometry

Sample	**Matrix**	**Density ($g.cm^{-3}$)**	**Radionuclide**	**Reference Value ($Bq.kg^{-1}$)**	**Measured value ($Bq.kg^{-1}$)**
IAEA381	liquid	1.02 ± 0.02	^{137}Cs	0.49 ± 0.01	0.53 ± 0.05
			^{40}K	11.4 ± 0.9	13.2 ± 1.6
IAEA375	Solid	1.69 ± 0.17	^{134}Cs	463 ± 9	455 ± 28
			^{137}Cs	5280 ± 106	5182 ± 108
			^{40}K	424 ± 8	412 ± 13
			$^{226}Ra(^{214}Pb)$	20 ± 2	19 ± 3

4.2 Results of soil samples for Arandis

Table 4.2: Results of activity concentrations of ^{226}Ra, ^{228}Ra, and ^{40}K, absorbed dose rates, annual dose equivalent, external hazard indices, internal hazard indices and radium equivalent activities for the town of Arandis

Sample ID	Radionuclide concentration (Bq/kg)			Absorbed dose rate	Annual dose Equivalent	Hex	Hin	Raeq
Radionuclide	Ra226	Ra228	K40	(nGy/h)	(mSv)	(Bq/kg)	(Bq/kg)	(Bq/kg)
AR1	52.45±1.22	174.59±6.6	652.4±26.1	163.18	0.2	0.95	1.10	352.35
AR2	76.49±3.86	282.59±2.41	724.37±28.9	246.17	0.3	1.45	1.67	535.86
AR3	65.48±2.15	234.30±6.47	684.48±27.4	208.75	0.26	1.22	1.41	453.23
AR4	58.17±3.11	287.05±9.81	641.85±25.7	237.35	0.29	1.4	1.57	518.07
AR5	55.60±1.19	213.42±11.09	607.59±24.3	187.61	0.23	1.1	1.26	407.58
AR6	46.73±1.18	83.29±0.70	489.42±19.6	95.3	0.12	0.55	0.68	203.52
AR7	53.01±4.15	92.61±3.33	519.66±21.0	105.43	0.13	0.61	0.76	225.46
Mean	58.28±9.88	195.36±83.0	617.1±85.4	177.69	0.22	1.04	1.21	385.15
Range (Min - Max)	46.73 76.49	83.29 287.05	489.42 724.37	95.3 246.17	0.12 0.3	0.55 1.45	0.68 1.67	203.52 535.86

Twenty (20) samples were collected in four (4) different residential areas of the town of Arandis with their coordinates recorded as shown in Chapter 3: Table 3.3 and Figure 3.4 respectively. Table 4.6 contains the results from the seven (7) composite or representative samples from the initial 20 samples and these 7 samples that were counted by the HPGe detector. This was done for each of the four towns.

The three essential primordial radionuclides being analysed in the areas of interest were ^{226}Ra, ^{228}Ra, and ^{40}K and the activity concentrations and absorbed dose rates, annual dose equivalent, and the radiological hazard indices have been calculated and summarised as shown in Tables; (4.5, 4.6, 4.7, 4.8, and 4.9). The average activity concentration for the town of Arandis for ^{226}Ra was 58.28 Bq/kg with a maximum of 76.49 Bq/kg and a minimum of 46.73 Bq/kg, for ^{228}Ra (^{232}Th). The average concentration was 195.36 Bq/kg with a maximum value of 287.05 Bq/kg and a minimum value of 83.29 Bq/kg, ^{40}K was the radionuclide with the highest activity concentration of 617 Bq/kg with a maximum value of 724.37 Bq/kg and minimum value of 489.42 Bq/kg. The mean activity concentration for ^{40}K had the highest mean activity concentration than both of ^{226}Ra and ^{228}Ra. This can be expected due to the fact that potassium (^{40}K) is usually the most abundant radionuclide in the soil all over the world. The mean activity concentrations of ^{226}Ra, ^{228}Ra, and ^{40}K from all the samples obtained from the towns are all higher than the world wide average activity concentrations whose world average activity concentrations due to ^{238}U, ^{232}Th, and ^{40}K in soil samples are 33, 45 and 412 Bq/kg respectively (UNSCEAR, 2008). This can be attributed to the underlying geology within the close proximity to the one of the world's largest scale of open pit uranium mining (Rössing Uranium Mine).

The absorbed dose rate for each of the homogenised samples in the town ranged from 95.3 to 246.37 nGy/h with a mean of 177.69 nGy/h. The mean value of the absorbed dose rate for the town was more than 3 times higher than the world's average value (58 nGy/h) (UNSCEAR, 2010)

The samples from the town was estimated to have an average annual dose equivalent of 0.22 mSv in the range of 0.12 to 0.30 mSv. The average annual dose equivalent was less than the reference level band of 1 - 10 mSv recommended by the public by the IRCP 60 (UNSCEAR, 2008).

The values of the external radiological hazard indices of Arandis was estimated to have an average of 1.04 within the range of 0.55 to 1.45, the average value was higher than unity. The external hazard indices represents external exposure to humans and could thus pose a risk to the health of the people living in this small town for a long period of time, the mean value being higher than the value of unity is attributed to the high activity concentrations of ^{226}Ra, ^{226}Ra, and ^{40}K of the soil samples. The high concentrations of radionuclides in some of the samples collected may be attributed to geological areas consisting of different granite rocks mainly feldspar, biotite, quartz, plagioclase and gneisses, which contain higher concentrations of thorium and potassium.

The average value for the internal hazard indices was 1.21 varying from 0.68 to 1.67, the maximum value and the average value are above the permissible limit of 1

The mean estimated value of Ra_{eq} was 385.15 Bq/kg ranging from 203.52 to 535.86 Bq/kg. The average Ra_{eq} values from the samples are higher than the safe limit of 370 Bq/kg and as recommended by the Organisation for Economic Cooperation and Development.

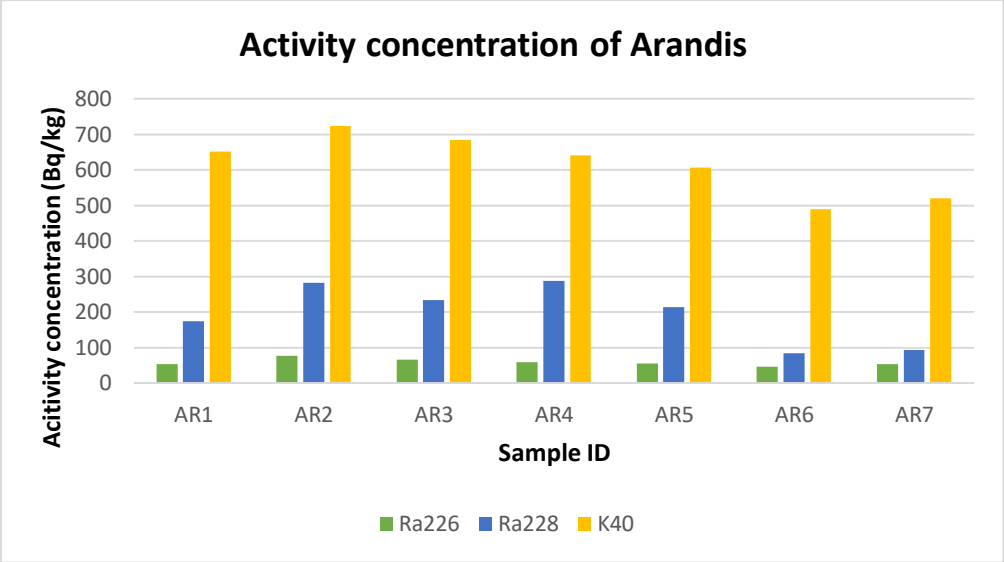

Figure 4.3: Comparison of the activity concentrations of ^{226}Ra, 228Ra and ^{40}K of the seven (7) homogenised samples from the town of Arandis

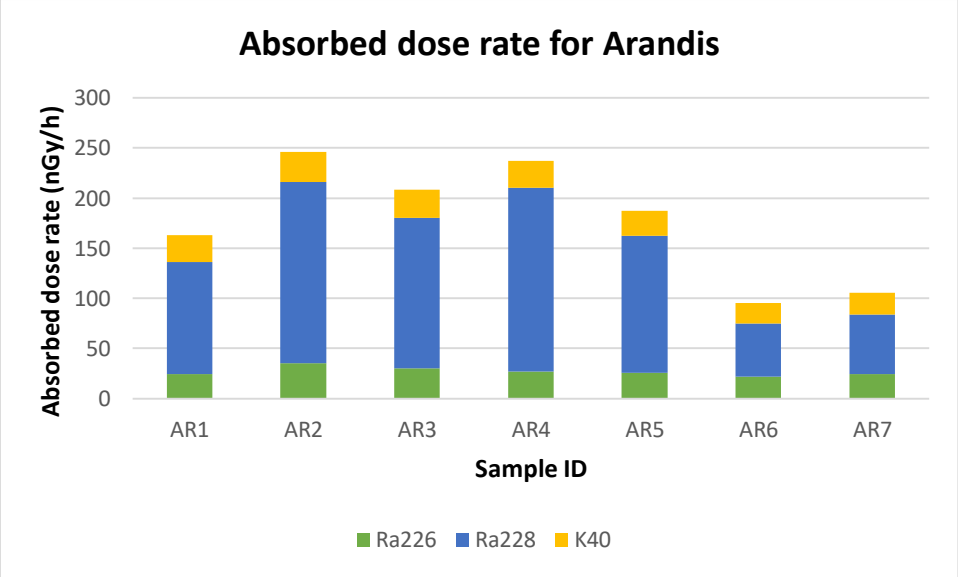

Figure 4.4: Comparison of the absorbed dose rates of the seven (7) homogenised samples from the town of Arandis

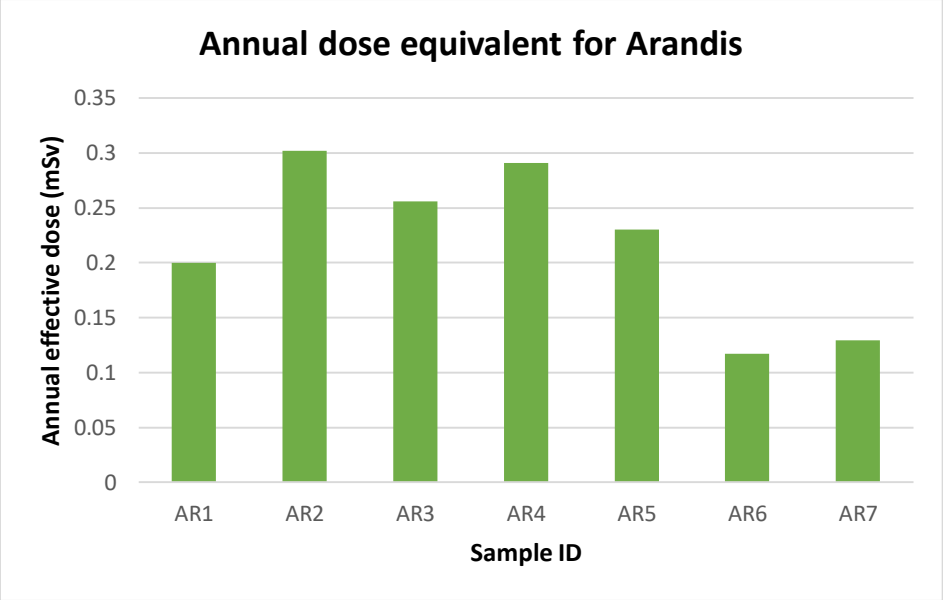

Figure 4.5: Comparison of the annual dose equivalent of the seven (7) homogenised samples from the town of Arandis

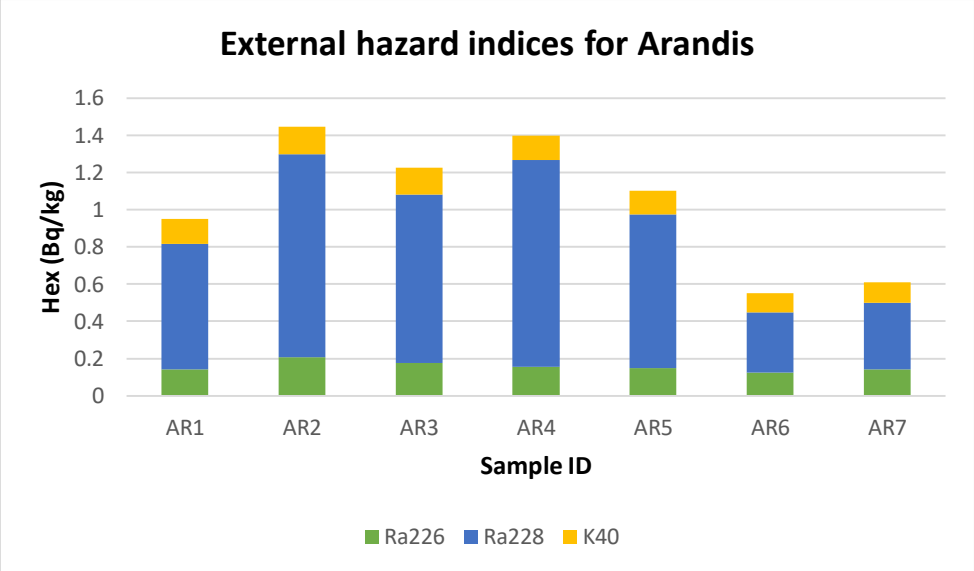

Figure 4.6: Comparison of the external hazard indices of the seven (7) homogenised samples from the town of Arandis

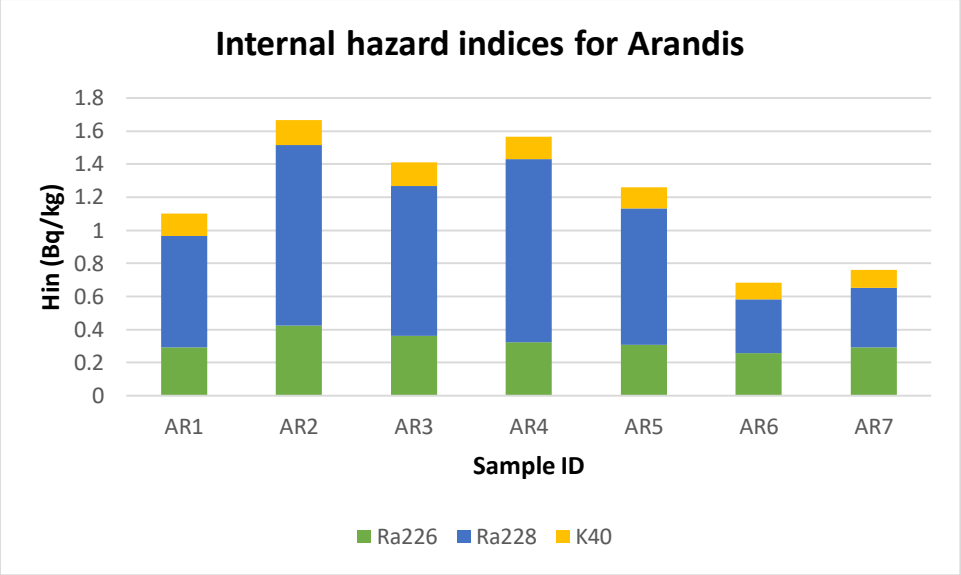

Figure 4.7: Comparison of the internal hazard indices of the seven (7) homogenised samples from the town of Arandis

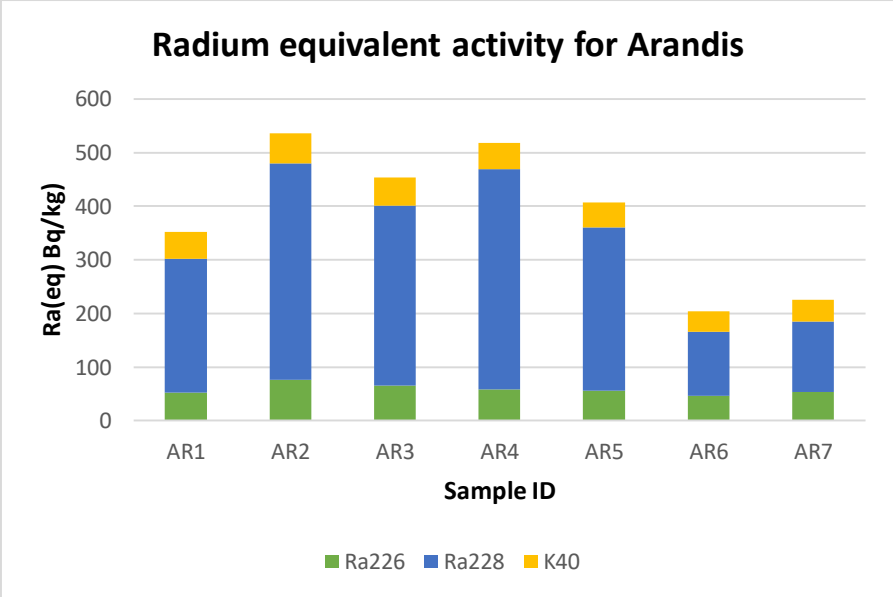

Figure 4.8: Comparison of the radium equivalent activity of the seven (7) homogenised samples from the town of Arandis.

4.3 Results of soil samples for Henties Bay

Table 4.3: Calculations of activity concentrations of ^{226}Ra, ^{228}Ra, and ^{40}K, absorbed dose rates, annual dose equivalent calculations, external hazard indices, internal hazard indices and radium equivalent activities for the town of Henties Bay

Sample ID	Radionuclide concentration (Bq/kg)			Absorbed dose rate	Annual dose equivalent	Hex	Hin	Raeq
Radionuclide	Ra226	Ra228	K40	(nGy/h)	(mSv)	(Bq/kg)	(Bq/kg)	(Bq/kg)
HB1	61.14±6.99	106.75±5.64	679.25±27.2	375.97	0.46	0.72	0.94	266.09
HB2	51.31±1.96	100.17±5.45	602.72±24.1	335.54	0.41	0.65	0.85	240.96
HB3	47.52±0.82	73.01±9.75	677.38±27.1	348.52	0.43	0.55	0.68	204.08
HB4	66.75±2.50	248.69±7.4	652.46±26.1	453.12	0.56	1.28	1.75	472.62
HB5	76.49±4.09	252.72±10.4	665.99±26.6	465.70	0.57	1.32	1.83	489.16
HB6	55.80±2.18	99.16±11.2	651.70±26.1	357.43	0.44	0.67	0.87	247.78
HB7	52.55±0.81	101.60±3.43	608.44±24.3	339.36	0.42	0.66	0.86	244.69
Mean	58.80±10.1	140.3± 76.2	648.28±31.1	382.24	0.47	0.84	1.11	309.34
Range (Min-Max)	47.52 76.49	73.01 252.72	602.72 679.25	335.54 465.70	0.41 0.57	0.55 1.32	0.68 1.83	204.08 489.16

Table 4.6 contains the results summarised from the seven (7) homogenised samples that were counted by the HPGe detector. From Table 4.6 the average activity concentration of ^{226}Ra (^{238}U) was 58.80 Bq/kg varying from 47.52 to 76.49 Bq/kg, which had the lowest activity concentration from all the other activity concentrations. The second highest average activity concentration was ^{228}Ra (^{232}Th) with a value of 140.30 Bq/kg varying from 73.01 to 252.72 Bq/kg. The activity concentration of ^{228}Ra ranged from 73.01 to 252.71 Bq/kg with an average value of 140 Bq/kg. ^{40}K has the highest average activity concentration of 648.28 Bq/kg varying from 602.72 Bq/kg to 679.25 Bq/kg. All the average concentrations of the radionuclides are above the world's average values of activity concentrations due to ^{238}U, ^{232}Th, and ^{40}K in soil samples are 33, 45 and 412 Bq/kg respectively (UNSCEAR, 2008). Henties Bay has the highest activity concentration of ^{40}K than all the other towns.

The values of the absorbed dose rates of the samples in Henties Bay vary from 335.54 to 465.70 nGy/h with an average absorbed dose rate of 382.24 nGy/h. It is interesting to note the highest absorbed dose rate value whose sample was collected in an effluent residential area. The average value of the absorbed dose rate for the town is more than 6 times higher than the world's average value (58 nGy/h) (UNSCEAR, 2010)

The average value of the annual dose equivalent was 0.47 mSv varying from 0.41 to 0.57 mSv. All these values are below the reference level band of 1 - 10 mSv value recommended by the (ICRP 60). The annual dose equivalent indicates that exposure in the town is within the recommended doses for the public.

The Hex values vary from the 0.55 to 1.32 with a mean value of 0.84. The highest external hazard indices value is higher than unity which indicates the radiation hazard

is significant and can be a health hazard for the more than 3000 people living in the town.

The estimated Ra_{eq} values obtained varied from 204.08 to 489.16 Bq/kg with an average value of 309.34 Bq/kg. The highest average value from the all the samples was higher than accepted value (370 Bq/kg), however the average values are lower than the 370 Bq/kg value of which it should not exceed.

The internal hazard indices for Henties Bay was estimated to have an average value of 1.11 varying from 0.68 to 1.83 the maximum value with the sample ID HB5 and the average value of Henties Bay are both above the permissible limit of 1.

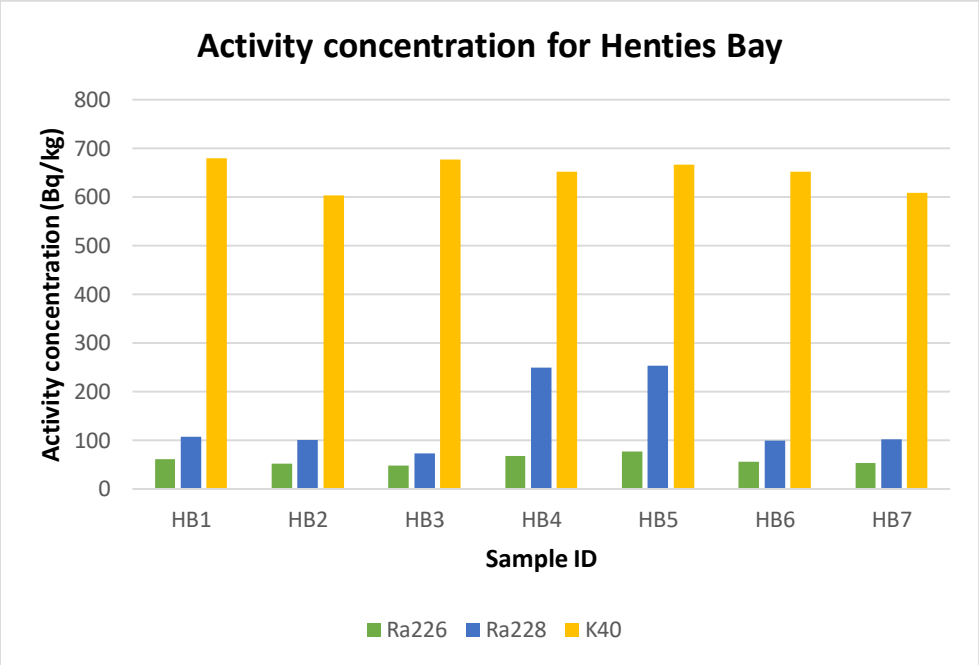

Figure 4.9: Comparison of the activity concentrations of ^{226}Ra, 228Ra and ^{40}K of the seven (7) homogenised samples from the town of Henties Bay

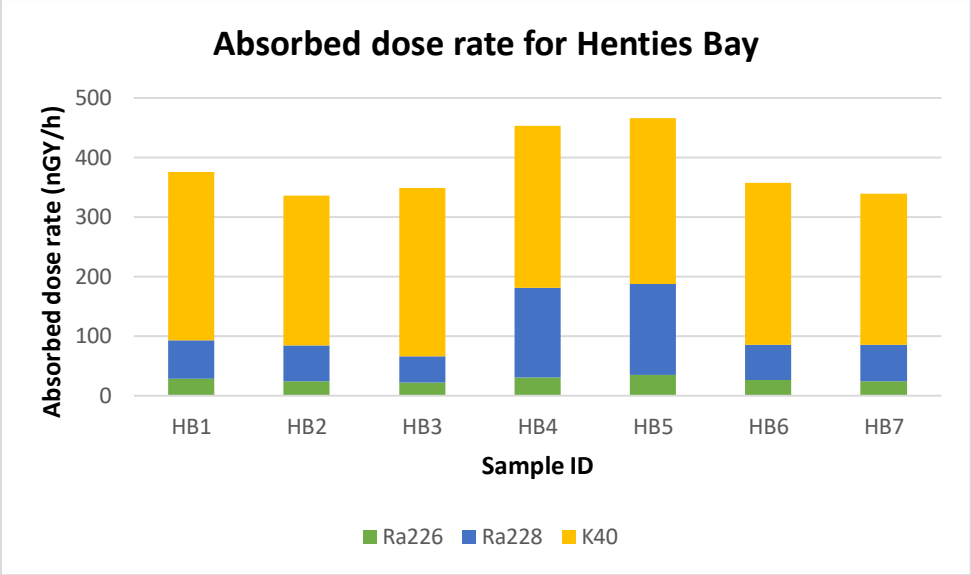

Figure 4.10: Comparison of the absorbed dose rates of the seven (7) homogenised samples from the town of Henties Bay

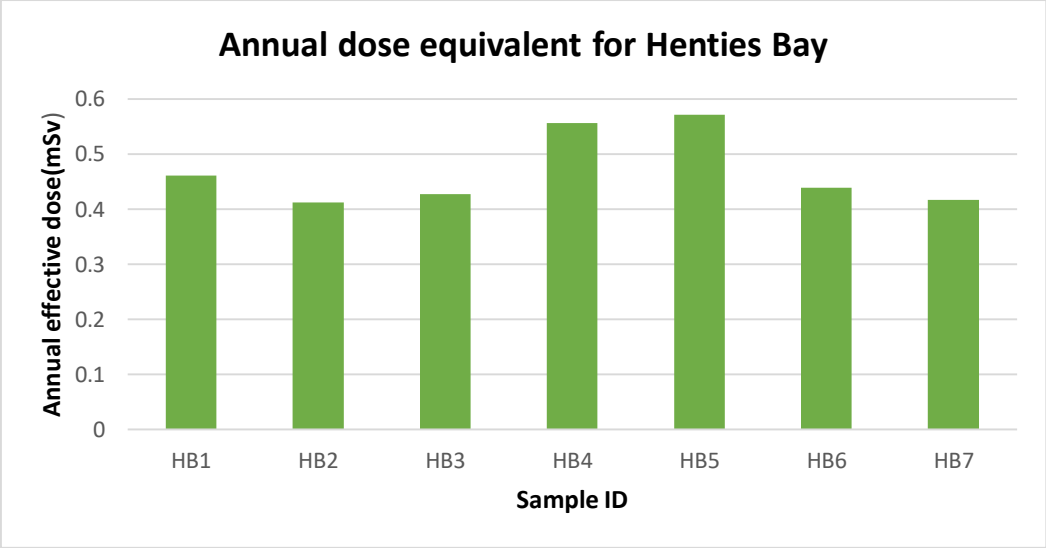

Figure 4.11: Comparison of the annual dose equivalent of the seven (7) homogenised samples from the town of Henties Bay

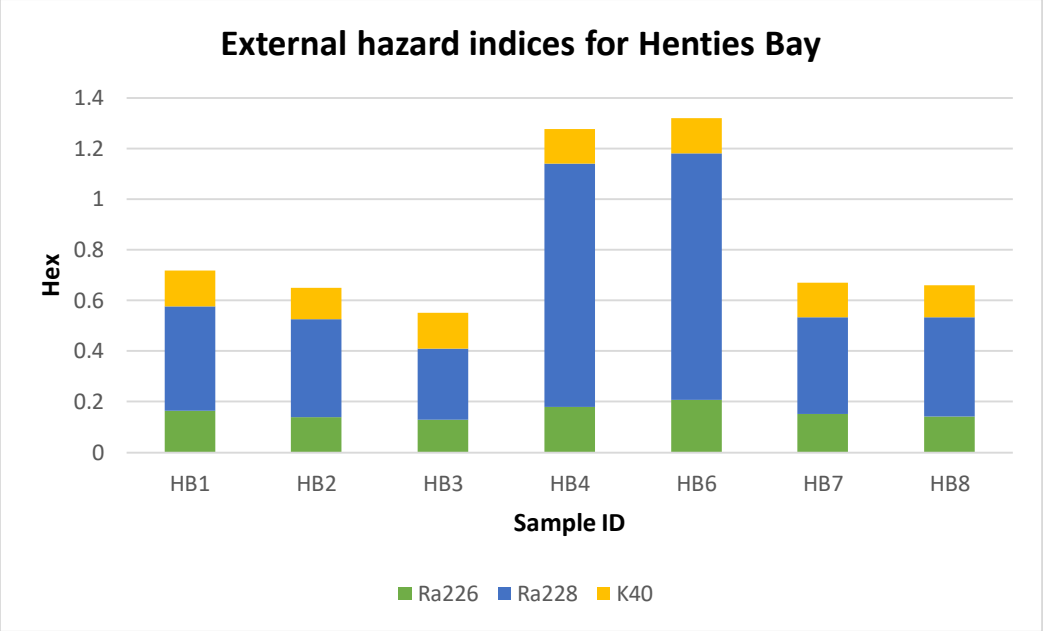

Figure 4.12: Comparison of the external hazard indices of the seven (7) homogenised samples from the town of Henties Bay

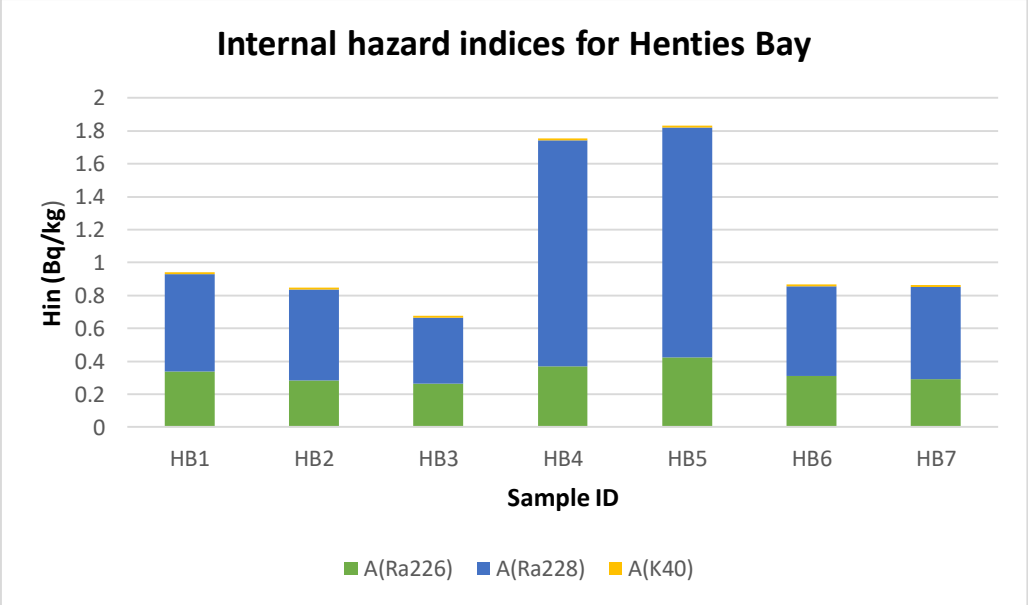

Figure 4.13: Comparison of the internal hazard indices of the seven (7) homogenised samples from the town of Henties Bay

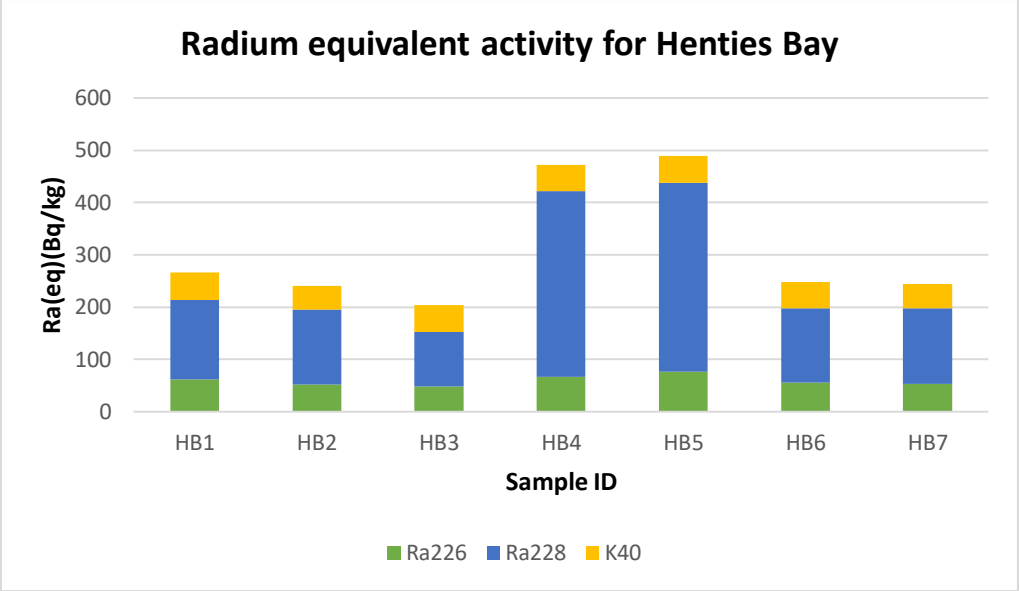

Figure 4.14: Comparison of the radium equivalent activity of the seven (7) homogenised samples from the town of Henties Bay

4.4 Results of soil samples of Walvis Bay

Table 4.4: Calculations of activity concentrations of ^{226}Ra, ^{228}Ra, and ^{40}K, absorbed dose rates, annual dose equivalent, external hazard indices, internal hazard indices and radium equivalent activities for the town of Walvis Bay

Sample ID	Radionuclide concentration (Bq/kg)			Absorbed dose rate	Annual dose equivalent	Hex	Hin	Raeq
Radionuclide	Ra226	Ra228	K40	(nGy/h)	(mSv)	(Bq/kg)	(Bq/kg)	(Bq/kg)
M1	12.44±1.25	14.90±3.41	332.23±13.3	28.60	0.035	0.16	0.16	59.33
M2	12.82±1.06	19.78±3.93	353.05±14.1	32.59	0.040	0.18	0.19	68.29
N1	14.04±2.14	17.35±12.8	285.18±11.4	28.86	0.035	0.16	0.18	60.81
S1	13.60±1.80	13.77±8.58	336.59±13.5	28.64	0.035	0.160	0.157	59.21
S2	15.57±1.82	16.93±6.44	350.14±14.0	32.02	0.039	0.18	0.19	66.74
T1	16.25±4.45	17.99±6.10	318.19±12.7	31.64	0.039	0.18	0.20	66.48
T2	0.86±0.60	0.36±0.88	25.69±1.03	1.69	0.0021	0.0091	0.0072	3.35
Mean	12.23 ±5.19	14.44 ±6.51	285.9 ±116.9	26.29	0.032	0.15	0.15	54.89
Range (Min - Max)	0.86 16.25	0.36 19.78	25.69 353.05	1.69 32.59	0.0021 0.040	0.0091 0.18	0.0072 0.20	3.35 68.29

The average activity concentration of ^{226}Ra (^{238}U) was estimated to be 12.23 Bq/kg with a range from 0.86 to 16.25 Bq/kg. The average activity concentration for ^{226}Ra was extremely low compared to the world's average activity concentration value of 33 Bq/kg. This can be attributed to the geological area of Walvis Bay having no granite rocks and other uranium bearing minerals. The average activity concentration of ^{226}Ra for Walvis is the lowest for all the towns. The average activity concentration for ^{228}Ra (^{232}Th) was 14.44 Bq/kg varying from 0.36 to 19.78 Bq/kg, the average value were both comparable to the low average activity concentration value of ^{226}Ra and the average value was consequently also below the worlds average activity concentration of 45 Bq/kg. The average activity concentration for ^{40}K was 285.87 Bq/kg with a range from 25.69 to 353.05 Bq/kg, comparing to the world's average activity concentration value of 412 Bq/kg, the average concentration value was lower, but much higher than the other radionuclide concentrations.

The estimated average value for the absorbed dose rate was 26.29 nGy/h varying from 1.69 to 32.59 nGy/h. The world's average value for absorbed dose rate is 58 nGy/h and the estimated average value was less than the world's average value. This correlates to the low concentrations of the radionuclide content.

The average annual dose equivalent value for the town of Walvis Bay was 0.032 mSv varying from 0.021 to 0.04 mSv. The average dose value was very low compared to the reference level band between 1 - 10 mSv recommended by the (ICRP 60).

The Hex average value was 0.15, varying from 0.00901 to 0.184, the highest Hex value of 0.184 was less than unity which means the radiation hazard is insignificant for people who reside in Walvis Bay. Ra_{eq} average value was 58.89 Bq/kg with a range from 3.35 to 68.29 Bq/kg. All the values were found to be less than 370 Bq/kg.

The average value of the internal hazard indices was estimated to be 0.15, with a variation from 0.0072 to 0.20, the average value was less than the limit of 1.

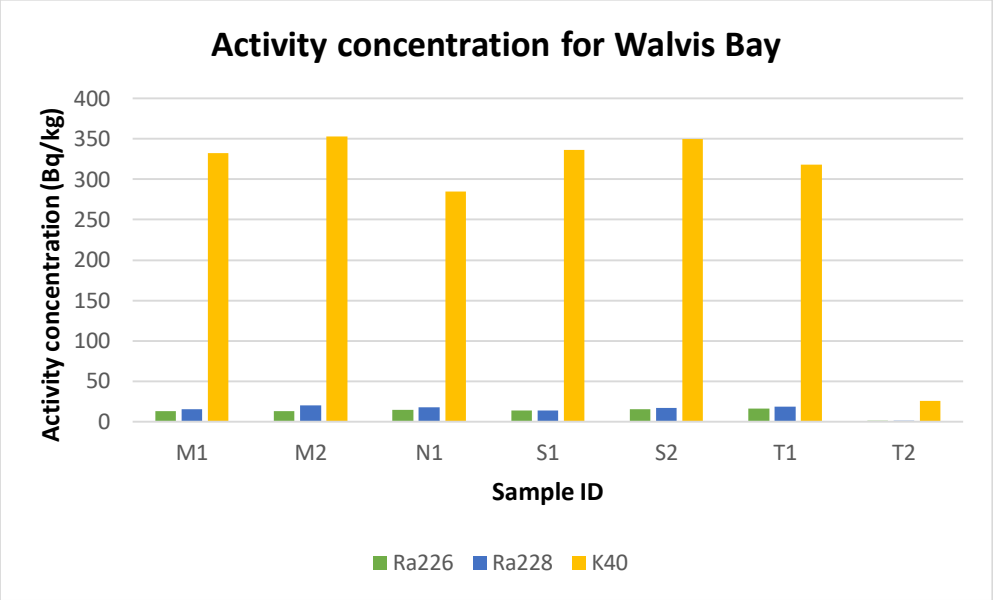

Figure 4.15: Comparison of the activity concentrations of ^{226}Ra, 228Ra and ^{40}K of the seven (7) homogenised samples from the town of Walvis Bay

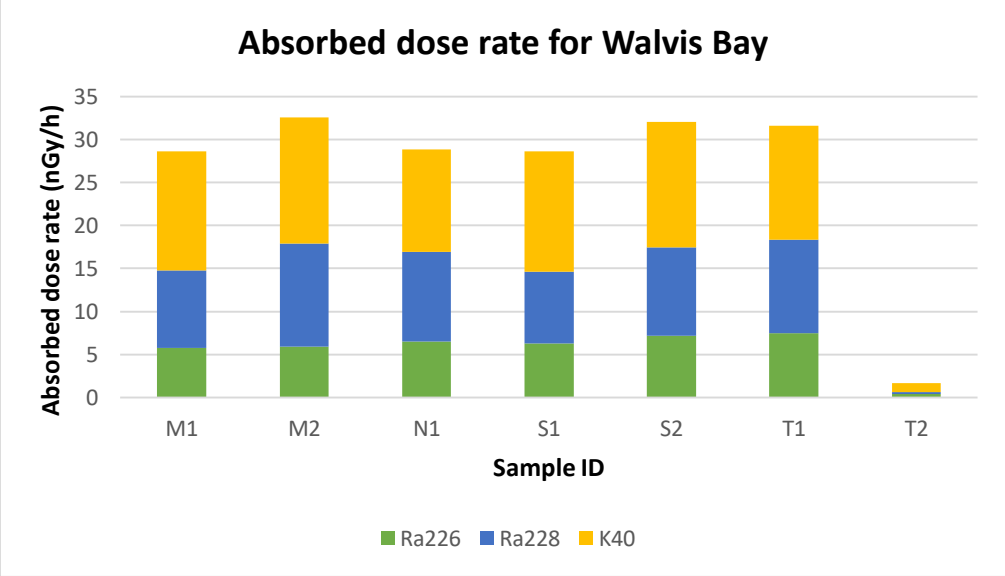

Figure 4.16: Comparison of the absorbed dose rates of the seven (7) homogenised samples from the town of Walvis Bay

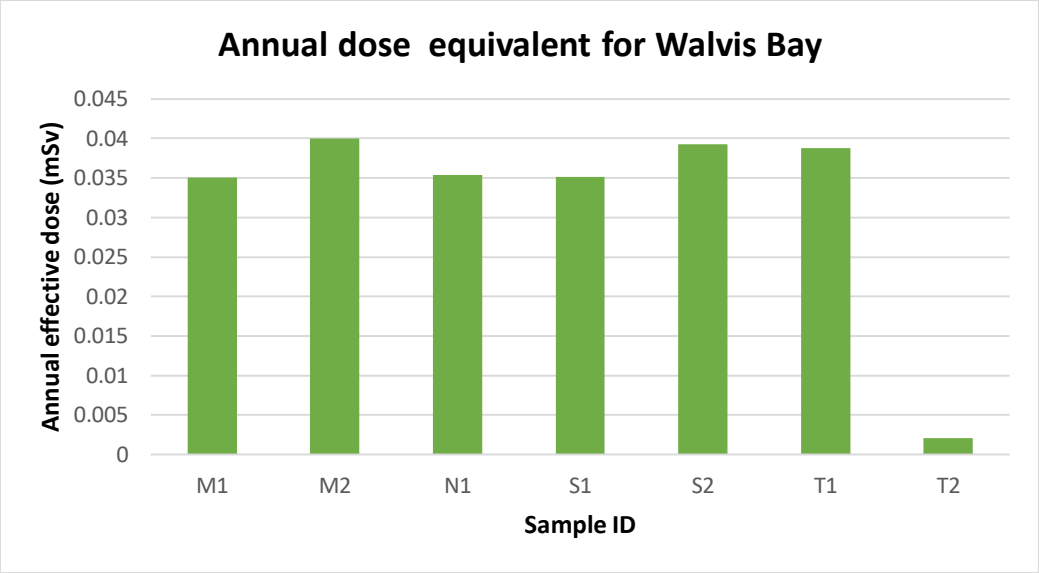

Figure 4.17: Comparison of the annual dose equivalent of the seven (7) homogenised samples from the town of Walvis Bay

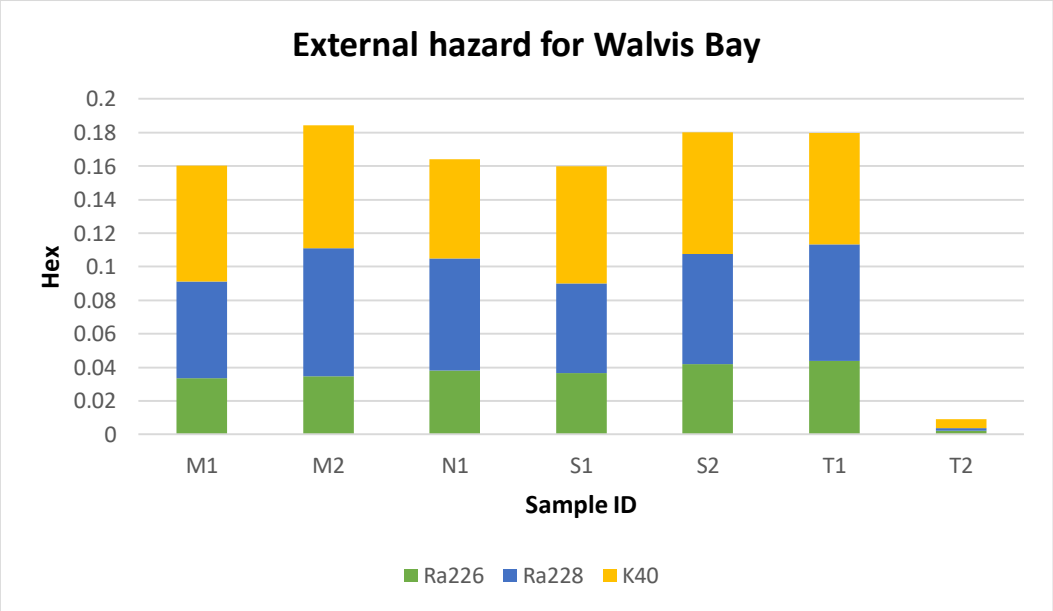

Figure 4.18: Comparison of the external hazard indices of the seven (7) homogenised samples from the town of Walvis Bay

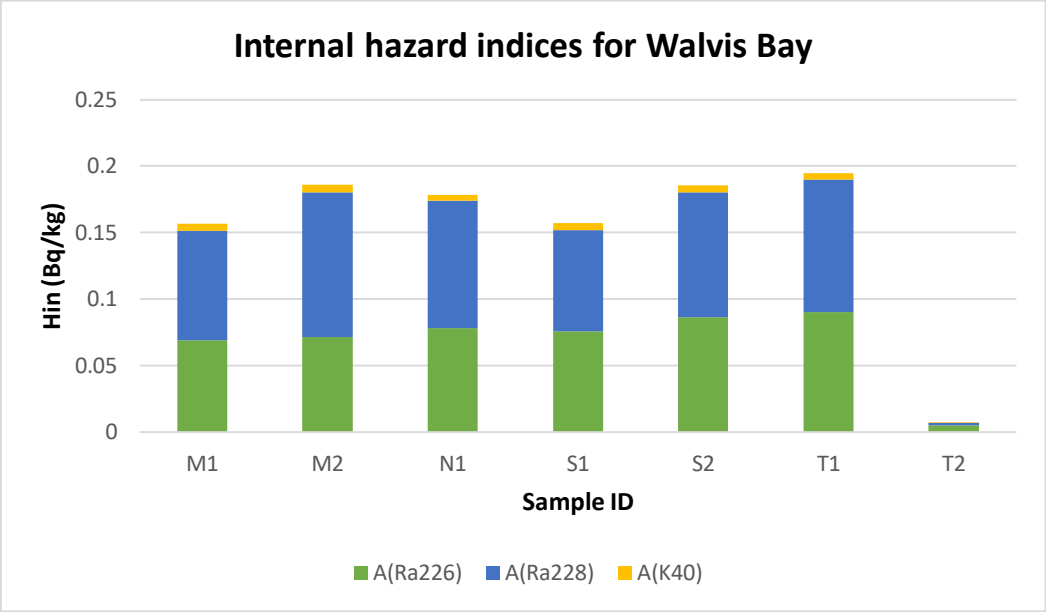

Figure 4.19: Comparison of the internal hazard indices of the seven (7) homogenised samples from the town of Walvis Bay

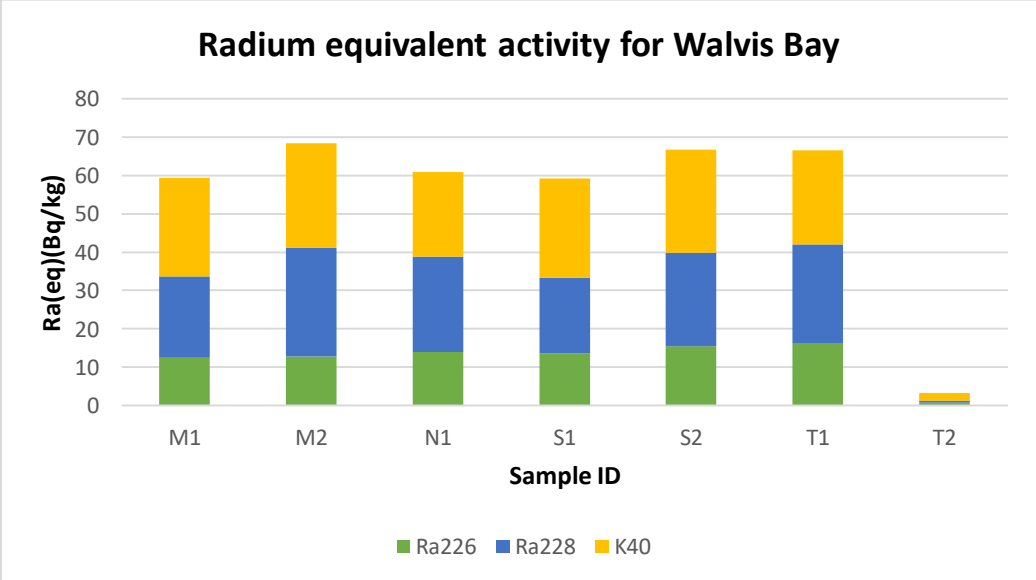

Figure 4.20: Comparison of the radium equivalent activity of the seven (7) homogenised samples from the town of Walvis Bay

4.5 Results of soil samples for Swakopmund

Table 4.5: Calculations of activity concentrations of ^{226}Ra, ^{228}Ra, and ^{40}K, absorbed dose rates, annual dose equivalent calculations, external hazard indices, internal hazard indices and radium equivalent activities for the town of Swakopmund

Sample ID	Radionuclide concentration (Bq/kg)			Absorbed dose rate	Annual dose equivalent	Hex	Hin	Raeq
Radionuclide	Ra226	Ra228	K40	(nGy/h)	(mSv)	(Bq/kg)	(Bq/kg)	(Bq/kg)
JB1	30.30±0.60	52.42±7.75	424.30±16.9	63.35	0.078	0.37	0.46	137.93
JB2	35.70±1.30	59.25±8.42	405.19±16.2	69.18	0.085	0.41	0.51	151.63
TW1	25.84±0.21	47.86 ±4.74	331.64±13.3	54.68	0.067	0.067	0.40	54.74
TW2	26.27±0.38	51.52±1.50	353.75±14.2	58.01	0.071	0.34	0.42	127.18
MD1	6.56±0.96	29.15±7.58	197.26±7.9	28.86	0.035	0.17	0.19	63.43
MD2	40.96±0.87	88.77±2.10	497.9±19.9	93.30	0.11	0.56	0.67	206.24
TM1	35.24±0.30	65.07±4.70	443.89±17.8	74.09	0.091	0.44	0.54	162.47
Mean	28.70±11.2	56.29± 18.2	379.15±97.5	63.07	0.07	0.34	0.46	129.09
Range (Min - Max)	6.56 40.96	29.15 88.77	197.26 497.9	28.86 93.30	0.035 0.11	0.067 0.56	0.19 0.67	54.74 206.24

The ^{226}Ra average activity concentration value was 28.70 Bq/kg varying from 6.56 to 40.96 Bq/kg. ^{226}Ra had the lowest activity concentration from the radionuclides (^{228}Ra and ^{40}K) and its average activity value was less than the world's average activity concentration of 33 Bq/kg as stated by (UNSCEAR, 2008). The second highest average activity concentration value of ^{228}Ra was 56.29 Bq/kg varying from 29.15 to 88.77 Bq/kg. The highest average activity concentration is from the radionuclide ^{40}K with a value of 379.15 Bq/kg ranging from 197.26 to 497.90 Bq/kg, however the average activity concentration value of ^{40}K was less than the world's average activity value of 412 Bq/kg. These estimated mean activity concentration values of Swakopmund are comparable to that of Walvis Bay, this can be attributed to the towns being in close proximity to each other of 30 km apart and being similar geological formations.

The average absorbed dose rate for Swakopmund was 63.07 nGy/h ranging from 28.86 to 93.30 nGy/h. The average absorbed dose rate is comparable to the world's average value of absorbed dose rate which is "58 nGy/h" (UNSCEAR, 2010).

The average annual dose equivalent for Swakopmund was found to be 0.070 mSv ranging from 0.035 to 0.11 mSv. All these values were below the limit of 1.0 mSv recommended by the IRCP (UNSCEAR, 2008). These low values are consequently attributed to both the low activity concentrations of the radionuclides under investigation in the Swakopmund area and the low absorbed dose rate values.

The Hex average value was 0.34 with a range from 0.067 to 0.56, all the values were lower than unity, which means the radiation hazard insignificant for the people living in Swakopmund.

The Ra_{eq} average value was 129.09Bq/kg with a range from 54.74 to 206.24 Bq/kg. All the estimated values were below the 370 Bq/kg value.

The internal hazard had an average value estimated to be 0.46 with a range from 0.19 to 0.67. All the values were less than the limit of 1.

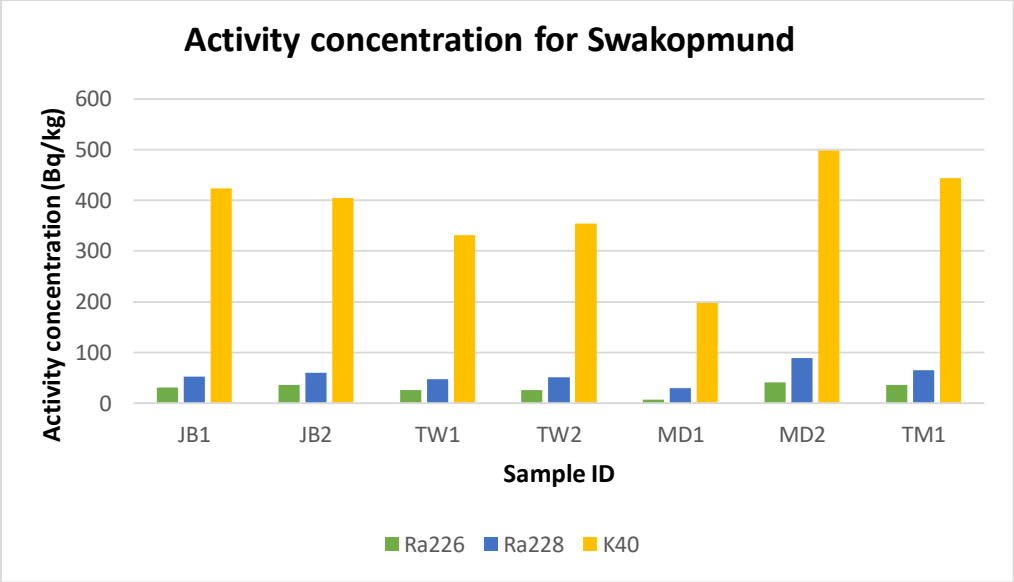

Figure 4.21: Comparison of the activity concentrations of ^{226}Ra, 228Ra and ^{40}K of the seven (7) homogenised samples from the town of Swakopmund

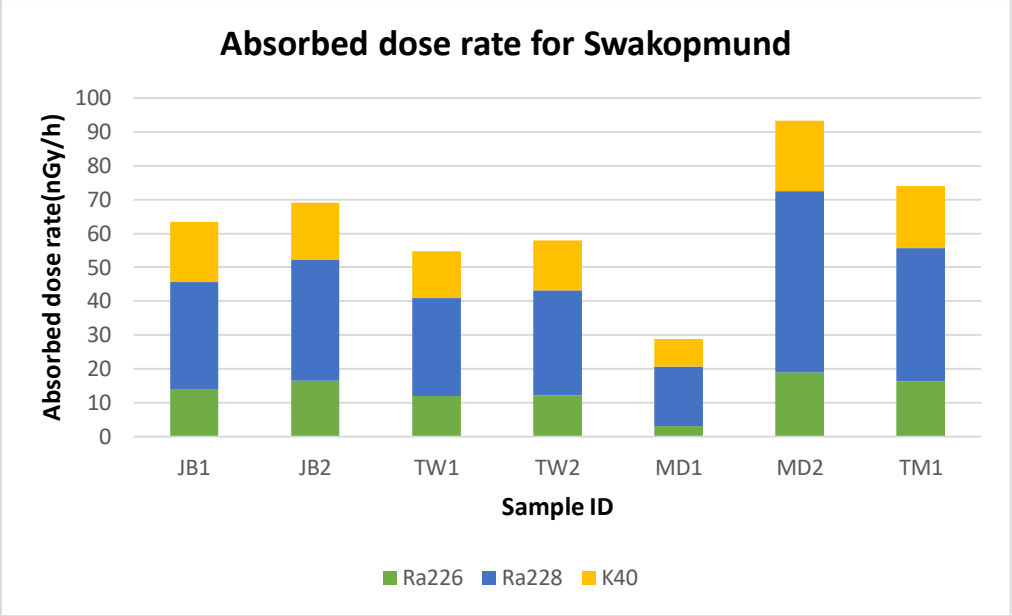

Figure 4.22: Comparison of the absorbed dose rates of the seven (7) homogenised samples from the town of Swakopmund

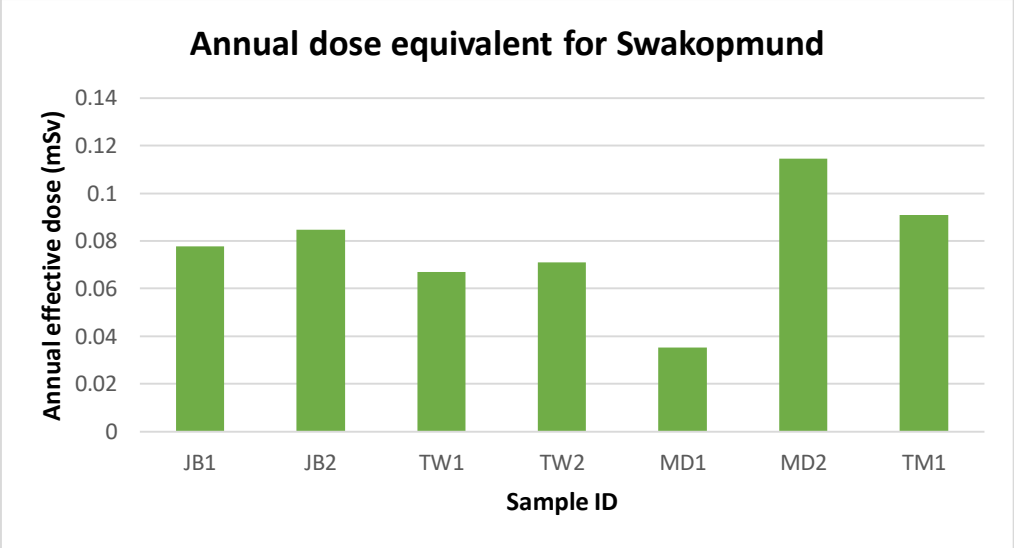

Figure 4.23: Comparison of the annual dose equivalent of the seven (7) homogenised samples from the town of Swakopmund

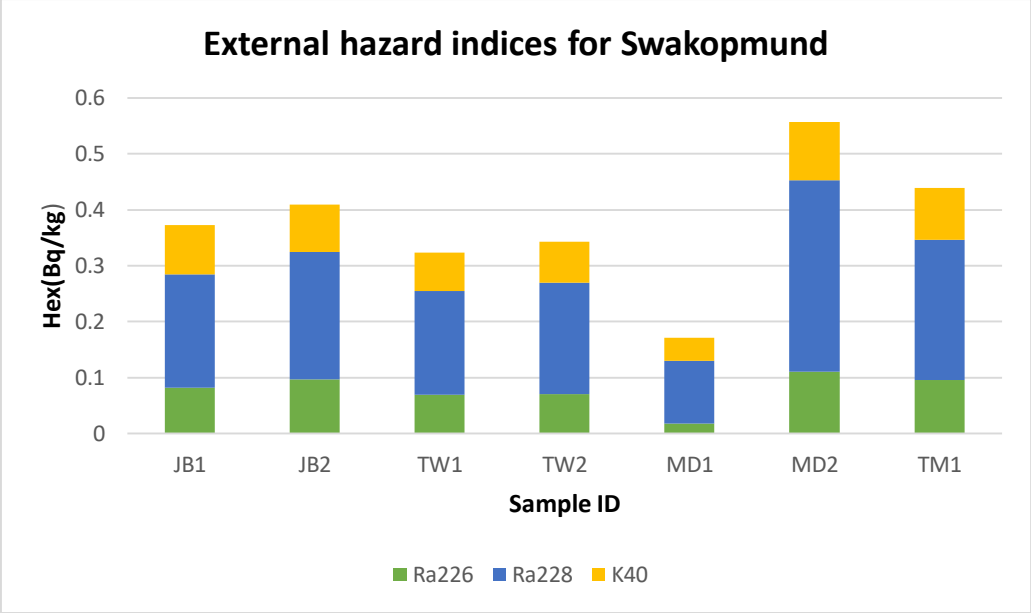

Figure 4.24: Comparison of the external hazard indices of the seven (7) homogenised samples from the town of Swakopmund

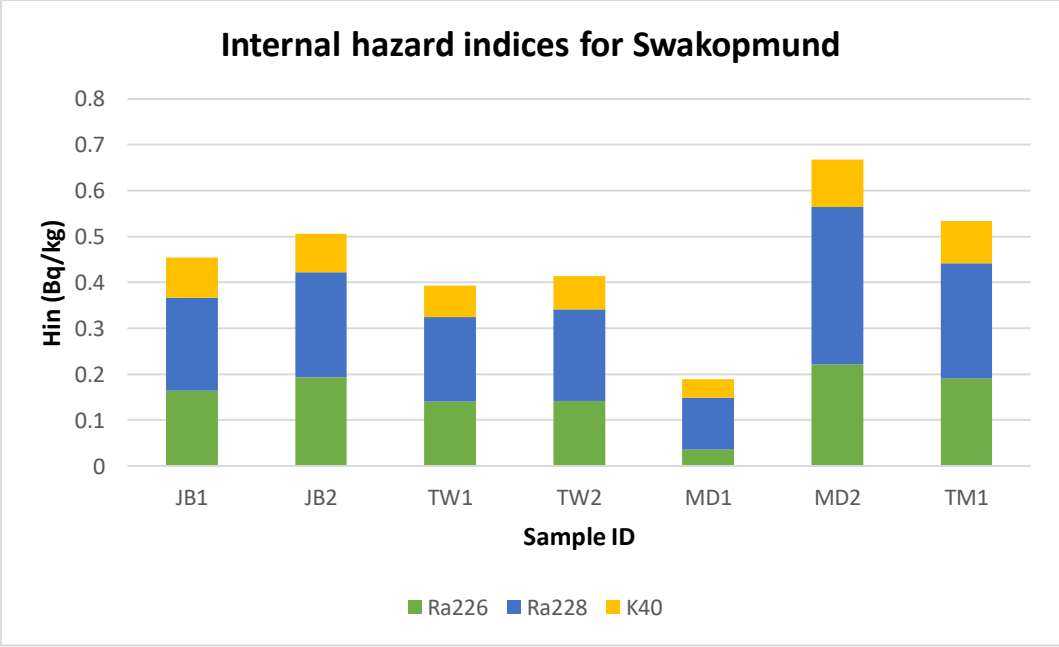

Figure 4.25: Comparison of the internal hazard indices of the seven (7) homogenised samples from the town of Swakopmund

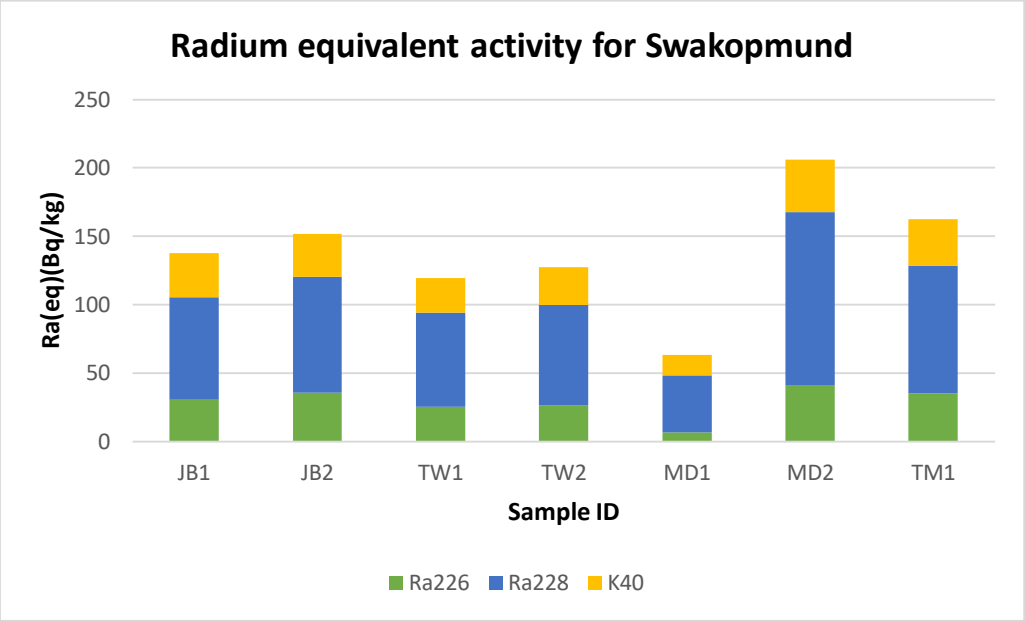

Figure 4.26: Comparison of the radium equivalent activity of the seven (7) homogenised samples from the town of Swakopmund

4.6 Comparison of natural radioactivity concentration (Bq/kg) in the soil samples of the four towns for present study with previous studies reported and published from different countries in the world.

Country/Town	Mean activity concentration (Bq/kg)				References
	Ra(226)	Th(232)	K(40)		
Namibian Towns:					
Arandis	47	195	617		Present Study
Henties Bay	58	140	648		Present Study
Walvis Bay	12	14	285		Present Study
Swakopmund	29	57	379		Present Study
Egypt	17	18	320		(UNSCEAR,2000)
Turkey	37	40	667		(Taskin, 2009)
Albaha Saudi Arabia	37	32	343		(Zaharani, 2012)
Algeria	50	25	370		(UNSCEAR,2000)
United States	40	35	420		(UNSCEAR,2000)
Denmark	17	19	460		(UNSCEAR,2000)
Portugal	44	51	840		(UNSCEAR,2000)
Iran	28	22	640		(UNSCEAR,2000)
Ghana	29	25	582		(Darko,2010)
Japan	33	28	310		(UNSCEAR,2000)
China	32	41	440		(UNSCEAR,2000)
Belgium	26	27	380		(UNSCEAR,2000)
Sweden	42	42	680		(UNSCEAR,2000)
Nigeria	7	29	229		(Kolo, 2012)
World Average	33	45	412		(UNSCEAR,2000)

Table 4.7 Results for lifetime cancer risk for the four towns

Lifetime Cancer Risk				
Town	**H_E(avg annual dose equivalent)**	**DL**	**RF**	**LCR**
Arandis	0.22	51.62	0.05	0.57×10^{-3}
Henties Bay	0.47	51.62	0.05	1.21×10^{-3}
Walvis Bay	0.032	51.62	0.05	0.0083×10^{-3}
Swakopmund	0.079	51.62	0.05	0.20×10^{-3}

Table 4.10: A comparison of the excessive lifetime cancer risk for the four towns

The excessive Lifetime cancer risks for each of the towns were estimated from the equation 4.0 in Chapter 3.

CHAPTER FIVE

CONCLUSION AND RECOMMENDATIONS

5.1 CONCLUSION

The overall objective is to assess the radiological impact and exposure of the members of the public living in the four areas.The research focus is on determinating the levels and the extent of the exposure of the naturally ocurring radionuclides of ^{226}Ra/ ^{228}Ra decay series as well as ^{40}K within the major four towns of the Erongo region. These four towns are close to the uranium mines that are at the highest scale of mining, and is essential to be monitoring the primordial radionuclide concentrations in the soils of these towns.

The radioactivity levels in soil at, Walvis Bay, Swakopmund,amd Henties Bay were within the global average values for ^{226,} Ra, ^{228}Ra and ^{40}K, except for Arandis.

The average activity concentration for the radionuclides; ^{226}Ra, ^{228}Ra and ^{40}K in the soils were determined inlcuding the absorbed dose rates, annual effective dose rates, external hazard indices, radium equivalent activities and the excessive ifetime cancer risks for each town was also determined.

^{40}K has been observed to have the highest activity concentration than ^{226}Ra and ^{228}Ra in all of the towns. The activity concentration of ^{40}K was found to be the highest specifically in Henties Bay and Arandis as a result it is responsible for the majority of the radioactivity in the soil.

The radioactivity levels in soil at, Walvis Bay, Swakopmund,amd Henties Bay were within the global average values for ^{226,} Ra, ^{228}Ra and ^{40}K, except for Arandis.

The average activity concentration for ^{226}Ra was observed to be the lowest than the radionuclides of ^{40}K and ^{228}Ra. All the towns were observed to have low activity concentration of ^{226}Ra.

The mean annual dose equivalent were estimated below the global average value of 0.48 mSv.

The radium equivalent activities for all the towns except Arandis was below the limit of 350 Bq/kg.

The mean external hazard indices and internal hazard indices for Walvis Bay, Swakopmund and Henties Bay were below the limit values except Arandis.

5.2 RECOMMENDATIONS

5.2.1 Scientific community

There is a need for continuous study to establish the effects of seasonal variations on the concentrations of the radionuclides. This study should include the analysis of the activities of alpha and beta particles in underground water. It can also include the aspect of internal dosimetry through inhalation of ^{220}Rn, ^{210}Po and ^{210}Pb in the soil or through direct measurement of Radon in houses in this communities.

5.2.2 Regulatory body

Results from this work should be used by the Namibian National Radiation Protection Authority as it radiologically maps the activity concentration of the Erongo region, which can be susceptible to radiological contamination in its soil and water. It is encouraged to use these data to establish radiation protection programs and regulatory procedures for monitoring of external radiation levels including radon concentrations in soil. It is advised that the regulatory authority in partnership with environmental agencies educate members of the public in the Erongo region on the activities of safe mining and how it can affect their communities. The Regulatory authority should focus on enacting regulations and guidance documents to enforce radiation protection in NORM Industry in Namibia compatible with International Radiation Protection and Safety Standards.

References

Ahmed, S. N. (2007). *Physics and Engineering of Radiation Detection.* Kingston: Elsevier 2007.

Al-Masri, M. S & Suman, H. (2003). ORM waste management in the oil and gas industry: The Syrian experience. *Journal of Radioanalytical and Nuclear Chemistry*, 256(1): 159 - 162.

Anderson, E. C. (2001). Numerical modelling of radon-222 entry into houses: an outline of techniques and results. *Science of the Total Environment*, 272 (1): 33-42.

Arandis Town Council. (2010). *Google Chrome*. Retrieved from Arandis Profile: http://www.arandistown.com/wp-content/uploads/2010/10/Arandis-Profile.pdf

Besler, H. (1994). Geomorphogenese und Paläoklima Namibias. Die Erde 125: 139- 165.

BIER. (2006). *Health risks from exposure to low levels of ionizing radiation: BEIR VII Phase 2, National Research Counci. Committee to Assess Health Risks from Exposure to Low Level of Ionizing Radiation.* Washington, D. C: The National Academic Press.

Cañete, S., Jose, S. P., Palad, L. J. H., Enriquez, E. B., Garcia, T. Y & Yulo-Nazarea, T. (2008). Leachable 226Ra in Philippine phosphogypsum and its implication in groundwater contamination in Isabel, Leyte, Philippines. *Environmental Monitoring and Assessment*, 142 (1-3): 337-344.

Cember, H., & Johnson, T. E. (2009). *Introduction to Health Physics fourth Edition.* New York: McGraw Hill Companies.

Chabaux, F., Riotte, J & Dequincey, O. (2003). U-Th-Ra fractionation during weathering and river transport. *Reviews in Mineralogy and Geochemistry*, 52 (1): 533-576.

Charette,. Mathew, A., Dulaiova, H., Gonneea, M. E., Henderson, P. B., Moore, W. S., Scholten, J. C., & Pham, M. K. (2012). GEOTRACES radium isotopes interlaboratory comparison experiment. *Limnology and Oceanography: Methods*, 10 (6): 451-463.

Chauhan, R. A. (2013). Study of radon transport through concrete modified with silica fume. *Radiation Measurements* , 59: 59-65.

Chernick C. L. (1962). Fluorine compounds of xenon and radon. *Science*, 138 (3537): 136-138.

Coastal Zone Management Project (CZM). (1999, August). *Coastal Profile of the Erongo Region.* (K. Bender, R. Barby, & J. Korrubel, Eds.) Retrieved July 25, 2011, from Environmental Information Service Namibia: http://www.the-eis.com/data/literature/Coastal%20profile%20of%20the%20Erongo%20Region.pdf

Darby, S. (2005). Radon in homes and risk of lung cancer: collaborative analysis of individual data from 13 European case-control studies. *Bmj*, 330 (7485): 223.

Darko, A. F. (2007). *Baseline radioactivity measurements in the vicinity of a Gold Treatment Plant.* Journal of Applied Science and Technology.

Debertin, K. A., (1988). *Gamma-and X-ray spectrometry with semiconductor detectors.* Amsterdam: North-Holland.

Dowdall, M. Ø., Gwynn, J. P & Dvids, C. (2004). Simultaneous determination of 226Ra and 238U in soil and environmental materials by gamma-spectrometry in the absence of radium progeny equilibrium. *Journal of Radioanalytical and Nuclear Chemistry*, 261(3): 513-521.

El-Gmal, A. (2007). Study of the Spatial distribution of Natural Radioactivity. *Journal of Radiation Measurements*, 457-465.

Esmaili., M. S. (2002). New public dose assessment of elevated natural radiation areas of Ramsar (Iran) for epidemiological studies. *Proceedings of the 5th International Conference on High Levels of Natural Radiation and Radon Areas* (pp. 15-24). Munich: Elsevier.

Gbadago, J. K., faanhof, A., Darko, E. O & Schandorf, C. (2011). Investigation of the Environmental Impacts of Naturally Ocuuring Radionuclides in the processing of Sulphide ores for Gold using Gamma Spectrometry. *Journal of Radiological Protection*, 31(3): 337-352.

Gilmore, G. (2008). *Practical gamma-ray spectroscopy. 2nd ed. Chichester.* Wiley.

Glass, W. A & Varma, M. N. (1991). Physical and chemical mechanisms in molecular radiation biology. New York: Plenum Press.

Green, R. H. (2019). Retrieved September 23, 2019, from Encyclopædia Britannica: https://www.britannica.com/place/Namibia

Hall, E. J. (1994). *Radiobiology for the Radiologist (Fourth Edition).* Philadelphia: J. B. Lippincott Company.

Hall, E. J. (2006). *Radiobiology for the Radiologist 6th edition.* Philadelphia: J.B Lippincott Company.

Hedemann-Jensen, P. (2010). Naturally occurring radiation sources: existing or planned exposure situation. *Journal of Radiological Protection* , 30(4):781-787

IAEA. (1989). *Measurement of Radionuclides in Food and Environment* . Austria: IAEA-Technical Report Series No. 295.

IAEA. (2003). *Guidelines for radioelement mapping using gamma ray spectrometry data.* Vienna: International Atomic Energy Agency Publication

IAEA. (2005). *Environmental and source monitoring for purposes of radiation protection:: safety guide RS-G-1.8.* Vienna: International Atomic Energy Agency Publication

IAEA. 2014. *Radiation protection and safety of radiation sources : international basic safety standards*. Vienna: International Atomic Energy Agency

IAEA. (2015). *Protection of the public against exposure indoors due to radon and other natural sources of radiation specific safety guide.* Vienna: International Atomic Energy Agency Publication.

ICRP. (2007). *Scope of Radiological Protection Control Measures.* ICRP Publication 104. Ann 35 (5).

ICRP. (2010). *Lung cancer risk from radon and progeny and statement on radon. ICRP Publication 115.* Annals of the ICRP 40 (1).

Oyedele, J. A & Shimboyo, S. (2008). Radionuclide Concentration in soils of Nothern Namibia, Southern Africa. *Radiation Protection Dosimetry*, 131(4): 482-286.

Jacob, J. D. (1990). Radon-222 as a test of convective transport in a general circulation model. *Tellus B* , 42 (1): 118-134.

Jacob, R. E. (1974). *The radioactive mineralisation in part of the central Damara belt, South West Africaand its possible origins.* Atomic Energy Board Rep. PIN 234(B/R), 17pp.

Johnston, C. H. (1978). *Report on Spitzkoppe Concession - Damaraland.* General Mining and Finance Corp. Ltd.

Kiefer, J. (1990). *Biological Radiation Effects.* Berlin: Springer Verlag.

Knoll, G. F. (2000). *Radiation Detection adn Measurements 3rd Edition.* New York: John Wiley and Sons.

Kohrs B, K. P. (2014). *Study on low level radiation of Rio Tinto's Rossing Uranium mine workers.* EJOLT & Earthlife Namibia.

Kolo, M. T (2014).Natural Radioacitivity and environmental risks assessment of Sokoto phosphate rock, Northwest Nigeria. *African Journalof Environmental Science and Technology:* 8(9): 532 - 538.

Lancaster, J., Lancaster, N & Seely, M. K. (1984). *Climate of the central Namib Desert.* Madoqua:14 (1):5-61

Nasim, A., Sabiha, J & Tufail, M (2012). *Enhancement of natural radioactivity in fertilized soil of Faisalabad, Pakistan.Environ SciPollut Res 2012, 19: 3327 - 338.*

Lombardo, A. J. (2008). *Measuring and Modeling Naturally Occurring Radioactive Material:Interpreting the Relationship Between the Natural Radionuclides Present.*

Martin, J. E. (2006). *Physics for Radiation Protection. Weinheim: WILEY-VCH Verlag GmbH & KGaA.*

Mathew, J. B. (1985). *Natural radioactivity of Australian Building materials, industrial wastes and by products . Health Physics , Vol 48: 87 - 95*

Mathew, P. J & Beretka, J (1985). *Natural radioactivity of Australian Building materials, industrial wastes and by-products.*

Mohammed Mahmud Abu Samreh, K. M. (2014). *Measurement of activity concentration levels of radionuclides in soil samples*. *Turkish Journal of Engineering & Environmental Sciences*, 113-125.

Mohanty, A, K., Sengupta, D., Das, S, K., SK Saha and KV Van. (2004). *Natural radioactivity and radiation exposure in the high background area at Chhatrapur beach placer deposit of Orissa, India. Journal of Environmental Radioactivity , 75(1): 15-33.*

Michielsen, N & Tymen, G. (2007). *Semi-continuous measurement of the unattached radon decay products size distributions from 0.5 to 5nm by an array of annular diffusion channels. Journal of Aerosol Science, 38 (11): 1129-1139*.

NUA. (2019, June 19). Google. Retrieved from namibian uranium association: http://www.namibianuranium.org/uranium-mining-in-namibia/

Porstendörfer, J. (1994). Properties and behaviour of radon and thoron and their decay products in the air. *Journal of Aerosol Science*, 25 (2): 219-263.

Porstendörfer, J. (1999). Radon: Characteristics in air and dose conversion factors. *Health Physics*, 76 (3): 300-305.

Schreiber, U. (1996). *The Geology of the Walvis Bay Area.* Windhoek: Geological Survey of Namibia.

Schubert, M. A. (2012). Air–water partitioning of 222Rn and its dependence on water temperature and salinity. *Environmental Science & Technology*, 46 (7): 3905-3911.

Siegel, P. (2013). Gamma spectroscopy of environmental samples. *American Journal of Physics*, 81(5):381 - 388.

Taljaard, J. (1979). *Low-level atmospheric circulation over the Namib.* Newsletter of the Weather Bureau of South Africa.

Taskin, H & Karavus, M. (2009). Radionuclide concentrations in soil and lifetime cancer risk due to gamma radioactivity in Kirklareli, Turkey. *J. Environmental Radioactivity*, 100 (1): 49 - 53.

Turner, J. E. (2007). *Atoms, Radiation and Radiation Protection 2nd Edition.* John Wiley and Sons.

UNSCEAR. (2000). *Exposure from natural radiation sources. United Nations Scientific Committee on the effects of Atomic Radiation.* New York.

UNSCEAR. (2006). *Sources-to-effects assessment for radon in homes and workplaces: United Nations Scientific Committee on the Effects of Atomic Radiation.* New York: IAEA.

UNSCEAR. (2008). *Exposures of the public and workers from various sources of radiation.* New York: IAEA.

UNSCEAR. (2008). *Sources and effects of ionizing radiation. United Nations Scientific Committee on The Effects of Atomic Radiation, Report to the General Assembly with Annexes. Vol. II.* New York: United Nations Publication.

UNSCEAR. (2010). *Sources and effects of ionizing radiation.* New York: United Nations .

UNSCEAR. (2010). *Summary of Low Dose Radiation on Health.* New York.

Walter, H. (1936). *Die ökologischen Verhältnisse in der Namib-Nebelwüste.* Leipzig : Gebrüder Borntraeger.

WHO. (2009). *Handbook on indoor radon.* Geneva: World Health Organization.

Zaharani, J. H. (2012). Radioactivity Measurements and Radiation Dose Assessments in Soil of Albaha Region (Saudi Arabia). *Life Science Journal*, 9(3)2391 - 2397.

APPENDICES

APPENDIX 1: Mixed radionuclide standard certificate

Seite 2
Page

030854
D-K-15203-01-00
2017-04

Geometry Reference Source

Source no.	AJ-9177
Drawing	VZ-1520-001
Volume	approximately 1000 ml
Density	approximately 1.0 g/cm³
Construction	The radionuclidic mixture is homogeneously incorporated in the matrix of the source.

Nuclide	Gamma-ray energy [MeV]	Activity [Bq]	Emission rate [s^{-1}]
Americium-241	0.060	3.42E03	1.23E03
Cadmium-109	0.088	1.52E04	5.58E02
Cobalt-57	0.122	5.22E02	4.47E02
Cerium-139	0.166	6.06E02	4.85E02
Mercury-203	0.279	8.00E02	6.52E02
Tin-113	0.392	2.01E03	1.30E03
Strontium-85	0.514	2.03E03	2.00E03
Caesium-137	0.662	2.83E03	2.40E03
Yttrium-88	0.898	4.31E03	4.05E03
Cobalt-60	1.173	3.25E03	3.25E03
Cobalt-60	1.333	3.25E03	3.25E03
Yttrium-88	1.836	4.31E03	4.28E03

Reference date	1 May 2017 at 12:00 UTC
Leakage and contamination test*	Wipe test according to ISO 9978.
Wipe test passed on	24 April 2017
Measuring method	The activity of the source was determined by weighing out calibrated single and/or mixed nuclide solutions. After production the source was verified with a high purity germanium detector with multi-channel analyzer. Temperature during the weighing: 21 °C ± 5 °C
Uncertainty*	The relative uncertainty of the activity is 3 % (Cd-109: 5 %).
Radioactive impurities	Rb-84<1 Bq; In-114m<4 Bq; Sb-124<1 Bq
Remark	201702217-LB SQ-012725

* please see HI001

End of Certificate